Technical Report ECOM-01870(E)-8-T April 1967

# THE PHASE SYNCHRONIZATION OF A PARAMETRIC SUBHARMONIC OSCILLATOR

C. E. L. Technical Report No. 7695-178

Contract No. DA 28-043-AMC-01870(E)

DA-Project No. 1 PO 21101 AO42. 01. 02

Prepared by

James L. Cockrell

COOLEY ELECTRONICS LABORATORY

Department of Electrical Engineering
The University of Michigan
Ann Arbor, Michigan

for

U. S. Army Electronics Command, Fort Monmouth, N. J.

## ABSTRACT

The general problem of phase determination for a parametric subharmonic oscillator is formulated. The analyses of several circuits are reduced to the solution of the canonical Mathieu equation. Solution is effected by the Floquet theorem and the parameters discussed in terms of the range of values encountered in experimental circuits. The transient portion of the solution produces arbitrary constants with two possible signs, yielding the two phase states of a growing oscillation. Conditions of oscillation are discussed, and the influence of signal and noise presented.

Pump unbalance, as a primary signal masking source is a natural outgrowth of the analysis of the usual balanced pumping circuits. This condition is discussed in terms of coherent and incoherent quenching, that is, where the pumping is initiated at the same pump phase angle each quench cycles (incoherent quenching). The error probability where this pump unbalance is controlled by a variety of means is shown to be adequately low over a dynamic range significantly greater than generally reported in the literature.

Experimental results are given demonstrating the various aspects of the analysis. Error probabilities of bistate phase detection are measured for noise and pump unbalance masking conditions and are shown to be represented adequately by the theory.

## ACKNOWLEDGEMENTS

The author wishes to express his gratitude to the many persons who have provided guidance, assistance, and support during the course of this study.

In particular it was Dr. D. K. Adams who suggested the initial formulation of the problem and guided the early effort toward its solution. To Dr. Toshio Fujisawa, Osaka University, Japan, go special thanks for his suggestions relating to the noise analysis while he was in this country as a visiting professor. Also acknowledged is the guidance of Dr. Peter Khan and Professor Alan Macnee, the doctoral committee chairman, during the evolution of the analysis, experimental work, and preparation of the manuscript.

The research conducted here was supported, in part, by the U. S. Army Electronics Command, Under Contracts DA-36-039 AMC-00059(E), DA-28-043 AMC-00029(E), and DA 28-043 AMC-01870(E). Thanks are due to Mr. Herb Brett of USAECOM, Fort Monmouth, New Jersey, for his encouragement and assistance.

TABLE OF CONTENTS

TABLE OF CONTENTS (cont.)

TABLE OF CONTENTS (Cont.)

## LIST OF SYMBOLS

| Symbol | Meaning | Defined by, or First used in equation |
|---|---|---|
| $y''$ | $\frac{d^2y}{dz^2}$ where $y$ is the dependent variable of the canonical Hill equation | 2.1 |
| $a$ | constant coefficient of dependent variable of Hill equation | 2.1 |
| $\phi(z)$ | general periodic function of $z$ | 2.1 |
| $g$ | coefficient of parametric excitation for canonical Hill equation | 2.1 |
| $z$ | general independent variable for canonical Mathieu-Hill equation | 2.1 |
| $e_s(t)$ | signal voltage, function of time | 2.3 |
| $R$ | series resistance of simple series circuit | 2.3 |
| $L$ | series inductance of simple series circuit | 2.3 |
| $S(t)$ | elastance of series circuit, a function of time, $t$ | 2.3 |
| $i$ | instantaneous current in series circuit | 2.3 |
| $q$ | instantaneous charge associated with elastance | 2.3 |
| $\Gamma$ | inverse inductance associated with series inductance $L$ | 2.3 |
| $f$ | a general function of the variable $y$ | 2.6 |
| $K$ | a function of $t$ | |
| $M$ | a function of $t$ | |
| $\lambda$ | flux linkage associated with the inductance | 2.7 |

## LIST OF SYMBOLS (cont.)

| Symbol | Meaning | Defined by, or First used in equation |
|---|---|---|
| $G$ | shunt conductance of a parallel circuit | |
| $\eta$ | coefficient of parametric excitation | 2.10 |
| $v_c$ | instantaneous elastance voltage | 2.10 |
| $S_0$ | constant part of pumped elastance | 2.10 |
| $\omega_1$ | $\frac{1}{2}$ pump angular frequency | 2.10 |
| $\theta$ | phase angle of pumped quantity at t = 0 | 2.10 |
| $V_c$ | a derived elastance voltage | 2.11 |
| $\Gamma_0$ | constant part of pumped inverse inductance | 2.14 |
| $I$ | derived current variable in series circuit with pumped inductance | 2.14 |
| $I_L$ | derived inductive current variable for parallel circuit with pumped inverse inductance | 2.15 |
| $V$ | derived voltage variable for parallel circuit | 2.16 |
| $V_e$ | lossless derived voltage variable | 2.17 |
| $Q_0$ | resonant circuit quality factor | 2.18 |
| $\omega_0$ | natural resonant angular frequency of passive circuit. | 2.18 |
| $a'$ | trial constant term in Mathieu equation | 2.20 |
| $g'$ | trial coefficient of parametric excitation in Mathieu equation | 2.21 |
| $\delta$ | fractional excursion of $\omega_1$ within passive resonance curve | following 2.23 |

## LIST OF SYMBOLS (cont.)

| Symbol | Meaning | Defined by, or First used in equation |
|---|---|---|
| $\Delta\omega_{max}$ | angular frequency variation from resonance to the half-power point | following 2.23 |
| $t'$ | translated time variable | 2.26 |
| A | arbitrary constant in solution equation (associated with growing term) | 3.2 |
| B | arbitrary constant in solution equation (associated with decaying term) | 3.2 |
| $\mu$ | characteristic exponent in solution to Mathieu equation | 3.2 |
| $\psi(z)$ | unspecified periodic function of z | 3.2 |
| $\sigma$ | phase angle in Mathieu equation solution | 3.3 |
| $s_{3,5..}$ | sine term coefficient in series representation of $\phi(z,\sigma)$ | 3.3 |
| $c_{3,5..}$ | cosine term coefficient in series representation of $\phi(z,\sigma)$ | 3.3 |
| $\theta_1'$ | translated pump phase angle | 3.5 |
| $\mu_L$ | general dimensionless loss parameter | 3.10 |
| $\theta_1''$ | pump phase angle purturbed by circuit losses | 3.13 |
| $i_s$ | instantanious signal current | 4.1 |
| $\omega_\ell$ | lower side angular frequency | 4.1 |
| $\Delta\omega_\xi$ | angular frequency excursion between $\omega_1$ and $\omega_\ell$ or $\omega_u$ | 4.1 |
| $\omega_u$ | upper side angular frequency | 4.1 |

## LIST OF SYMBOLS (cont.)

| Symbol | Meaning | Defined by, or First used in equation |
|---|---|---|
| $\theta_\ell$ | phase angle of lower side frequency | 4.1 |
| $\theta_u$ | phase angle of upper side frequency | 4.1 |
| $I_\ell$ | phasor representing lower side frequency signal current | 4.2 |
| $I_u$ | phasor representing upper side frequency signal current | 4.2 |
| $C$ | circuit capacitance (time function) | 4.3 |
| $C_0$ | constant part of circuit capacitance | 4.3 |
| $V_\ell$ | lower side frequency circuit voltage phasor | 4.5 |
| $V_u$ | upper side frequency voltage phasor | 4.5 |
| $*$ | denotes complex conjugate | 4.4 |
| $\xi$ | fractional displacement of side frequencies from half-pump frequency $\omega_1$ | 4.6 |
| $\Pi$ | complex pumping parameter | 4.7c |
| $V_{\ell N}$ | lower side frequency voltage phasor in absence of pumping | 4.9 |
| $V_{uN}$ | upper side frequency voltage phasor in absence pumping | 4.9 |
| $g_\xi$ | complex gain factor | 4.11 |
| $g_m$ | complex gain at frequency $\omega_1$ | 4.12a |
| $\zeta$ | fractional excursion of signal frequency from half-pump frequency, $\omega_1$ in the pumped, or active state | 4.14 |

## LIST OF SYMBOLS (cont.)

| Symbol | Meaning | Defined by, or First used in equation |
|---|---|---|
| $\zeta'$ | detuned $\zeta$ | 4.14 |
| $\Pi'$ | complex pumping parameter in the detuned state | 4.14 |
| $g_{\phi\ell}$ | phase factor associated with lower side frequency | 4.17 |
| $g_{\phi u}$ | phase factor associated with upper side frequency | 4.17 |
| $g_{\phi}$ | phase factor for high gain situation | 4.20 |
| $\theta_2$ | consolidated phase angle (for convenience of manipulation) | 4.20 |
| $g_{\phi max}$ | maximum value of $g_{\phi}$ | 4.21 |
| $g_{\phi min}$ | minimum value of $g_{\phi}$ | 4.21 |
| $v_{ss}(t)$ | instantaneous circuit voltage in steady-state condition | 4.23 |
| $v_{\ell}(t)$ | instantaneous lower side frequency circuit voltage | 4.23 |
| $v_u(t)$ | instantaneous upper side frequency circuit voltage | 4.23 |
| $I_s$ | degenerate signal current phasor | 4.25 |
| $\theta_s$ | signal phase angle | 4.25 |
| $V_{2\omega_p}$ | circuit voltage at pump frequency | 4.29 |
| $C_1$ | capacitance of one side of a balanced circuit | 4.29 |
| $C_2$ | capacitance of the other side of an balanced circuit | 4.29 |
| $E_1$ | drive voltage phasor of one side of a balanced circuit | 4.29 |

## LIST OF SYMBOLS (cont.)

| Symbol | Meaning | Defined by, or First used in equation |
|---|---|---|
| $E_2$ | drive voltage phasor of the other side of a balanced circuit | 4.29 |
| $E_p$ | common drive voltage phasor of a perfectly balanced pump transformer | 4.30 |
| $e_1$ | instantaneous pump voltage associated with $E_1$ | 4.30 |
| $e_2$ | instantaneous pump voltage associated with $E_2$ | 4.30 |
| c | relative capacitance unbalance | 4.31 |
| $\mu_g$ | growing term dimensionless parameter | 5.1 |
| $\mu_d$ | decaying term dimensionless parameter | 5.1 |
| $v(0)_+$ | instantaneous circuit voltage just after pumping begins | 5.1 |
| $v(0)_+$ | instantaneous circuit voltage just time derivative just after pumping begins | 5.1 |
| a, b, d, e | coefficients of A and B in the pair of simultaneous equations in A and B | 5.5 |
| $c_+$ | capacitance just after pumping begins | 5.9 |
| $C(0)_-$ and $c_-$ | capacitance just before pumping begins | 5.9 |
| $v_+$ | circuit voltage just after pumping begins | 5.9 |
| $v_-$ | circuit voltage just before pumping begins | 5.9 |
| $\alpha, \beta, \gamma, \varphi$ | phase angles grouped for convenience of manipulation | 5.16 |
| $\sigma'$ | departure of Mathieu phase angle from $\frac{\pi}{4}$ radians | 5.29 |
| $\sigma''$ | $\sigma'$ perturbed by a detuning quantity | 5.30 |

## LIST OF SYMBOLS (cont.)

| Symbol | Meaning | Defined by, or First used in equation |
|---|---|---|
| $\alpha_\ell$, $\alpha_\mu$ | convenience angles, related to lower and upper side frequencies | 5.32 |
| $\Pi''$ | $\Pi'$ purturbed by detuning | 5.34 |
| $A_{deg}$ | value of A for the degenerate case | 5.37 |
| $A_{deg}$ $\delta=0$ | value of A for the degenerate tuned case | 5.38 |
| $P_s$ | signal power delivered to the tuned circuit | 5.41 |
| $P_s'$ | signal power delivered to the detuned circuit | 5 41 |
| $( )$ | the mean value of | 5.43 |
| $i_1$ | sine component sum of upper and lower side frequency signal circuits | 5.44 |
| $i_2$ | cosine component sum of upper and lower side frequency signal currents | 5.44 |
| $i_N$ | a root mean square signal current | 5.45 |
| $A_{\zeta'}$ | A due to excitations of differential bandwidth $d_{\zeta'}$ at $\pm \zeta'$ | 5.45 |
| dN | thermal noise power delivered to circuit within the bandwidth $d_{\zeta'}$ | |
| K | Bottzmann constant, Joules $^oK$ | 5.47 |
| T | absolute temperature in degrees Kelvin | 5.47 |
| df | incremental frequency, cycles per second | |
| N | total thermal noise associated with a passive resonant circuit | 5.51 |
| N' | thermal noise associated with an active resonant circuit | 5.53 |

## LIST OF SYMBOLS (cont.)

| Symbol | Meaning | Defined by, or First used in equation |
|---|---|---|
| $A_N$ | root-mean-square value of A due to thermal noise | 5.56 |
| $a_N$ | normalized gaussian random variable | 5.57 |
| $B_{deg}$ | value of B for degenerate case | 5.62 |
| $B_{deg}$ $\delta=0$ | value of B for degenerate, tuned case | 5.63 |
| $B_{\zeta'}$ | RMS value of B in differential band $d_{\zeta'}$ | 5.64 |
| $B_N$ | RMS value of B due to thermal noise | 5.65 |
| $A_{noise}$ | A due to noise. Equal to $A_N$ if thermal noise is only noise source | 6.1 |
| $v_0$ | output circuit voltage peak | 6.2 |
| $v_i$ | input circuit signal voltage peak | 6.2 |
| $v_{om}$ | maximum peak output voltage of oscillation | 6.3 |
| $v_{im}$ | maximum input peak voltage | 6.3 |
| $g_v$ | voltage gain | 6.3 |
| $f_m$ | maximum data frequency | 6.4 |
| M | figure of merit | 6.4 |
| $y(\frac{\theta_1}{2}, \sigma'')$ | function of $\frac{\theta_1}{2}$ and $\sigma''$ in pump unbalance consideration | 6.6 |
| $A_{pu}$ | A due to pump unbalance | 6.8 |
| $e_1(1)$ | pump voltage for 1st quench cycle | 6.15 |

## LIST OF SYMBOLS (cont.)

| Symbol | Meaning | Defined by, or First used in equation |
|---|---|---|
| $e_2(2....)$ | pump voltage for 2nd, quench cycle | 6.15 |
| $\theta_1(2)$ | initial pump phase angle of 2nd quench cycle | 6.15 |
| $\theta_1(n)$ | initial pump phase angle of nth quench cycle | 6.16 |
| $p_0$ | minimum value of $P_s / P_{pu}$ for zero error | 6.17 |
| $V_{envelope}$ | envelope of peak voltage | 7.1 |
| $V_1$, $V_2$ | successive observations of circuit voltage peak envelope | 7.2 |
| $v_{ss\ max}$ | maximum steady-state voltage due to signal phase shift | 7.17 |
| $v_{ss_{min}}$ | minimum steady-state voltage due to signal phase shift | 7.17 |
| $C_n$ | nth harmonic of time varying capacitance C | III.1 |
| $V_k$ | kth harmonic of the capacitor voltage | III.1 |
| $\omega_k$ | unidentified angular frequency | III.1 |
| $I_c$ | capacitive current | III.5 |

## LIST OF ILLUSTRATIONS

LIST OF ILLUSTRATIONS (cont.)

## LIST OF APPENDICES

# I. INTRODUCTION

## 1.1 General Problem Area. Parametric Subharmonic Oscillator (SHO)

The parametric subharmonic oscillator has been something of a curiosity to theoretical and experimental investigators for a period of at least one hundred years. As mentioned by E. Goto (Ref. 21) in 1959, and others before him, most of us have experienced the basic phenomena in attempting to cause our childhood swing to operate without any actual contact with the ground. In the child's heuristic manner he finds that appropriate bending (shortening) of the suspension at certain points in the cycle is effective in increasing the amplitude of oscillation. Quite appropriately named pumping, this effort patiently applied will cause the swing to proceed from no observable motion to dramatically violent oscillations. The phenomnon, though not new, is finding application in a world particularly sensitive to an inherent property of that phenomenon. The resulting oscillation possesses two intrinsically identifiable, stable states. Von Neumann (Ref. 45) and Goto (Ref. 22), at about the same time recognized that the subharmonic oscillation of order one-half observed in a parametrically excited resonant circuit always had one of two possible phase positions with respect to the pumping phase. The logical extension of these states to the "o" and "1" of the binary world quickly followed. It was further recognized that the device, being a resonant system, could be scaled to extremely high frequencies, with resultingly high possible binary data rates. Thus the principle held promise for exploitation in digital devices.

## 1. 2 Prior Art

The volume of literature that bears closely on the general subjects of parametric amplifiers and the parametric subharmonic oscillator is large and stems from many sectors of the international literature. The emphases are identifiable into the subject categories which follow and present a variety of depth and elegance.

Observations of subharmonic oscillations were reported in 1859 by F. E. Melde (Ref. 112) and in 1883 by Lord Rayleigh (Ref. 110). They had observed the sustained vibrations of a stretched wire at frequency f when the tension of the wire was varied by attachment to a tuning fork vibrating at frequency 2f. The oscillations were always phased so that as the wire moved away from the static position the tension was decreasing. Conversely as the wire moved toward the static position the tension was increasing and kinetic energy was being added to the system. A similar observation in a mechanical system was made by Stephenson in 1908 (Ref. 113) when he discussed the theory of the stability of an inverted pendulum by periodic movements of its point of support. The electrical analog of these observations have been subsequently reported by a great number of authors. Typical of the earlier effort is the work of R. V. L. Hartley (Ref. 28) in 1936 when he used the saturating effect of iron-cored inductors to produce parametric excitation. The work of Goto (Ref. 21) in Japan and a group of his colleagues has brought the understanding of the inductive SHO to a high level of practical importance by using ferrites. Computing schemes employing thousands of these devices have been built in Japan. In this country the

work has centered on devices constructed around the semiconductor diode as a voltage controllable capacitance. The primary reason for this emphasis is the high component quality factor (Q) obtainable into the gigahertz frequency region and possible extension of use to higher speed computers.

Another general category of investigation profusely reported and bearing on the SHO is that of parametric amplification. The SHO is a degenerate form of the parametric amplifier and techniques used to analyze these devices are highly developed. In particular, (Ref. 15) methods of handling the steady-state analysis for perturbations about the degenerate condition have come from the study of double side-band parametric amplifiers.

The analysis of the differential equations which result from parametric excitation have a long history. These discussions are included in a classic work by McLachlan (Ref. 103) published in 1946 and containing 226 references to the international literature. The refinement of methods of solution of initial value problems where the equations are of the Mathieu-Hill type is evidenced by the work of L. A. Pipes (Ref. 56).

The detailed study of oscillators invariably leads to large signal analyses where nonlinearities are the limiting influence. Much of the literature on the SHO concerns this region of operation since it is in the large-signal state that the operation is observed and logic operations effected. These studies deal with methods of handling the nonlinearities of the reactive elements. Goto (Ref. 21) has used an interesting graphical presentation to display stable states at large signal levels. Wang (Ref. 46) developed a model of a thin magnetic film parametron (SHO) and demon-

strated a computer solution to a high saturation steady-state level. The extreme nonlinearities of magnetic components were used in a unique analysis by Lavi (Ref. 26) in a dissertation at Carnegie Tech and later presented in a national publication (Ref. 25). The authors whose work most directly leads to the ideas and form of analysis used in this study are Bura (Ref. 17) and Phillips (Ref. 104). In particular Bura concerns himself with the expression for the operation of the parametric amplifier close to the degenerate condition. The results of his work differ considerably from some of the analytical and experimentally confirmed results of the study under discussion (c.f. paragraph 4. 16 and 7. 4). Phillip's contribution was primarily in the transient analysis and the evolution of the mathematical forms describing the phenomena as deriveable from actual circuit components.

An additional segment of the prior art is concerned with the extension of the understanding of the SHO to applications in signal detection schemes and in computer technology. Radar front-ends have been built using the degenerate parametric amplifier (Ref. 23) in the amplifying mode. Wang and Wade (Ref. 10) have analyzed a similar device in the superregenerative mode. In the computer literature moderate frequency devices (10 to 50 MHz) are discussed and have assumed practical importance in computers in Japan (Ref. 14). In this country the effort has been to construct microwave computer elements using the semiconductor diode as the active element and to develop methods of handling information at the elevated data rates made possible by gigahertz pumping.

## 1.3 Statement of the Problem

In the various studies mentioned in the prior art the emphasis has been on the dynamic process of growth of the subharmonic oscillation. The authors have mentioned that a form of gain is possible in that a very small signal can positively establish the phase of growing oscillation. Only minimal attention has been given to optimizing that "gain" or finding the limitations of the gain. In none of the studies has significant attention been given to the mechanisms of phase-state determination. In such a binary signal detection scheme the resulting oscillation bears the information with a finite probability of error. Therefore, it is the purpose of this study:

1) to explore the mechanisms of phase determination and to identify the disturbing factors.
2) to express quantitatively, where possible, the limitations of sensitivity and error-probability in the determination of oscillation phase by a signal phase.
3) to demonstrate the validity of the analysis by suitable experimental procedures.

## 1.4 Topics of Investigation

The objectives lead naturally to limiting the study to very low levels of oscillation. In this region, where the phase determination actually occurs, the circuit elements are considered linear, and the pumped element

is a linear time-varying capacitance. Step quenching[1] has been used throughout since in these days of high speed switching circuits it is a mode easily achieved and thus of practical importance.

Along these lines progress has been made on these specific topics:

1) Formulation of the problem as an initial value problem where regions of consideration are
   (a) passive circuit, where only signal and noise are imposed on the circuit,
   (b) active circuit, where periodic pumping has been initiated abruptly and the values of (a) at the interface become the initial values of (b).
2) Consideration of circuit response to signal (degenerate condition) and noise (quasi degenerate condition).
3) Consideration of practical circuitry and the results of pump unbalance in nearly balanced pumping.
4) Consideration of coherent vs incoherent quenching.

It is interesting to note that at the inception of the study the importance of pump unbalance in imposing limitations on the response of the SHO to signal phase information was not recognized. Nor has it been discussed in the literature. Appreciation of these limitations grew out of attempts to correlate laboratory results with the analysis evolved from topic 2 above.

---

[1] Quenching, a term conceived in the superregenerative amplifier field refers to the initiation and termination of the conditions permitting oscillation. These conditions can be inserted and removed smoothly, or abruptly, as in "step" quenching.

Finally as the pump unbalance problem was identified the concepts of coherent and incoherent quenching were found to divide these limitations into two families.

The chapters which follow describe in detail the evolution of the analysis and the supporting experimental work. The mathematical formulation in Chapter II is not new but is glossed over without careful consideration by most authors. The material on the transient solution in Chapter III and in Appendices I and II has significant additions to material found in the literature. These additions permit a better understanding of operation away from the ideal "tuned, lossless situation." Chapter IV deals with the steady-state solution which is necessary to the complete solution even in the oscillating region of operation since this is the "particular integral" of that solution. Chapters V and VI take the earlier results and develop analytical forms for error-probabilities under the various operating conditions. Chapter VII contains the experimental results which have proceded hand-in-hand with the development of the analytical results. The final chapter summarizes the results of the study and attempts to project the consequences of the findings into the present uses of the subharmonic oscillator and into some possible applications.

## II MATHEMATICAL FORMULATION

Possible circuit models of parametric subharmonic oscillators are discussed. The variables are chosen so that, after suitable changes, the canonical Mathieu equation results. In this process approximations are made and discussed. The general method of solution is presented.

### 2.1 Type of Problem - Conceptual Formulation

This discussion assumes that the oscillating system is controlled by external (information) signals where the level of oscillation is very low, and in the limit is in the vicinity of circuit noise. At this low level reactive circuit elements which are otherwise characterized by high level nonlinearities may be considered as linear elements. In particular when such elements are forced to vary periodically about a quiescent value by an external means a linear time - varying element is achieved. Such an element has the potential for transforming energy from the source of periodic variation (the pump) to the circuit to which the element is connected. (Ref. 15, 70, and others)

The mathematical treatment of a resonant circuit having a linear time-varying reactive element as has been suggested by several authors (Ref. 21, 26), is closely related to the equations of Mathieu and Hill. Where the pumping is a general periodic function of the independent variable z the Hill equation results. (Ref. 103)

$$y'' + [a - g\phi(z)]\, y = 0 \qquad (2.1)$$

where a and g are constants.

A special case of the Hill equation is the Mathieu form, which is

characterized by a simple harmonic pump frequency, thus:

$$y'' + (a - 2g \cos 2z)y = 0 \qquad (2.2)$$

It is the purpose of this chapter to show that the Mathieu equation (2.2) can be used to describe a resonant circuit characterized by moderately high passive Q and sinusoidal pumping of a reactive element.

## 2.2 Circuit Models, Variables

Consider the series resonant circuit with a linear time-varying elastance in Fig. 2.1. The differential equation around the loop is

$$e_s(t) = Ri + L\frac{di}{dt} + S(t)q \qquad (2.3)$$

Using the elastance charge q as the independent variable

$$\left.\begin{aligned} i &= \frac{dq}{dt} = \dot{q} \\ \frac{di}{dt} &= \frac{d^2q}{dt^2} = \ddot{q} \\ L &= \frac{1}{\Gamma} \end{aligned}\right\} \qquad (2.4)$$

Eq. 2.3 becomes

$$\Gamma e_s(t) = \ddot{q} + R\Gamma\dot{q} + S(t)\Gamma q \qquad (2.5)$$

Eq. (2.5) is an example of a canonical form which we shall restate in general terms

$$f = \ddot{y} + K\dot{y} + My \qquad (2.6)$$

Where K, M, and f in general are functions of independent variable t.

As a second circuit example, consider the series resonant circuit where the inductance is pumped rather than the elastance or capacitance Fig. 2. lb. In this instance the inductance voltage is $\frac{d\lambda}{dt}$ where the time variations are implicit in the constitution of the flux linkage, $\lambda$. The circuit equation is written in terms of $\lambda$ as the dependent variable, while the inverse inductance, $\Gamma$, is identified as the pumped quantity.

$$\dot{e}_s(t) = \ddot{\lambda} + R\Gamma(t)\dot{\lambda} + [R\dot{\Gamma} + S\Gamma(t)]\lambda \qquad (2.7)$$

Equation 2. 7 is also in the form of 2. 6 although complicated somewhat by the time dependence of the K coefficient and the additional term in the M coefficient.

The circuits of Fig. 2. 1 have their exact duals in parallel configurations and the equations for them can be written in the canonical form from Eqs. 2. 5 and 2. 7 at once.

Parallel circuit, pumped inductance

$$Si_s(t) = \ddot{\lambda} + GS\dot{\lambda} + \Gamma(t)S\lambda \qquad (2.8)$$

Parallel circuit, pumped capacitance

$$\dot{i}_s(t) = \ddot{q} + GS(t)\dot{q} + [G\dot{S} + \Gamma S(t)]q \qquad (2.9)$$

It will be noted that in the examples presented up to this point the reactive elements are represented as elastance and inverse inductance. This

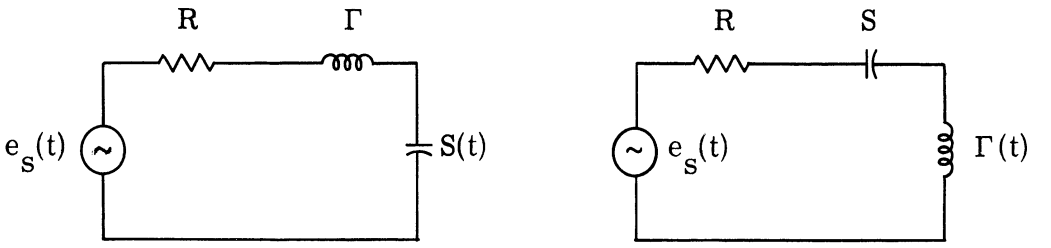


$$S(t) = \frac{1}{C} = S_o[1 - \eta \sin(2\omega_1 t + \theta_1)]$$

$$\Gamma(t) = \frac{1}{L} = \Gamma_o[1 - \eta \sin(2\omega_1 t + \theta_1)]$$

(a)

Pumped Elastance

(b)

Pumped Inverse-Inductance

Fig. 2.1 Series circuits.

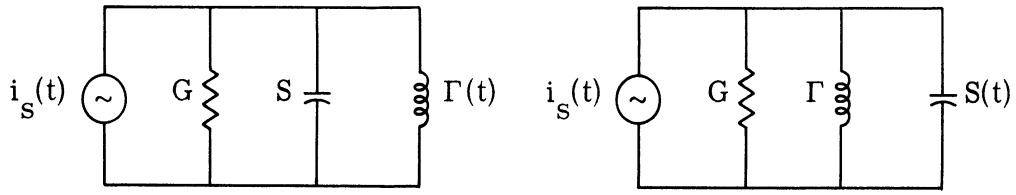


(a)

Pumped Inverse Inductance

(b)

Pumped Elastance

Fig. 2.2 Parallel circuits.

is done for two reasons. First, the form of the equations is simpler because the terms all appear having only numerator values; and second, time variations are constrained to the numerator where the simple harmonic variations are represented in concise closed form rather than in a series of terms. The question arises, of course, about whether it is actually capacitance or elastance that is being pumped sinusoidally. The answer is related specifically to the particular element being pumped, and the manner of pumping. For small values of $\eta$, the index of parametric excitation, these differences become small in any event. The primary effect is the reversal of sign as the explicit time variation is transferred from the denominator to the numerator.

We have seen how the simple resonant circuit models having a single time-varying reactive element produce similar differential equations (2. 6). When the elastance is pumped the charge is the natural variable. For the pumped inductance the flux linkage is the natural variable. Neither of these quantities is particularly amenable to direct measurement in the laboratory nor do most workers in the field have facility in thinking specifically of these quantities. This problem has led several writers (e. g. , Ref. 21) to find derived current and voltage variables which very nearly represent the actual current and voltage of the circuits and which can be represented by the form of Eq. 2. 6.

For example, if in the series circuit with pumped capacitance we note that:

$$q = \frac{v_c}{S} = \frac{v_c}{S_0 [1 - \eta \sin (2\omega_1 t + \theta_1)]} \tag{2.10}$$

then we can define a new elastance voltage

$$V_c = \frac{v_c}{[1 - \eta \sin (2\omega_1 t + \theta_1)]} \tag{2.11}$$

from which

$$q = \frac{V_c}{S_0} \qquad \dot{q} = \frac{\dot{V}_c}{S_0} \qquad \ddot{q} = \frac{\ddot{V}_c}{S_0} \tag{2.12}$$

and now Eq. 2.5 becomes

$$S_0 \Gamma e_s(t) = \ddot{V}_c + R\Gamma \dot{V}_c + S(t)\, \Gamma V_c \tag{2.13}$$

The variable $V_c$ is very nearly the actual elastance voltage $v_c$, differing from the actual only by the index of parametric excitation, $\eta$, which appears as a time variation at the pump radian frequency $2\omega_1$, and its harmonics.

Similarly, for the series circuit with pumped inductance the derived variable is the current I, and Eq. 2.7 becomes

$$\Gamma_0 \dot{e}_s(t) = \ddot{I} + R\ddot{\Gamma}(t)\, \dot{I} + [R\dot{\Gamma} + s\Gamma(t)]\, I \tag{2.14}$$

and for the parallel circuits with pumped inductance and pumped capacitance Eq. 2.8 and Eq. 2.9 respectively become:

$$\Gamma_0 S i_s = \ddot{I}_L + G S \dot{I}_L + \Gamma(t) S I_L \tag{2.15}$$

$$S_0 \dot{i}_s = \ddot{V} + G S(t) \dot{V} + [G\dot{S} + S(t)\Gamma] V \tag{2.16}$$

where $V = \frac{C}{C_0} v$ derived from $q = Cv = C_0 V$

It has been shown that each of the simple resonant circuits having a pumped reactive element is described by the same form of Eq. 2.6 and is given explicitly in Eqs. 2.5, 2.7, 2.8, and 2.9. In addition, a group of derived variables, closely approximating the actual variables are described by the same form. It follows that a reduction of the canonical form Eq. 2.6 to a Mathieu equation is tantamount to reducing all the explicit representations to the same form. Therefore from this point on only a single form will be considered, and the particular one chosen is that most closely describing the circuit investigated in the laboratory. This circuit is the parallel circuit having a pumped capacitance. The equation representing the derived variable, V, the circuit voltage is the point of departure, Eq. 2.16. It is worth noting that this equation and its dual, Eq. 2.14, are somewhat more involved than Eqs. 2.13 and 2.15 because of the appearance of time variations of the coefficient of the first derivative.

## 2.3 Reduction to Canonical Mathieu Form

The Mathieu Eq. 2.2 contains no first derivative and thus a change of variable in (2.16) will be considered. This variable has the same dimensional form as V but is multiplied by an exponential factor which exactly compensates for the normal dissipation. This is a mathematical artifice and is described

in detail in Appendix I. Under this transformation Eq. 2.16 becomes:

$$S_0 \epsilon^{\frac{G}{2}\int S(t)dt} \cdot i_s = \ddot{V}_e + \left\{ -\frac{[GS(t)]^2}{4} + \frac{G\dot{S}(t)}{2} + S(t)\Gamma \right\} V_e \qquad (2.17)$$

where

$$V_e = V \epsilon^{\frac{G}{2}\int S(t)\,dt}$$

In order to proceed we consider the case of simple harmonic parametric excitation of the form

$$S = S_0[1 - \eta \sin(2\omega_1 t + \theta_1)] \qquad (2.18)$$

$\eta$ is the coefficient of parametric excitation.

Circuit quality factor is variously stated as:

$$Q_0 = \frac{R}{\omega_0 L} = \frac{1}{G\omega_0 L} = \frac{\omega_0 C_0}{G} = \frac{\omega_0}{GS_0}$$

where $\omega_0^2 \equiv S_0\Gamma$.

When the passive circuit resonant radian frequency $\omega_0^2$ is factored out of the bracket and the substitutions of Eq. 2.18 are made; Eq. 2.17 becomes

$$S_0 \epsilon^{\frac{G}{2}\int S\,dt} \dot{i}_s = \ddot{V}_e + \omega_0^2 \left\{ \frac{1}{4Q_0^2} \left[1 - \eta \sin(2\omega_1 t + \theta_1)\right]^2 \right.$$

$$\left. - \frac{\eta\,\omega_1}{Q_0 \omega_0} \cos(2\omega_1 t + \theta_1) + \left[1 - \eta \sin(2\omega_1 t + \theta_1)\right] \right\} V_e \qquad (2.19)$$

The terms in the bracket contribute primarily the two kinds of terms in the canonical Mathieu equation, namely a constant term, and a double frequency pumping term.

Let us call the constant term a', and note:

$$a' = 1 - \frac{1}{4Q_0^2} + \frac{\eta^2}{8Q_0^2} \qquad (2.20)$$

The double frequency coefficient we will call 2g' (to conform with McLachlan's canonical form of the Mathieu equation, c.f. ref. 103). This term then is:

$$2g' = -\eta\left[\left(1 - \frac{1}{2Q_0^2}\right) \sin(2\omega_1 t + \theta_1) + \frac{\omega_1}{\omega_0} \frac{1}{Q_0} \cos(2\omega_1 t + \theta)\right. \qquad (2.21)$$

For moderate $Q_0$ factors of 10 or larger this double frequency term is

$$2g' \approx \eta \sin(2\omega_1 t + \theta_1 + \tan^{-1} \frac{1}{Q_0}) \qquad (2.22)$$

($\eta$ accurate to the order of 1 part in $8Q_0^4$ and $2g' \cong \eta$)

In addition to the constant, and double-frequency terms, there is a very small cos $4\omega_1$ term which is of the order of $\frac{\eta^2}{4Q_0^2}$. If this very small (1 part in 1000) $4\omega_1$ term is neglected the remaining equation is a dimensional form of the Mathieu equation.

$$f = \ddot{V}_e + \omega_0^2[a' - 2g' \sin(2\omega_1 t + \theta_1 + \tan^{-1}\frac{1}{Q_0})]\, V_e \qquad (2.23)$$

where

$$f \equiv S_0 \epsilon^{\frac{G}{2}\int S\, dt}_{i_s}$$

We now consider the relation between the passive circuit resonance radian frequency $\omega_0$ and the half-pump radian frequency $\omega_1$ in terms of a normalized dimensionless variable $\delta$.

$$\delta \equiv \frac{(\omega_1 - \omega_0)}{\Delta\omega_{max}}$$

$\Delta\omega_{max}$, the half power point of the resonance curve, is known from passive circuit theory in terms of the center frequency and circuit Q factor to be $\frac{\omega_0}{2Q_0}$.

$$\text{Thus } \omega_0 = \frac{\omega_1}{1 + \frac{\delta}{2Q_0}} \qquad (2.24)$$

and $\omega_0^2 \cong^* \omega_1^2 (1 - \frac{\delta}{Q_0})$ (* read $\cong$ is very nearly equal to --)

And now if we let

$$a \equiv a'(1 - \frac{\delta}{Q_0})$$

and

$$g \equiv g'(1 - \frac{\delta}{Q_0})$$

then (2. 25)

$$a' \omega_0^2 = a\omega_1^2$$

and

$$2g'\omega_0^2 = 2g\omega_1^2$$

and choose the origin of time t' such that $\cos 2\omega_1 t' = \sin (2\omega_1 t + \theta_1 + \tan^{-1} \frac{1}{Q_0})$ Eq. 2. 23 becomes

$$f(t) = \ddot{V}_e + \omega_1^2 [a - 2g \cos 2\omega_1 t'] V_e \quad (2. 26)$$

Now let $z \equiv \omega_1 t'$

$$V_e(t') = V_e (\frac{z}{\omega_1}) = y(z)$$

$$\frac{f(t)}{\omega_1^2} = y'' + [a - 2g \cos 2z] y \quad (2. 27)$$

2. 4 Circuit Relation to Matrix Parameters, a, g. As we shall see later, the transient solution to this equation (2. 27) is governed completely by the values of a and g. Therefore it is worthwhile emphasizing how these two quantities are related to the circuit parameters.

In a circuit of moderate Q (e. g., $Q_0 \geqq 10$) a is in the vicinity of unity

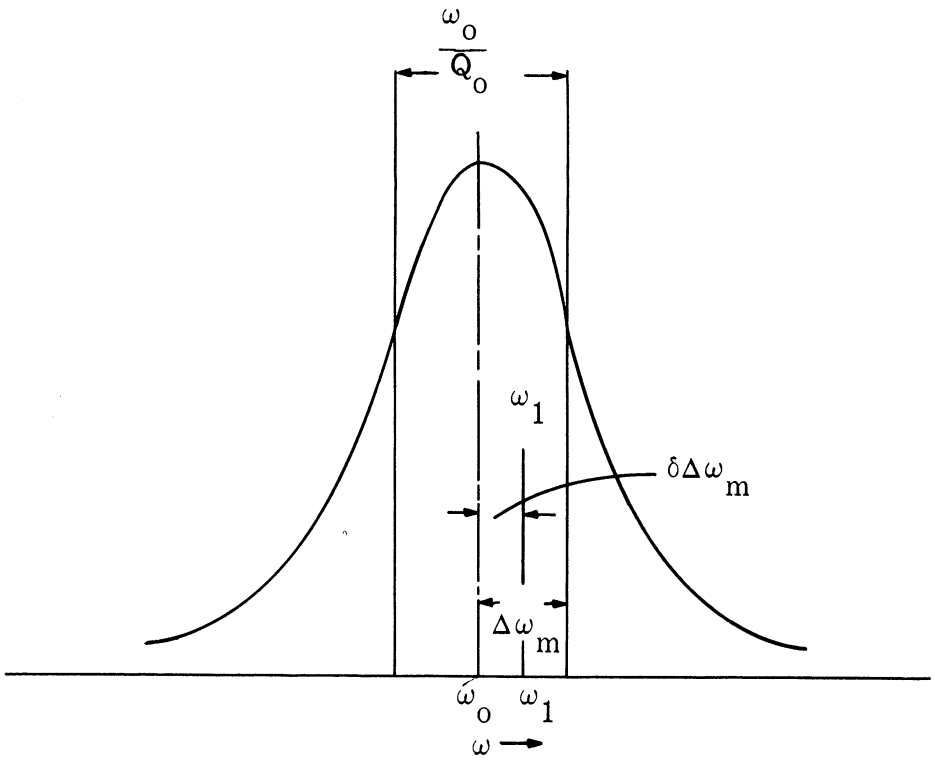


Fig. 2.3 Pump-passive resonance relations.

and is essentially the ratio of the squares of the passive circuit resonant frequency to the half pump frequency. A departure from this value occurs as we saw in Eq. 2. 20. Orders of magnitude are shown in the dimensionless form below

$$a = \left(1 - \frac{\delta}{Q_0}\right)\left(1 - \frac{1}{4Q_0^2} + \frac{\eta^2}{8Q_0^2}\right) \qquad (2.28)$$

detuning losses pumping

Noting that within the normal pass band $-1 \leqq \delta \leqq +1$, the detuning has by far the greatest effect on a, but even that is a small perturbation, about unity. However, as we shall see, the effect is quite significant.

The factor 2g is also affected by the detuning parameter $\delta$, but the influence on the solution usually is small enough to be neglected. (Ref. 46)

The fact that the ratio of $\frac{a}{2g}$ is not a function of pump frequency (i. e., detuning) but only of $\eta$, the index of parametric excitation, is shown by Eqs. 2. 25, 2. 21, and 2. 22. The significance of this will be evident as the transient solution is discussed in the next chapter.

Finally, the phase angle of the pump, is perturbed by a small angle $(\tan^{-1} \frac{1}{Q_0})$ due to the losses.

It has been shown above that the lossless Mathieu equation can be used to describe resonant circuits having a reactive element which is being pumped at approximately twice the resonant frequency of the passive elements. For circuit quality factors of 10 or above the terms of the final equation become quite simple. The dominating parameters are circuit detuning and

pumping level. A series of variable changes was made to convert the differential equation of the chosen circuit to the canonical Mathieu equation form. This allows the body of literature on that equation to be used in the transient solution.

## 2. 5 Method of Solution

The solution of the final Eq. 2. 27 will be made in the classic manner of solving separately the complementary equation, finding a particular integral to accommodate the inhomogeneous member of the original equation, and adapting the constants to constraints appropriate to the problem.

The complementary equation will be solved according to a classic reference on the Mathieu equation (Ref. 103) noting the particular range of circuit parameters involved, and evolving a graphic solution for the natural response of parameters of the system.

The particular integral can be found using mathematical procedures appropriate to this class of problems, such as the so-called "variation of parameters" method. Such procedures will indeed produce a solution, as shown by Bura (Ref. 17) in a recent paper about the general degenerate form of parametric amplifier. However, these methods offer less insight into what actually happens in the circuit than the steady-state solution approach familiar to the engineer. This latter approach will be used following the general methods suggested by D. K. Adams in Ref. 15.

The initial conditions which prevail when the circuit is switched from a passive circuit to an active, unstable, oscillating circuit provide the basis for imparting information to the active circuit. When thermal noise combines

with signal in the information handling process the problem becomes a statistical one where only the average performance over a large number of samples has a direct meaning. Included in this sampling process are other disturbing factors such as signal leakage and pump frequency unbalance. These can and frequently do have a predominant effect in determining the low-level signal limitations of the device as a sampled data digital signal amplifier.

# III TRANSIENT SOLUTION

## 3.1 Mathieu Form

The response of the active resonant systems presented in Chapter II has been shown to be constrained by the classic Mathieu equation. These systems are resonant circuits containing a single time-varying reactive element. The actual circuits contain dissipating members but by suitable changes of variable are represented by the lossless Mathieu equation, repeated for convenience below:

$$y'' + [a - 2g \cos 2z]y = 0 \qquad (3.1)$$

From the general theory of linear differential equations we learn that the solution is of the type

$$y = A\epsilon^{\mu z} \phi(z) + B\epsilon^{-\mu z}\psi(z) \qquad (3.2)$$

where A and B denote arbitrary constants, $\mu$ is the characteristic exponent which depends on a and g, and $\phi$ and $\psi$ are periodic functions of z (Floquet's Theorem). In the words of Professor E. T. Whittaker in 1914 (Ref. 106) "While the general character of the solution from the function theory point of view is thus known its actual analytical determination presents great difficulties." Professor Whittaker went on to introduce a new variable, $\sigma$, which we shall also use here. This variable is the phase angle of the periodic portions of the solution Eq. 3.2 and has a very definite physical significance.

3.1.1. The a-g Plane. The "analytical determination" mentioned

above is not nearly so difficult in the particular case of interest as in the more general case. The stability of the general transient solution is best understood by referring to the a-g plane. Figure 3.1 (Ref. 2-4) shows the various regions of stable solutions, the lines dividing these regions being periodic solutions. Of interest in the problem at hand are the unstable regions, and of particular concern is the plane in the vicinity of $a = 1$. For our problem we find that the area bounded by $a = (1 \pm .15)$ and $g$ between 0 and .2 is sufficient to display the full range of solutions of the transient problem.

3.1.2 $\mu$ and $\sigma$ Parameters. Examination of the selected region of Fig. 3.1 shows that the values of $\mu$ and $\sigma$ can be given explicitly in terms of the equation parameters (3.1), $a$ and $g$. The details of the development of Fig. 3.2 are of considerable interest and are touched upon in an abbreviated form by Phillips (Ref. 104) in a recent paper. In Fig. 3.2 the direct presentation of the variable, $\sigma$, on the a,g, plane is a significant addition to this method of understanding the transient solution. The development of these curves is given in Appendix II.

Noting that the characteristic exponent, $\mu$, is uniquely determined by the values of a and g, only the nature of $\phi(z)$ and $\psi(z)$ remains in order to understand the transient solution. Here the restricted region of a and g assist us considerably. Following Whittaker's development he supposed that $\phi(z)$ can be represented by $\phi(z, \sigma)$ as a Fourier series introducing $\sigma$ as a phase angle, thus:

$$\phi(z,\sigma) = \sin(z-\sigma) + s_3 \sin(3z-\sigma) + s_5 \sin(5z-\sigma) + \ldots\ldots + c_3 \cos(3z-\sigma) + c_5 \cos(5z-\sigma) + \ldots\ldots \tag{3.3}$$

The s's and c's are functions of g and $\sigma$. The substance of Whittaker's development was to show that the missing terms in Eq. 3.3 introduce non-periodic terms in $\phi(z, \sigma)$ and that the coefficients $s_n$ and $c_n$ are convergent series in g and $\sigma$. The coefficient of the sin $(z-\sigma)$ is arbitrarily chosen to be unity. The series expressions for the s's and c's are given in Appendix II and tabulated in table 3.1 to show the maximum relative magnitudes.

Table 3.1

| Term | Largest Term | Max. value for g = .2 % of unity |
|---|---|---|
| $s_3$ | $-g/8$ | 2.5 |
| $c_3$ | $\frac{3}{64} g^2 \sin 2\sigma$ | .19 |
| $s_5$ | $\frac{1}{192} g^2$ | .021 |
| $c_5$ | $\frac{-7}{2304} g^3 \sin 2\sigma$ | .0024 |
| $s_7$ | $-\frac{1}{9216} g^3$ | .00009 |
| $c_7$ | $\frac{35}{442368} g^4 \sin 2\sigma$ | .000013 |

Table 3.1 shows that the $s_3$ term is by far the largest, other than the reference term, $\sin(z-\sigma)$. Thus for the region of the transient solution under discussion we find that it is nearly a pure sinusoid having at most a 3rd harmonic of 2.5%. Consistent with the objective to find a comprehensive picture of the

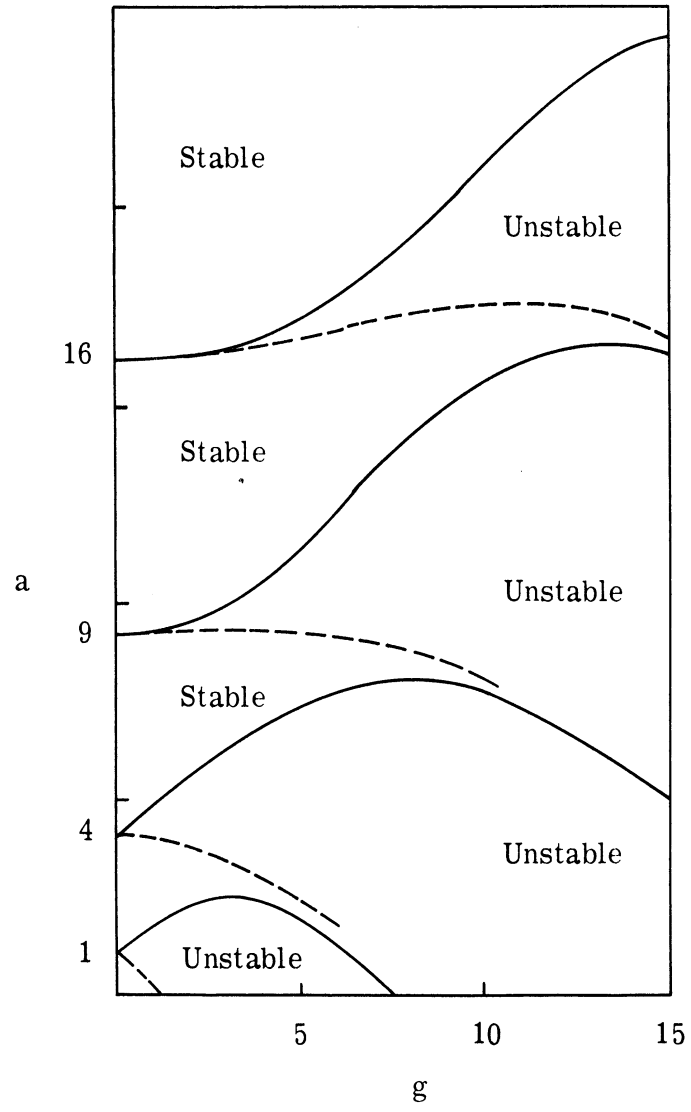


Fig. 3. 1 Stability of solutions.

mechanisms involved in the phase synchronization in the simplest possible form only the $\sin(z-\sigma)$ term will be used in the material which follows.

The second independent solution is obtained by writing $-\sigma$ in Eq. 3.3 so that the complete solution to Eq. 3.1 in the region of interest for this problem is:

$$y = A\epsilon^{\mu z}\sin(z-\sigma) + B\epsilon^{-\mu z}\sin(z+\sigma) \qquad (3.4)$$

## 3.2 Reversal of Variable Changes

The changes made in Chapter II to arrive at the Mathieu equation are now reversed to restore the original variables. The individual changes are reversed one at a time in order to show the effect of the particular changes on the form of the final solution.

$$\omega_1 t' = z \qquad y(z) = V_e(t')$$

$$V_e = A\epsilon^{\mu\omega_1 t'}\sin(\omega_1 t' - \sigma) + B\epsilon^{-\mu\omega_1 t'}\sin(\omega_1 t' + \sigma) \qquad (3.5)$$

from Eq. 2.25

$$\omega_1 t' = \omega_1 t + \frac{\theta_1}{2} \quad \text{and} \quad \theta_1' \equiv \theta_1 + \tan^{-1}\frac{1}{Q_0} - \frac{\pi}{2}$$

$$V_e = A'\epsilon^{\mu\omega_1 t}\sin(\omega_1 t + \frac{\theta_1'}{2} - \sigma) + B'\epsilon^{-\mu\omega_1 t}\sin(\omega_1 t + \frac{\theta_1'}{2} + \sigma) \qquad (3.6)$$

A' and B'; are merely new arbitrary constants.

$V_e$ is the lossless variable and is related to the true variable with losses by

$$V = V_e \epsilon^{-\int \frac{GS(t)}{2}} \tag{3.7}$$

The fact that S(t) is time-varying makes the form of V more difficult to relate to the problem. Using the substitution that $GS_0 = \omega_0 / Q_0$

$$V = V_e \epsilon^{\frac{-\omega_0 t}{2Q_0}} \epsilon^{\frac{-\omega_0 \eta}{\omega_1 4Q_0}} \cos(2\omega_1 t + \theta_1) \tag{3.8}$$

Since $\frac{\omega_0}{\omega_1}$ is approximately unity the second exponential term is simply a time perturbation of V and has values within the range, $(1 \pm \frac{\eta}{4Q_0})$. For values of $\eta < .2$ and $Q_0 > 10$ this perturbation is of the order of .25% or less.

Using Eq. 3.8 in 3.6 (neglecting the second exponential in Eq. 3.8)

$$V = A'\epsilon^{(\mu - \mu_L)\omega_1 t} \sin(\omega_1 t + \frac{\theta_1'}{2} - \sigma) + B'\epsilon^{-(\mu + \mu_L)\omega_1 t} \sin(\omega_1 t + \frac{\theta_1'}{2} + \sigma) \tag{3.9}$$

where

$$\theta_1' \equiv (\theta_1 + \tan^{-1} \frac{1}{Q_0} - \frac{\pi}{2})$$

and

$$\mu_L \equiv \frac{\frac{\omega_0}{\omega_1}}{2Q_0} \cong \frac{(1 - \frac{\delta}{2Q_0})}{2Q_0} \tag{3.10}$$

Equation 3.9 is a solution to the homogeneous differential Eq. 2.16 and but for the small variations introduced in paragraph 2.2 is the actual elastance voltage. A new quantity has been introduced in $\mu_L$, which expresses explicitly the circuit losses, and the detuning.

## 3.3 Criterion for Oscillation

In Eq. 3.9 the criterion for oscillation is that V grow without limit as t increases. Since $\mu$ is always positive in the region of interest this criterion is satisfied only when

$$\mu > \mu_L \tag{3.11}$$

In order to visualize this criterion one can identify the iso-$\mu$ curves of Fig. 3.2 as iso-$Q_0$ curves. For example if $Q_0 = 10$, from Eq. 3.10 we note that $\mu_L \cong .05$. Thus the $\mu = .05$ curve of Fig. 3.2 divides the a-g plane into an unstable region above $\mu = .05$, and a stable region below. This is portrayed again in Fig. 3.3 where the curves are laid out on the "a" axis (as ordinates versus g) and the iso-$\mu$ curves are labeled with $Q_0$ values. Each of the $Q_0$ values divides the plane into stable and unstable regions for that particular $Q_0$.

Having defined stability regions it is desired now to visualize movement within the regions for a given problem. As discussed in paragraph 2.4 and by Phillips (Ref. 2) the ratio of $\frac{a}{2g}$ is determined by $\eta$ and is not a function of frequency. Thus, as the circuit is detuned with respect to the half-pump frequency (i.e., $\omega_0$ with respect to $\omega_1$) the ratio of $\frac{a}{2g}$ is described by a straight line through the origin.

The stability of the circuit is understood in terms of the intersections

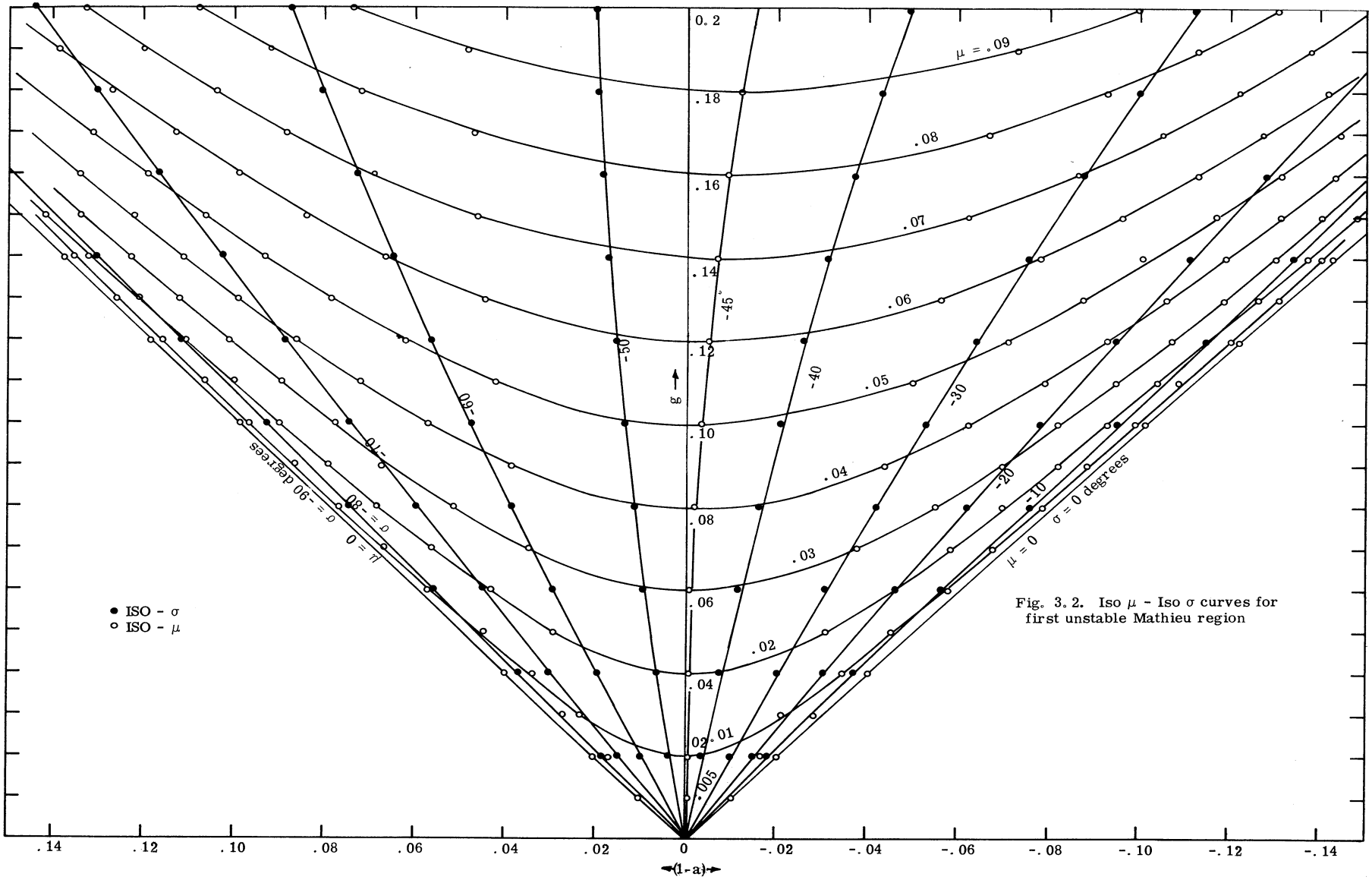


Fig. 3.2. Iso $\mu$ - Iso $\sigma$ curves for first unstable Mathieu region

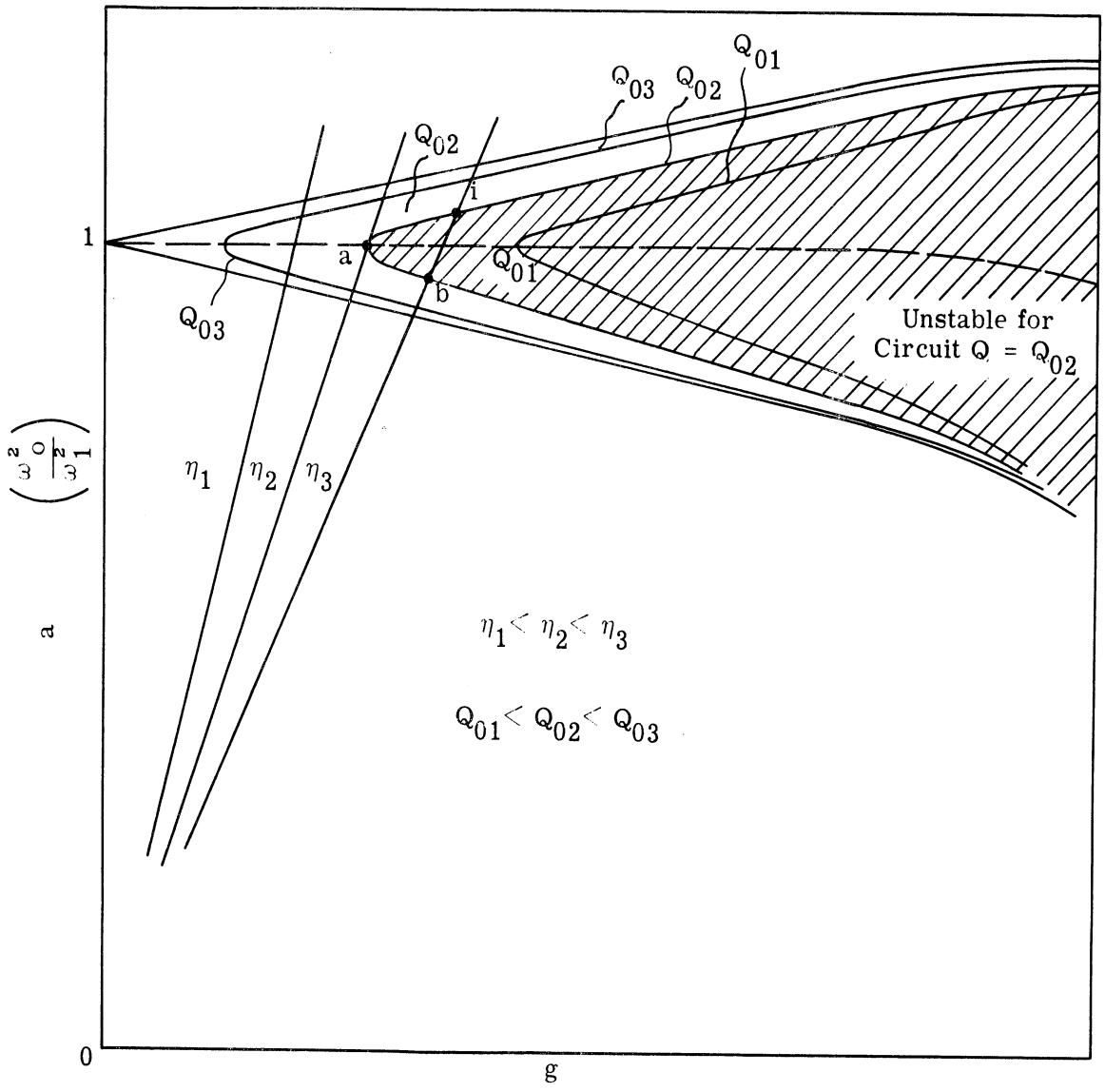


Fig. 3.3 Oscillation criteria for a SHO circuit with losses.

of this straight line with the particular $Q_0$ curve describing the passive circuit. If no intersection occurs, the circuit is stable. If the constant-$\eta$ line is tangent to the $Q_0$ curve, oscillation at just one frequency is possible. For two intersections oscillation over a band of frequencies is possible. Using the $Q_{02}$ of Fig. 3. 3 as a case in point and noting the increasing $\eta$ lines in the sequence $\eta_1$, $\eta_2$, $\eta_3$ the geometry of the oscillation criterion becomes evident. In particular, we note asymmetry in the frequency excursion over which oscillation is possible for $\eta = \eta_3$ as shown by the unequal distance from a = 1 along the "a" axis.

## 3. 4 Simplifications under Various Operating Modes

Equation 3. 9 is the transient solution to the original differential Eq. 2. 16. It is instructive, particularly as to understanding the substance of a given expression, if some of the members or terms representing small departures from the central representation are stripped away. Let us note the significance of constraining the passive resonant frequency ($\omega_0$) to the half-pump frequency ($\omega_1$). Returning to Fig. 3. 2 we note that for a = 1, $\sigma \cong -45^0$ ($\frac{-\pi}{4}$) radians) and $\mu \cong \frac{g}{2} \cong \frac{\eta}{4}$

then

$$\mu_L = \frac{1}{2Q_0} \tag{3.12}$$

and Eq. 3. 9 becomes

$$V = A'\epsilon^{(\frac{\eta}{4} - \frac{1}{2Q_0})\omega_1 t} \sin(\omega_1 t + \frac{\theta''_1}{2}) + B''\epsilon^{-(\frac{\eta}{4} + \frac{1}{2Q_0})\omega_1 t} \cos(\omega_1 t + \frac{\theta''_1}{2})$$

$$V = A'\epsilon \tag{3.13}$$

where

$$\theta_1'' = \theta_1 + \tan^{-1} \frac{1}{Q_0} \text{ and } B'' = -B'$$

Note that $\theta_1''$ is essentially the pump phase angle and that for $Q_0 = 10$ the phase shift in Eq. 3.13 due to the losses is less than 3 degrees. Thus we see that the natural solution to the problem attacked is an exact subharmonic oscillation of order $\frac{1}{2}$, whose phase angle is determined by the pump phase, and where the pump level and losses are explicitly represented in terms of a simple oscillation criterion.

At this point it is worth examining Eq. 3.13 qualitatively to note that the phase relationship of the solution is appropriate to the phase of the pump signal and the energy relationships which are occuring. In order to deliver energy continuously from the pump source to the tank circuit work must be done on the system during a portion of the cycle, but not extracted by the pump at other times. Using the simple example of Adams (Ref. 15) we note that work will be done on the system if at the time a voltage occurs across the capacitor the capacitance is decreased. Energy will not be extracted from the capacitor if at the time no voltage occurs across the capacitor the capacitance is increased.

That such conditions prevail in the analytical forms above is shown simply by noting:

capacitance variation from Eq. 2.18

$$C = C_0[1 + \eta \sin 2(\omega_1 t + \frac{\theta_1}{2})] \qquad (3.14)$$

Voltage variation from Eq. 3.13 (growing exponential part)

$$V = A'\epsilon^{\mu_g \omega_1 t} \sin(\omega_1 t + \frac{\theta''_1}{2}) \qquad (3.15)$$

When the capacitor voltage is zero $[(\omega_1 t + \frac{\theta''_1}{2}) = \eta\pi)$ the capacitance is at $C_0$ but increasing. When the capacitor voltage is maximum $(\omega_1 t + \frac{\theta''_1}{2}) = (2\eta + 1)\frac{\pi}{2}]$ the capacitance is at $C_0$ but decreasing. These relationships are shown vividly by the photographs of experimental transients in Chapter VII, Figs. 7.10 and 7.11.

For the problem at hand, that of understanding the manner and limits of controlling the system, the growing exponential term is the most important, since, after a significant number of time constants of this term, the decaying term will be negligible. In conventional superregenerative devices the growing exponential term is used as a measure of the magnitude of A. Of particular interest in this study is the phase ambiguity of the growing output as represented by the two possible signs of A. The subharmonic oscillator phase is by its very nature bistable.

# CHAPTER IV

## THE STEADY-STATE SOLUTION

The steady-state solution is that part of the general solution of a differential equation which results from the non-homogeneous member in the original equation. In the particular circuit under consideration this member represents the driving or signal function. The signal is characterized in terms most suitable for the degenerate parametric device being studied, so that both signal and noise can be described by the same analytical form. For our problem of understanding the mechanism of the transfer of information from the signal to the growing oscillation, the initial conditions are the vital link between the passive circuit and active circuit. Prior to initiation of pumping the circuit will be assumed to be under the steady-state constraint of the signal (information and noise). After initiation of pumping this signal experiences amplification via the active circuit parameters. In both cases we will be using the instantaneous values of the steady-state solution in the time domain. The generation of these forms produces a gain function which has a value both below and above a threshold for oscillation and as given by Adams (Ref. 15) contains explicitly the information about that threshold.

### 4.1 Derivation of General Steady-State Form

4.1.1 Signal Characterization. The signal current, $i_s$, of Fig. 2.2b, is now characterized in a form which is convenient for the

quasi-degenerate parametric amplifier. The juxtaposition of frequencies under consideration is shown in Fig. 4. 1. Each signal current at a frequency in the vicinity of $\omega_1$ but below $\omega_1$ (named $\omega_\ell$, a lower side frequence), separated from $\omega_1$ by $\Delta\omega_\xi$ together with the time-varying capacitance generate a response at $(2\omega_1 - \omega_\ell)$. This becomes part of $\omega_u$, the upper side frequency. This frequency at $\omega_u$, together with the time-varying capacitance generate a response at $(2\omega_1 - \omega_u)$, which is back exactly at the original lower side frequency, $\omega_\ell$. In addition to this amplitude characteristic there is also a phase characteristic peculiar to the signal but not the noise. Accordingly we will represent the signal $i_s$ by this double side-frequency, each component carrying an explicit phase angle.

$$i_s = |I_\ell| \cos(\omega_\ell t + \theta_\ell) + |I_u| \cos(\omega_u t + \theta_u) \tag{4.1}$$

where

$$\left.\begin{aligned} \omega_\ell &\equiv \omega_1 - \Delta\omega_\xi \\ \omega_u &\equiv \omega_1 + \Delta\omega_\xi \end{aligned}\right\}$$

and side frequency phasors are:

$$\left.\begin{aligned} I_\ell &\equiv |I_\ell| \, \epsilon^{j\theta_\ell} \\ I_u &\equiv |I_u| \, \epsilon^{j\theta_u} \end{aligned}\right\} \tag{4.2}$$

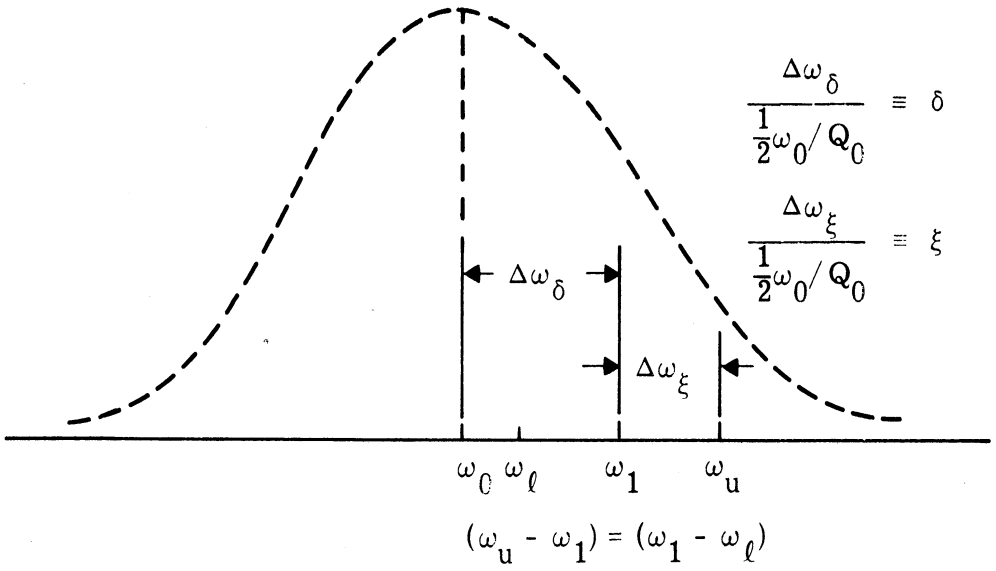


Fig. 4.1 Side-Frequency Locations.

4.1.2 Phasor Description. We now describe the currents at the lower and upper side frequencies associated with a time varying capacitance. For a general monochromatic sine pump of the form:

$$C = C_o[1 + \eta \sin(2\omega_1 t + \theta_1)] \tag{4.3}$$

the expression for the currents is shown in Appendix III to be

$$\begin{bmatrix} I_\ell \\ I_u^* \end{bmatrix}_C = \begin{bmatrix} j\,\omega_\ell\, C_o & \omega_\ell \frac{\eta}{2} C_o \epsilon^{j\theta_1} \\ \omega_u \frac{\eta}{2} C_o \epsilon^{-j\theta_1} & -j\,\omega_u\, C_o \end{bmatrix} \begin{bmatrix} V_\ell \\ V_u^* \end{bmatrix}_C \tag{4.4}$$

(C subscripts identifying values related to the capacitance.)

When the reactive element of Eq. (4.4) is placed in the circuit of Fig. 2.2b with the driving function of Eq. (4.1) the equilibrium is expressed by:

$$\begin{bmatrix} I_\ell \\ I_u^* \end{bmatrix} = \begin{bmatrix} G + \frac{\Gamma}{j\omega_\ell} + j\omega_\ell\, C_o & \omega_\ell \frac{\eta}{2} C_o \epsilon^{j\theta_1} \\ \omega_u \frac{\eta}{2} C_o \epsilon^{-j\theta_1} & G + \frac{\Gamma}{-j\omega_u} - j\omega_u\, C_o \end{bmatrix} \begin{bmatrix} V_\ell \\ V_u^* \end{bmatrix} \tag{4.5}$$

The source current phasors are represented explicitly in the left-hand member. Equation 4.5 carries all the information about the steady-

state, and when the conversion matrix is inverted the side frequency voltages are given explicitly. Some effort will now be expended to expressing Eq. (4.5) in terms which will be significantly more descriptive of the circuit and much more useful in the development which follows.

4.1.3 Conversion Matrix. In general, the resonant frequency of the circuit, $\omega_0$, departs from the half-pump frequency, $\omega_1$. This variation can be specified, as in Fig. 4.1, as a fractional part, $\delta$, of the half-bandwidth. In addition, symmetrically disposed about the half-pump frequency the side-frequencies appear. Their displacement is described similarly by the fraction, $\xi$, of the half-bandwidth. If these components are to have significant amplitudes, their frequency displacements must be restricted to the region $-1 \leqq (\delta + \xi) \leqq +1$.

From Fig. 4.1 we write

$$\begin{aligned} \omega_\ell &= \omega_0 + \Delta\omega_\delta - \Delta\omega_\xi \cong \omega_0 \left(1 + \frac{\delta - \xi}{2Q_0}\right) \\ \omega_u &= \omega_0 + \Delta\omega_\delta + \Delta\omega_\xi \cong \omega_0 \left(1 + \frac{\delta + \xi}{2Q_0}\right) \end{aligned} \tag{4.6}$$

Where $Q_0$ is the quality factor of the passive circuit and is defined:

$$Q_0 \equiv \frac{\omega_0 C}{G} = \frac{\Gamma}{\omega_0 G} \tag{4.7a}$$

and $\omega_0$ is the resonant angular frequency:

$$\omega_0^2 \equiv \frac{\Gamma}{C} \tag{4.7b}$$

In order to simplify the notation let us introduce a complex pumping parameter, $\Pi$, where:

$$\Pi \equiv \frac{\eta Q_0}{2} \epsilon^{j\theta_1} \tag{4.7c}$$

Now, if the conductance, G, is factored out of all the elements of the conversion matrix, the elements of resultant matrix are dimensionless.

$$\begin{bmatrix} I_\ell \\ \\ I_u^* \end{bmatrix} = G \begin{bmatrix} 1 + j(\delta - \xi) & \Pi \\ \\ \Pi^* & 1 - j(\delta + \xi) \end{bmatrix} \begin{bmatrix} V_\ell \\ \\ V_u^* \end{bmatrix} \tag{4.8}$$

We would like to develop a "gain" expression. In order to do this the side frequency voltages appearing in the absence of pumping are needed.

Define

$$V_{\ell N} \equiv \frac{I_\ell}{G[1 + j(\delta - \xi)]}$$

$$V_{uN} \equiv \frac{I_u}{G[1 + j(\delta + \xi)]} \tag{4.9}$$

where the "N" in each case signifies that this is the normalized circuit voltage that is observed in the absence of pumping.

$$\begin{bmatrix} V_{\ell N} \\ V_{uN}^{*} \end{bmatrix} = \begin{bmatrix} 1 & \dfrac{\Pi}{1 + j(\delta - \xi)} \\ \dfrac{\Pi^{*}}{1 - j(\delta + \xi)} & 1 \end{bmatrix} \begin{bmatrix} V_{\ell} \\ V_{u}^{*} \end{bmatrix} \tag{4.10}$$

Inverting (4.10) now gives the desired expression for the voltages produced at the side frequencies, the gain appearing explicitly as the reciprocal of the determinant of the conversion matrix.

$$\begin{bmatrix} V_{\ell} \\ V_{u}^{*} \end{bmatrix} = g_{\xi} \begin{bmatrix} 1 & \dfrac{-\Pi}{1 + j(\delta - \xi)} \\ \dfrac{-\Pi^{*}}{1 - j(\delta + \xi)} & 1 \end{bmatrix} \begin{bmatrix} V_{\ell N} \\ V_{uN}^{*} \end{bmatrix} \tag{4.11}$$

where

$$g_{\xi} \equiv \frac{1}{1 - \left( \dfrac{\Pi \Pi^{*}}{1 + (\delta^{2} - \xi^{2}) - j2\xi} \right)} \tag{4.12}$$

When $\xi$ is zero, the degenerate condition is defined, and $g_{\xi}$ has a maximum value, $g_{m}$, thus:

$$g_{m} \equiv \frac{1}{1 - \dfrac{|\Pi|^{2}}{1 + \delta^{2}}} \tag{4.12a}$$

Equations 4. 11 can be thought of as consisting of three separate factors; gain, passive circuit voltage, and phase response. Each will be examined in the paragraphs which follow, according to the description by magnitude and phase angle.

4. 1. 4 Gain. $g_\xi$ is examined in detail in Appendix IV. It is given the gain significance in that it is a factor representing amplification when $\Pi$, the pumping parameter is not zero. When $\Pi$ is zero (no pumping) $g_\xi$ is unity and the passive circuit voltages result. Equations 4. 11 and 4. 12 show $g_\xi$ is the only factor which can produce gain, and that for oscillation to exist $g_\xi$ must be able to go to infinity. From Eq. (4. 12) we see that two conditions must be satisfied for g to increase without limit. They are:

$$\begin{aligned} \xi &= 0 \\ |\Pi|^2 &= 1 + \delta^2 \end{aligned} \qquad (4.13)$$

In the problem under study the steady-state term is not used when the band center gain is infinite, but at pumping levels above this point. When the gain is defined as in (4. 12) and the second condition of (4. 13) is exceeded $\left(\frac{|\Pi|^2}{1+\delta^2} > 1\right)$, the gain as such has less meaning (i. e., relating to a growing oscillation) but is still an essential part to the general solution of the original differential equation. The magnitude of $g_m$ decreases with increasing pump level ($\eta$) and the sign is everywhere negative. (cf. Fig. 4. 2). We note that for values of $\Pi/\sqrt{1+\delta^2}$ in the vicinity of 1

the effective band is narrowed as the gain increases and (4. 12) can be expressed simply

$$g_\xi \cong g_m \frac{1}{1 - j\zeta'} = g_m \frac{1}{\sqrt{1+(\zeta')^2}} \epsilon^{j \tan^{-1}\zeta'} \qquad (4.14)$$

where

$$\zeta \equiv 2g_m \xi$$

and

$$\zeta' \equiv \frac{\zeta}{1 + \delta^2}$$

Further define

$$|\Pi'| \equiv \frac{|\Pi|}{\sqrt{1+\delta^2}} \text{ then } g_m = \frac{1}{1 - |\Pi'|^2}$$

--the primed notation ($\zeta'$, $\Pi'$) introduced to allow implicit expression of the detuning, $\delta$.

4. 1. 5 Passive Circuit Voltages. The right-hand column matrix of (4. 11) carries the information about the passive circuit, the elements being defined in (4. 9). When $V_{\ell N}$ and $V_{uN}$ are expressed as magnitudes and angles they become

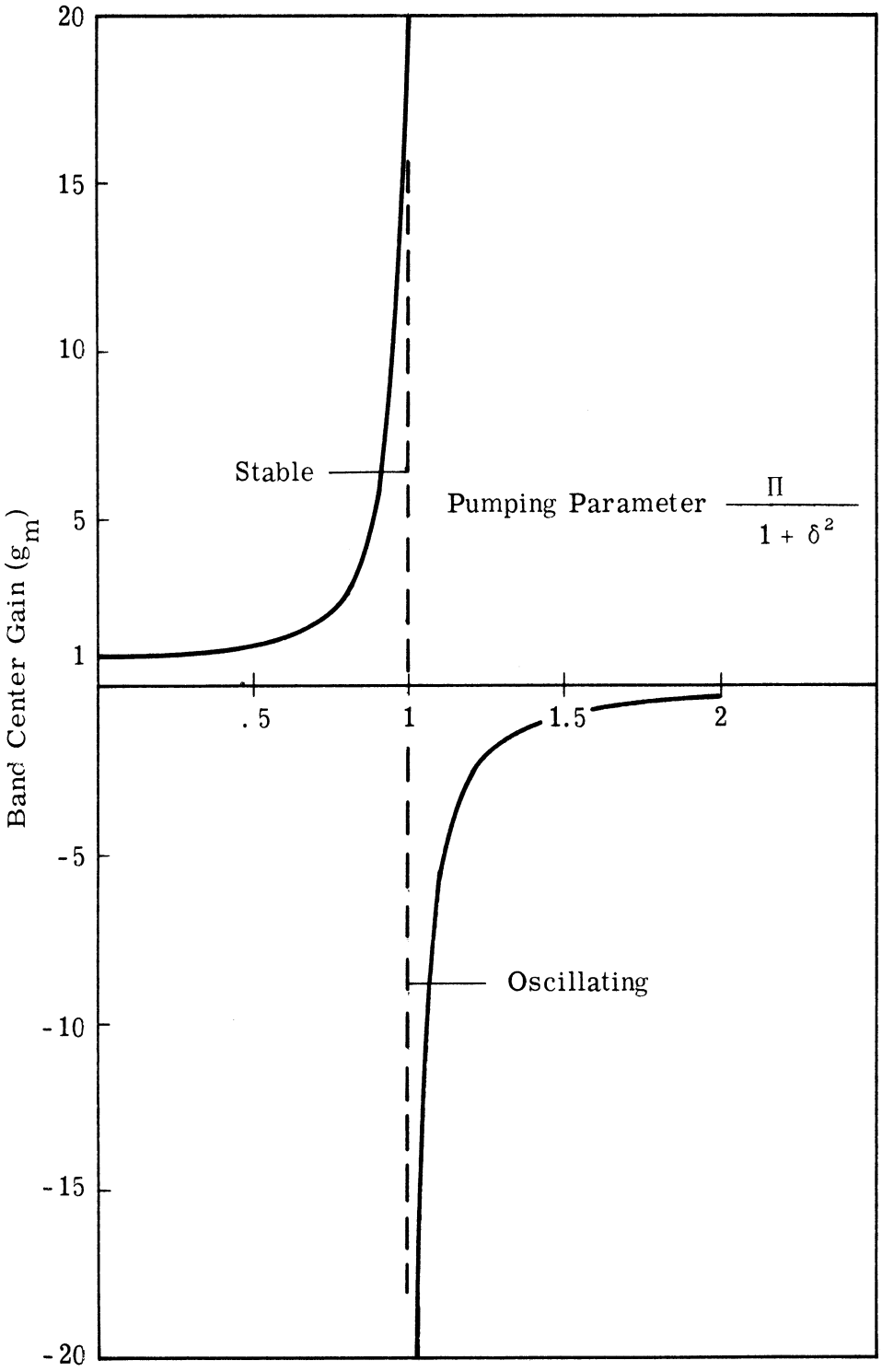


Fig. 4. 2 Band center gain vs. pumping parameter.

$$V_{\ell N} = \frac{I_\ell}{G\sqrt{1+(\delta-\xi)^2}\,\epsilon^{j\tan^{-1}(\delta-\xi)}} = \frac{|I_\ell|\,\epsilon^{j[\theta_\ell - \tan^{-1}(\delta-\xi)]}}{G\sqrt{1+(\delta-\xi)^2}}$$

$$V_{uN} = \frac{I_u}{G\sqrt{1+(\delta+\xi)^2}\,\epsilon^{j\tan^{-1}(\delta+\xi)}} = \frac{|I_u|\,\epsilon^{j[\theta_u - \tan^{-1}(\delta+\xi)]}}{G\sqrt{1+(\delta+\xi)^2}} \qquad (4.15)$$

We will be discussing an active band where the values of $\xi << 1$, and the expressions (4. 15) may be approximated:

$$V_{\ell N} \cong \frac{|I_\ell|\,\epsilon^{j[\theta_\ell - \tan^{-1}\delta]}}{G\sqrt{1+\delta^2}}$$

$$V_{uN} \cong \frac{|I_u|\,\epsilon^{j[\theta_u - \tan^{-1}\delta]}}{G\sqrt{1+\delta^2}} \qquad (4.16)$$

The forms (4. 16) are the usual ones for passive resonant circuits showing the explicit effect of the detuning. Note particularly that because of the assumption of small $\xi$ the phase angle sign is the same for both side frequencies.

4. 1. 6 Signal Phase Relations. The off-diagonal terms of Eq. (4. 11) carry explicit phase information. If the passive circuit voltages are factored out the equations become:

$$V_{\ell} = g_{\xi} V_{\ell N} g_{\phi\ell}$$
$$V_u^* = g_{\xi} V_{uN}^* g_{\phi u}^* \qquad (4.17)$$

where $g_{\phi\ell}$ and $g_{\phi u}$ are the factors associated with the lower and upper side frequency voltages respectively and which predominantly show the effect of the signal phase position.

$$g_{\phi\ell} = \left[1 - \left(\frac{\Pi}{1 + j(\delta-\xi)}\right) \frac{V_{uN}^*}{V_{\ell N}}\right]$$
$$g_{\phi u}^* = \left[1 - \left(\frac{\Pi^*}{1 - j(\delta+\xi)}\right) \frac{V_{\ell N}}{V_{uN}^*}\right] \qquad (4.18)$$

Consider the case when the excitation currents $|I_{\ell}|$ and $|I_u|$ Eq. (4.14) are equal and make up a double side frequency signal. For this case Eq. (4.18) becomes:

$$g_{\phi\ell} = 1 - \frac{|\Pi| \epsilon^{j[\theta_1 - \theta_{\ell} - \theta_u + \tan^{-1}(\delta+\xi)]}}{\sqrt{1+(\delta+\xi)^2}}$$
$$g_{\phi u}^* = 1 - \frac{|\Pi| \epsilon^{-j[\theta_1 - \theta_u - \theta_{\ell} + \tan^{-1}(\delta-\xi)]}}{\sqrt{1+(\delta+\xi)^2}} \qquad (4.19)$$

Within the active band at nominal gain levels ($g_m \geqq 10$) the value of $\xi << 1$. Under this condition we can write a single expression for the two equations of (4.18):

$$g_{\phi\ell} = g_{\phi u} = g_\phi = 1 - \frac{|\Pi|}{\sqrt{1+\delta^2}} \epsilon^{j\theta_2} = 1 - |\Pi'| \epsilon^{j\theta_2} \qquad (4.20)$$

where

$$\theta_2 = (\theta_1 - \theta_u - \theta_\ell + \tan^{-1} \delta)$$

Equation 4.20 is visualized as the sum of two phasors of nearly equal magnitude. The maximum magnitude occurs when $\epsilon^{j\theta_2} = -1$, i.e., $\theta_2 = \pm\pi$ radians. The minimum occurs when $\epsilon^{j\theta_2} = +1$, i.e., $\theta_2 = 0$ radians. The ratio of the maximum to the minimum is

$$\frac{g_{\phi max}}{g_{\phi min}} = \frac{1 + |\Pi'|}{1 - |\Pi'|} \cong 4\, g_m \qquad (4.21)$$

Thus we see that the $g_\phi$ term has a profound influence on the steady state circuit voltage under the particular type of signal discussed above (i.e., $|I_\ell| = |I_u|$).

4.1.7 General Side Frequency Signals. When the side frequency signal currents are not equal in amplitude the simple visualization of Eq. 4.20 is no longer possible. Under noise excitation the independence of the side frequency "signal" currents must be preserved in order that random amplitudes and phases can be ascribed explicitly. The development

which follows contains all the information of paragraph 4. 1. 6 but loses the conceptual picture of the discrete frequency excitation.

Expanding Eq. (4. 11) using (4. 14), and (4. 16)

$$V_\ell = \frac{g_m}{G\sqrt{(1+\delta^2)(1+\zeta'^2)}} \left[ |I_\ell| \epsilon^{j(\theta_\ell - \tan^{-1}\delta - \tan^{-1}\zeta')} - |\Pi'|\,|I_u|\,\epsilon^{j(\theta_1 - \theta_u - \tan^{-1}\zeta')} \right]$$

$$V_u = \frac{g_m}{G\sqrt{(1+\delta^2)(1+\zeta'^2)}} \left[ -|\Pi|\,|I_\ell|\,\epsilon^{j(\theta_1 - \theta_\ell + \tan^{-1}\zeta')} + |I_u|\,\epsilon^{j(\theta_u - \tan^{-1}\delta + \tan^{-1}\zeta')} \right] \qquad (4.22)$$

## 4. 2 Reduction to Instantaneous Values

The instantaneous values of the upper and lower side frequencies are derived directly from Eq. (4. 22) and since both represent voltages within the passband the net circuit voltage is the sum of the lower and upper side frequency components.

$$v_{ss}(t) = v_\ell(t) + v_u(t)$$

where

$$v_\ell(t) = \mathrm{Re}\left(V_\ell\, \epsilon^{j\omega_\ell t}\right)$$
$$v_u(t) = \mathrm{Re}\left(V_u\, \epsilon^{j\omega_u t}\right) \qquad (4.23)$$

from which

$$v_{ss}(t) = \frac{g_m}{G\sqrt{(1+\delta^2)(1+\zeta')}}\Big[|I_\ell|\Big\{\cos(\omega_\ell t + \theta_\ell - \tan^{-1}\delta - \tan^{-1}\zeta') - |\Pi'|\cos(\omega_u t + \theta_1 - \theta_\ell + \tan^{-1}\zeta')\Big\} + |I_u|\Big\{-|\Pi'|\cos(\omega_\ell t + \theta_1 - \theta_u - \tan^{-1}\zeta') + \cos(\omega_u t + \theta_u - \tan^{-1}\delta + \tan^{-1}\zeta')\Big\}\Big] \qquad (4.24)$$

Equation 4.24 describes the instantaneous steady state circuit voltage in terms of circuit values, signal constraints, and circuit adjustments. It applies to all pumping levels ($\Pi'$) including zero. Where the point-by-point time domain value of the solution to the original differential equation is needed in the vicinity of $t=0$ this is the equation which must be handled.

In looking at this steady state term in view of the solution to the transient problem and recognizing that after a few cycles the only term of significance in the general solution will be the growing exponential we note that the significance of Eq. (4.24) is identifying the value of

$v_{ss}(t)$ at $t = 0_+$ so that the arbitrary constants of the differential equation solution can be evaluated. This will be done in paragraph 5.4 of the next chapter.

## 4.3 Solution Under Special Cases

When the side frequencies approach $\omega_1$ exactly, the degenerate amplifier results. Under this condition the separate signals coincide in magnitude and phase. Thus in Eq. (4.24) we set:

$$\zeta' = 0$$

$$\theta_\ell = \theta_u = \theta_s \tag{4.25}$$

$$|I_\ell| = |I_u| = \frac{|I_s|}{2}$$

where $\theta_s$ and $I_s$ are the phase angle and phasor associated with the degenerate signal.

Equation 4.24 becomes

$$v_{ss}(t) = \frac{g_m}{G\sqrt{1+\delta^2}} |I_s| \left[\cos(\omega_1 t + \theta_s - \tan^{-1}\delta) - |\Pi'| \cos(\omega_1 t + \theta_1 - \theta_s)\right] \tag{4.26}$$

In order to visualize just what Eq. (4.26) means, we may make another simplification by letting $\theta_1$ (pump phase angle) be zero and the detuning, $\delta$, be zero. For moderate gains ($\Pi \geq 5$) the steady-state voltage

becomes approximately:

$$v_{ss}(t) = \frac{-g_m}{G} |I_s| \sin \omega_1 t \sin \theta_s \qquad (4.27)$$

Equation (4.27) is a maximum when $\theta_s$ is $\frac{\pi}{2}$ or $\frac{3\pi}{2}$. Recalling that the signal currents are given by Eq. 4.1 we see that the instantaneous signal current which will produce the maximum steady-state response is

$$i_s = -|I_s| \sin \omega_1 t \qquad (4.28)$$

-- simply a signal current in phase, and of the same sign as the preferred steady-state response.

## 4.4 Introduction of Pump Unbalance

One of the direct results of the experimental phase of this study is the realization that voltages at the pump frequency do appear across the resonant circuit and these unbalance voltages very significantly affect the minimum signal response of the system. Although the pump frequency voltage does not experience amplification it can have a magnitude which completely dominates the observed voltages. Effectively the pump unbalance presents a coherent interference which the information carrying signal must exceed in order to achieve efficient phase determination.

This aspect of the problem arises because of imperfections in the balance of the circuit used to accomplish pumping. From Fig. 4.3 which is a typical balanced circuit, the pump frequency voltage appearing across the circuit is simply

$$V_{2\omega_1} = \frac{C_1E_1 - C_2E_2}{C_1 + C_2 - \frac{1}{4\omega_1^2 L}} \tag{4.29}$$

where $E_1$ and $E_2$ are the phasor pump voltages associated with $e_1$ and $e_2$. Resistance terms in an actual circuit do not change the values much since the reactive terms dominate. From Eq. (4.29) an unbalance of the capacitances or pump voltages $e_1$ and $e_2$ in magnitude or phase, causes a voltage of pump frequency to appear across the circuit. Resistance unbalance in the actual circuit would introduce second order unbalance in amplitude and phase. Since $e_1$ and $e_2$ can be generated by bifilar secondary windings on a toroidal transformer, the degree of symmetry in the pump voltage source can be very high. The rest of the circuit is made mechanically and electrically symmetrical to insure a high degree of pump rejection. Matching the capacitances is much more difficult, and herein lies the principle source of unbalance. If we assume that the capacitances are connected to produce positive circuit capacitance variations for positive pump voltages, and

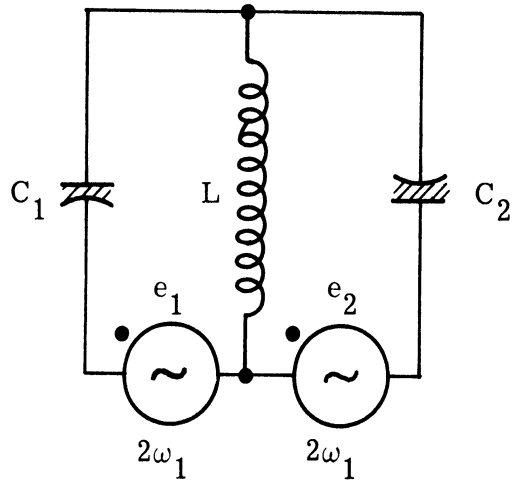


Fig. 4. 3 Balanced Pump Circuit.

$$e_1 = e_2 = |E_p| \sin(2\omega_1 t + \theta_1) \ , \tag{4.30}$$

the instantaneous value of pump unbalance voltage can be written

$$v_{2\omega_1} = c\,|E_p| \sin(2\omega_1 t + \theta_1) \tag{4.31}$$

Where we define the relative capacitance unbalance as

$$c \equiv \frac{C_1 - C_2}{\left(C_1 + C_2 - \dfrac{1}{4\omega_1^2 L}\right)} \tag{4.32}$$

since $\omega_1^2 L(C_1+C_2) = 1$, by the resonance condition (Ew. 4.7), the relative capacitance imbalance is:

$$c = \frac{4}{3}\,\frac{(C_1 - C_2)}{(C_1 + C_2)} \tag{4.33}$$

# CHAPTER V

## GENERAL SOLUTION

The general solution is derived. The dependence of the values of the constants on the initial conditions is shown. From these values the solution for the degenerate signal at exactly $\omega_1$ radians per second is presented. Finally the solution under the noise-forcing function is derived.

### 5.1 Form of Solution for Constants

The general solution for the circuit voltage is the sum of the steady-state and transient solutions. Thus, from Eq. (3.9):

$$v(t) = v_{ss}(t) + A\,\epsilon^{\mu_g \omega_1 t}\left(\sin\ \omega_1 t + \frac{\theta_1'}{2} - \sigma\right) + B\,\epsilon^{-\mu_d \omega_1 t}\left(\sin\ \omega_1 t + \frac{\theta_1'}{2} - \sigma\right) \qquad (5.1)$$

where $\mu_g = (\mu - \mu_L)$ $\mu_d = (\mu + \mu_L)$

The constants A and B are the only quantities yet undetermined in the solution. Two independent conditions are required in order to determine these coefficients. The ones available are the initial value and initial derivative of the circuit voltage. These quantities are determined by independent energy considerations at the time of the initiation of pumping.

Thus, when $t = 0_+$ (just after pumping begins) from Eq. 5.1

$$v(0)_+ = v_{ss}(0)_+ + A \sin\left(\frac{\theta_1'}{2} - \sigma\right) + B \sin\left(\frac{\theta_1'}{2} + \sigma\right)$$

$$\dot{v}(0)_+ = \dot{v}_{ss}(0)_+ + A\,\omega_1\left[\cos\left(\frac{\theta_1'}{2} - \sigma\right) + \mu_g \sin\left(\frac{\theta_1'}{2} - \sigma\right)\right]$$

$$+ B\,\omega_1\left[\cos\left(\frac{\theta_1'}{2} + \sigma\right) - \mu_d \sin\left(\frac{\theta_1'}{2} + \sigma\right)\right] \qquad (5.2)$$

The steady-state terms become a part of the constant terms in a pair of simultaneous equations in A and B.

Thus, when the coefficients of A and B are labeled a, b, d, and e (5.2) becomes

$$\left(v(0)_+ - v_{ss}(0)_+\right) = a\,A + b\,B$$

$$\left(\dot{v}(0)_+ - \dot{v}_{ss}(0)_+\right) = d\,A + e\,B \qquad (5.3)$$

The solutions for A and B follow from Cramer's rule directly.

$$A = \frac{\begin{vmatrix} \left(v(0)_+ - v_{ss}(0)_+\right) & b \\ \left(\dot{v}(0)_+ - \dot{v}_{ss}(0)_+\right) & e \end{vmatrix}}{\begin{vmatrix} a & b \\ d & e \end{vmatrix}} \qquad B = \frac{\begin{vmatrix} a & \left(v(0)_+ - v_{ss}(0)_+\right) \\ d & \left(\dot{v}(0)_+ - \dot{v}_{ss}(0)_+\right) \end{vmatrix}}{\begin{vmatrix} a & b \\ d & e \end{vmatrix}} \qquad (5.4)$$

$$a = \sin\left(\frac{\theta_1'}{2} - \sigma\right) \qquad b = \sin\left(\frac{\theta_1'}{2} + \sigma\right)$$

$$d = \omega_1\left[\cos\left(\frac{\theta_1'}{2} - \sigma\right) + \mu_g \sin\left(\frac{\theta_1'}{2} - \sigma\right)\right]$$

$$e = \omega_1\left[\cos\left(\frac{\theta_1'}{2} + \sigma\right) - \mu_d \sin\left(\frac{\theta_1'}{2} + \sigma\right)\right] \tag{5.5}$$

## 5.2 Denominator - The Determinant of the Matrix

The determinant, $\begin{vmatrix} a & b \\ d & e \end{vmatrix}$, reduces to:

$$\begin{vmatrix} a & b \\ d & e \end{vmatrix} = \omega_1\left[\sin(-2\sigma) - \mu\left\{\cos 2\sigma + \sin\left(\theta_1 + \tan^{-1}\frac{1}{Q_0}\right)\right\}\right] \tag{5.6}$$

When the detuning, $\delta$, is zero the phase angle, $\sigma$, very closely approaches $\frac{-\pi}{4}$. c.f. Fig. 3.2 for a = 1, then (5.6) reduces to

$$\begin{vmatrix} a & b \\ d & e \end{vmatrix} = \omega_1\left[1 + \mu \sin\left(\theta_1 + \tan^{-1}\frac{1}{Q_0}\right)\right] \tag{5.7}$$

Noting that $\mu << 1$, the denominator for the tuned case is very nearly $\omega_1$.

## 5.3 Initial Conditions

Time is marked from the beginning of pumping. That is, for $t < 0$ the circuit elastance (Fig. 2.2b) is $S_0$, and capacitance $\frac{1}{S_0} = C_0$. At $t = 0$ the elastance value switches to the functional form

$$S = S_0 [1 - \eta \sin (2\omega_1 t + \theta_1)] \cong \frac{1}{C_0 [1 + \eta \sin (2\omega_1 t + \theta)]} \tag{5.8}$$

Since all parameter values discussed in this paragraph are evaluated arbitrarily close to $t = 0$ we use the notation

$$\begin{aligned} C(0)_+ &= c_+ \quad \text{and} \quad C(0)_- = c_- \\ V(0)_+ &= v_+ \quad \text{and} \quad V(0)_- = v_- \end{aligned} \tag{5.9}$$

Thus

$$c_- = C_0 \qquad c_+ = C_0(1 + \eta \sin \theta_1)$$

In general, the capacitance experiences a discontinuity, and a resulting voltage discontinuity. The charge associated with C cannot change abruptly, so therefore:

$$c_- v_- = c_+ v_+ \quad \text{and} \quad v_+ = v_- \frac{c_-}{c_+} \tag{5.10}$$

or

$$v_+ \cong v_-(1 - \eta \sin \theta_1) \tag{5.11}$$

$v_-$ is evaluated from the steady-state solution before $t = 0$, that is, for no pumping. Since $\eta << 1$ we note that the discontinuity in the circuit voltage, v, is small and that whenever $\theta_1 = n\pi$ there is no

discontinuity. Equation (5. 11) is one of the values required to solve Eq. (5. 4).

Recalling that we are concerned with the parallel circuit of 2. 2b, the initial derivative is obtained from consideration of instantaneous currents at the instant pumping begins. (t = 0) The current in the inductance must be continuous for a constant inductance. If we require the signal current to be continuous at t = 0, then a current discontinuity in C is matched by a current discontinuity in G. Thus

$$G(v_+ - v_-) = \frac{d(v_+ c_+)}{dt} - \frac{d(v_- c_-)}{dt} \tag{5. 12}$$

Solving Eq. (5. 12) for $\dot{v}_+$

$$\dot{v}_+ = \frac{G}{c_+}(v_+ - v_-) + \frac{1}{c_+}(v_- \dot{c}_- + c_- \dot{v}_-) - v_+ \frac{\dot{c}_+}{c_+} \tag{5. 13}$$

which after some manipulation using Eqs. (5. 9) and (5. 11) becomes

$$\dot{v}_+ = (1-\eta \sin\theta_1)\left[-v_-\left\{\frac{G}{C_0}\,\eta \sin\theta_1 + (1-\eta \sin\theta_1)(2\omega_1 \eta \cos\theta_1)\right\} + \dot{v}_-\right] \tag{5. 14}$$

and since $\eta \ll 1$ we note

$$v_+ \cong -v_-\left(\frac{G}{C_0}\,\eta \sin\theta_1 + 2\omega_1 \eta \cos\theta_1\right) + v_- \tag{5. 15}$$

This is the second value required to solve Eq. (5. 4).

## 5.4 General Expression for A

5.4.1 $(v_+ - v_{ss+})$. The terms $(v_+ - v_{ss+})$ and $(v_+ - v_{ss+})$ of Eq. (5.4) are now evaluated. We proceed directly from Eq. (4.24), the steady-state solution and include the pump unbalance term of Eq. (4.31). In order to simplify the expression and keep all the information about the various phase shifts intact, Eq. (4.24) is evaluated using the new angular parameters:

$$\begin{aligned} \alpha &\equiv \theta_\ell - \tan^{-1}\delta - \tan^{-1}\zeta' \\ \beta &\equiv \theta_1 - \theta_\ell + \tan^{-1}\zeta' \\ \gamma &\equiv \theta_u - \tan^{-1}\delta + \tan^{-1}\zeta' \\ \phi &\equiv \theta_1 - \theta_u - \tan^{-1}\zeta' \end{aligned} \tag{5.16}$$

$$\begin{aligned} v_{ss}(t) = \frac{g_m}{G\sqrt{(1+\delta^2)(1+\zeta^2)}} & \Big[ |I_\ell| \left\{ \cos(\omega_\ell t + \alpha) - |\Pi'| \cos(\omega_u t + \beta) \right\} \\ & + |I_u| \left\{ \cos(\omega_u t + \gamma) - |\Pi'| \cos(\omega_\ell t + \phi) \right\} \Big] \\ & + c\,|E_p| \sin(2\omega_1 t + \theta_1) \end{aligned} \tag{5.17}$$

hen $t = 0_+$

$$v_{ss+} = \frac{g_m}{G\sqrt{(1+\delta^2)(1+\zeta'^2)}} \left[ |I_\ell| (\cos\alpha - |\Pi'| \cos\beta) + |I_u| (\cos\gamma - |\Pi'| \cos\phi) \right] + c\,|E_p| \sin\theta_1 \qquad (5.18)$$

The derivative of the steady state is written from (5.17) and evaluated at $t = 0$. Noting that $\frac{\omega_u}{\omega_1}$ and $\frac{\omega_\ell}{\omega_1} \approx 1$.

$$\dot{v}_{ss+} = \frac{-g_m \omega_1}{G\sqrt{(1+\delta^2)(1+\zeta'^2)}} \left[ |I_\ell| (\sin\alpha - |\Pi'| \sin\beta) + |I_u| (\sin\gamma - |\Pi'| \sin\phi) \right] + 2\omega_1 c\,|E_p| \cos\theta_1 \qquad (5.19)$$

Using Eq. 5.11 for $v_+$ and evaluating $v_-$ from Eq. 5.17 by noting that it applies before $t = 0$ if we note that $g_m = 1$, $|\Pi'| = 0$, and $|E_p| = 0$

$$v_+ = \frac{\left(1 - \eta \sin\theta_1\right)}{G\sqrt{(1+\delta^2)(1+\zeta'^2)}} \left[ |I_\ell| \cos\alpha + |I_u| \cos\gamma \right] \qquad (5.20)$$

Now using Eqs. 5.20 and 5.18 $(v_+ - v_{ss+})$ is written. Note that $v_+$ is not multiplied by a "gain" factor and that the effect of the discontinuity at $t = 0$ (manifested by the $\eta \sin\theta_1$ term) is of second order since we have assumed small changes in C due to pumping.

$$(v_+ - v_{ss+}) = \frac{1}{G\sqrt{(1+\delta^2)(1+\zeta'^2)}} \left[ |I_\ell| \left\{ \cos\alpha - g_m(\cos\alpha - |\Pi'| \cos\beta) \right\} \right.$$

$$\left. + |I_u| \left\{ \cos\gamma - g_m(\cos\gamma - |\Pi'| \cos\phi) \right\} \right] - c\,|E_p| \sin\theta_1 \quad (5.21)$$

In Eq. 5.21 the effect of the initial conditions ($v_+$) and the steady-state expression can be consolidated by noting that:

$$(1 - g_m) = -|\Pi'|^2 g_m \quad (5.22)$$

$$(v_+ - v_{ss+}) = \frac{|\Pi'|\, g_m}{G\sqrt{(1+\delta^2)(1+\zeta'^2)}} \left[ |I_\ell| (-|\Pi'| \cos\alpha + \cos\beta) \right.$$

$$\left. + |I_u| (-|\Pi'| \cos\gamma + \cos\phi) \right] - c\,|E_p| \sin\theta_1 \quad (5.23)$$

5.4.2 $(\dot{v}_+ - \dot{v}_{ss+})$. $\dot{v}_+$, the voltage derivative just after pumping starts, is obtained from Eq. 5.15. Note that $\frac{G}{C_0}$ is very nearly equal to $\frac{\omega_1}{Q_0}$.

$$\dot{v}_+ = \dot{v}_- - 2\omega_1 \eta\, v_- \left( \frac{1}{2Q_0} \sin\theta_1 + \cos\theta_1 \right) \quad (5.24)$$

$\dot{v}_-$ and $v_-$ are evaluated from the steady-state solution just before $t = 0$. Since $\frac{1}{2Q_0} << 1$ the last factor of Eq. 5.24 is very nearly $\cos\theta_1$ and Eq. 5.24 becomes:

$$\dot{v}_+ = \frac{-\omega_1}{G\sqrt{(1+\delta^2)(1+\zeta'^2)}} \left[ |I_\ell| \, (\sin\alpha + 2\eta \cos\theta_1 \cos\alpha) \right.$$

$$\left. + \, |I_u| \, (\sin\gamma + 2\eta \cos\theta_1 \cos\gamma) \right] \qquad (5.25)$$

Equations 5.25 and 5.19 are now combined to give:

$$(\dot{v}_+ - \dot{v}_{ss+}) = \frac{-\omega_1}{G\sqrt{(1+\delta^2)(1+\zeta'^2)}} \left[ |I_\ell| \, \{(\sin\alpha + 2\eta \cos\theta_1 \cos\alpha) \right.$$

$$- \, g_m \, (\sin\alpha - |\Pi'| \sin\beta)\}$$

$$+ \, |I_u| \, \{(\sin\gamma + 2\eta \cos\theta_1 \cos\gamma)$$

$$\left. - \, g_m \, (\sin\gamma - |\Pi'| \sin\phi)\} \right]$$

$$- \, 2\omega_1 \, c \, |E_p| \cos\theta_1 \, . \qquad (5.26)$$

If the terms representing the effect of the initial conditions are consolidated again with those of the steady-state by using Eq. 5.22, Equation 5.26 becomes:

$$(\dot{v}_+ - \dot{v}_{ss+}) = \frac{-\omega_1 |\Pi'| \, g_m}{G\sqrt{(1+\delta^2)(1+\zeta'^2)}} \left[ |I_\ell| \left( -|\Pi'| \sin\alpha + \sin\beta + \frac{2\eta}{g_m |\Pi'|} \cos\theta_1 \cos\alpha \right) \right.$$

$$\left. + \, |I_u| \left( -|\Pi'| \sin\gamma + \sin\phi + \frac{2\eta}{g_m |\Pi'|} \cos\theta_1 \cos\alpha \right) \right] - 2\omega_1 \, c \, |E_p| \cos\theta_1$$

$$(5.27)$$

In the previous equations all the terms of Eq. 5.4 have been developed in terms of the circuit parameters and independent side frequency forcing terms. Substituting in Eq. 5.4 the equations 5.21, 5.5, 5.27, and 5.6 gives a general expression for A

$$A = (v_+ - v_{ss+}) \frac{\omega_1\left[\cos\left(\frac{\theta_1'}{2} + \sigma\right) - \mu_d \sin\left(\frac{\theta_1'}{2} + \sigma\right)\right] - (\dot{v}_+ - \dot{v}_{ss+}) \sin\left(\frac{\theta_1'}{2} + \sigma\right)}{\omega_1\left[\sin(-2\sigma) - \mu\left\{\cos 2\sigma + \sin\left(\theta_1 + \tan^{-1}\frac{1}{2Q_0}\right)\right\}\right]} \tag{5.28}$$

A change in notation here will help to reveal the significance of various operating conditions on Eq. 5.28. $\theta_1'$ is the pump phase angle which includes a phase shift due to circuit loading $\left(\tan^{-1}\frac{1}{Q_0}\right)$ and another phase shift due to the form of the transient solution $(-\frac{\pi}{2})$. c.f. Eq. 3.9. Since $\sigma$ is very nearly $-\frac{\pi}{4}$ when the passive circuit is tuned to the half-pump frequency ($\omega_0 = \omega_1$), it is convenient to define:

$$\sigma' \equiv \sigma + \frac{\pi}{4} \tag{5.29}$$

$\sigma'$ is approximately the departure of $\sigma$ from the tuned value.

Recalling the $\theta''$ notation of Eq. 3.13, Eq. 5.28 becomes

$$A = \frac{(v_+ - v_{ss+})\left[\sin\left(\frac{\theta''_1}{2} + \sigma'\right) + \mu_d \cos\left(\frac{\theta''_1}{2} + \sigma'\right)\right] + \frac{(\dot{v}_+ - \dot{v}_{ss+})}{\omega_1} \cos\left(\frac{\theta''_1}{2} + \sigma'\right)}{\cos 2\sigma' + \mu(-\sin 2\sigma' + \sin \theta''_1)}$$

When the small phase shift due to the finite $Q_0$ found in $\theta''_1$ is combined with the phase shift of the transient solution due to detuning in the form

$$\sigma'' \equiv \sigma' + \frac{1}{2} \tan^{-1} \frac{1}{Q_0}$$

and the small perturbation of the value of A due to the "$\mu$" term of the denominator is neglected we have:

$$A = \frac{(v_+ - v_{ss+})\left[\sin\left(\frac{\theta_1}{2} + \sigma''\right) + \mu_d \cos\left(\frac{\theta_1}{2} + \sigma''\right)\right] + \frac{(\dot{v}_+ - \dot{v}_{ss+})}{\omega_1} \cos\left(\frac{\theta_1}{2} + \sigma''\right)}{\cos 2\sigma'} \qquad (5.30)$$

5.4.3 General Form - Quasi-Degenerate Solution. Equations 5.23, 5.27, and 5.30 are now brought together to provide an explicit form for A. It will be convenient to separate the pump-unbalance terms and express them at the end of the equation.

$$A = \frac{|\Pi'|\, g_m}{\cos 2\sigma' G\sqrt{(1+\delta^2)(1+\zeta'^2)}} \left[ \left\{ |I_\ell| \left(-|\Pi'| \cos\alpha + \cos\beta\right) + |I_u| \left(-|\Pi'| \cos\gamma + \cos\phi\right) \right\} \right.$$

$$\left\{ \sin\left(\frac{\theta_1}{2} + \sigma''\right) + \mu_d \cos\left(\frac{\theta_1}{2} + \sigma''\right) \right\}$$

$$+ \left\{ |I_\ell| \left( |\Pi'| \sin\alpha - \sin\beta - \frac{-2\eta}{|\Pi'|\, g_m} \cos\theta_1 \cos\alpha \right) \right.$$

$$\left. + |I_u| \left( |\Pi'| \sin\gamma - \sin\phi \frac{-2\eta}{|\Pi'|\, g_m} \cos\theta_1 \cos\gamma \right) \right\} \cos\left(\frac{\theta_1}{2} + \sigma''\right) \Bigg]$$

$$\frac{-c\,|E_p| \sin\theta_1 \left\{ \sin\left(\frac{\theta_1}{2} + \sigma''\right) + \mu_d \cos\left(\frac{\theta_1}{2} + \sigma''\right) \right\} - 2c\,|E_p| \cos\theta_1 \cos\left(\frac{\theta_1}{2} + \sigma''\right)}{\cos 2\sigma'}$$

(5.31)

In order to establish dominant effects a judgement is imposed at this point in the development. Recalling Eqs. 3.12 and 3.13 where $\mu$, $\mu_g$, and $\mu_d$ are defined we note that $\mu_d << 1$. In addition the term $\frac{2\eta}{|\Pi'|\, g_m} << 1$. Neglecting the contributions of these terms, which produce only very small phase shifts, the remaining terms combine using the sine of difference angles identity. Introducing a new angle notion the expression for A is:

$$\alpha_\ell = \left(\theta_\ell - \frac{\theta_1}{2} - \tan^{-1}\zeta'\right) \qquad \alpha_u = \left(\theta_u - \frac{\theta_1}{2} + \tan^{-1}\zeta'\right)$$

$$A = \frac{|\Pi'|\, g_m}{\cos 2\sigma' G\sqrt{(1+\delta^2)(1+\zeta'^2)}} \left[ |I_\ell| \left\{ |\Pi'| \sin(\alpha_\ell - \sigma'' - \tan^{-1}\delta) + \sin(\alpha_\ell + \sigma'') \right\} \right.$$

$$\left. + |I_u| \left\{ |\Pi'| \sin(\alpha_u - \sigma'' - \tan^{-1}\delta) + \sin(\alpha_u + \sigma'') \right\} \right] + \frac{-2c|E_p|}{\cos 2\sigma'} \, y\left(\frac{\theta_1}{2}, \sigma''\right) \tag{5.32}$$

where $y\ \frac{\theta_1}{2}, \sigma''$ is a pump unbalance factor to be considered later.

Now when the sine functions are expanded by separating $\alpha_\ell$ and $\alpha_u$ from the rest of the angular expression, and the results grouped by sines and cosines of $\alpha_\ell$ and $\alpha_u$:

$$A = \frac{|\Pi'|\, g_m}{\cos 2\sigma' G\sqrt{(1+\delta^2)(1+\zeta'^2)}} \left[ |I_\ell| \sin\alpha_\ell \left\{ |\Pi'| \cos(\sigma'' + \tan^{-1}\delta) + \cos\sigma'' \right\} \right.$$

$$- |I_\ell| \cos\alpha_\ell \left\{ |\Pi'| \sin(\sigma'' + \tan^{-1}\delta) - \sin\sigma'' \right\}$$

$$+ |I_u| \sin\alpha_u \left\{ |\Pi'| \cos(\sigma'' + \tan^{-1}\delta + \cos\sigma'') \right\} - |I_u| \cos\alpha_u \left\{ |\Pi'| \sin \right.$$

$$\left. \left. (\sigma'' + \tan^{-1}\delta) - \sin\sigma'' \right\} \right]$$

$$- \text{pump unbalance terms} \tag{5.33}$$

In Eq. 5.33 the signal current magnitudes appear as independent sine and cosine components of the $\alpha$ phase angles associated with the upper and lower side frequencies. A common factor for the sums of the components has appeared also. Performing the cosine operation on $(\sigma'' + \tan^{-1}\delta)$

and defining:

$$\Pi'' \equiv \frac{\Pi'}{\sqrt{1+\delta^2}} = \frac{\Pi}{(1+\delta^2)} \tag{5.34}$$

$$|\Pi'| \cos(\sigma'' + \tan^{-1}\delta) + \cos\sigma'' = (1+|\Pi''|)\left(\cos\sigma'' - \frac{|\Pi'|}{(1+|\Pi''|)} \sin\sigma''\right)$$

$$|\Pi'| \sin(\sigma'' + \tan^{-1}\delta) - \sin\sigma'' = (1+|\Pi''|)\left[\frac{(1-|\Pi''|)}{(1+|\Pi''|)}(-\sin\sigma'') + \frac{\delta|\Pi''|}{(1+|\Pi''|)}\cos\sigma''\right] \tag{5.35}$$

Applying Eq. 5.35 to Eq. 5.33 and noting that $\frac{(1-|\Pi''|)}{(1+|\Pi''|)} << 1$,

$$A \approx \frac{|\Pi''|(1+|\Pi''|)g_m}{\cos 2\sigma' \sqrt{1+\zeta'^2}\, G}\left[(|I_\ell| \sin\alpha_\ell + |I_u| \sin\alpha_u)\left(\cos\sigma'' - \frac{\delta|\Pi''|}{(1+|\Pi''|)}\sin\sigma''\right)\right.$$

$$\left. - (|I_\ell| \cos\alpha_\ell + |I_u| \cos\alpha_u)\left(\frac{\delta|\Pi''|}{1+|\Pi''|}\cos\sigma''\right)\right] + \frac{-2c|E_p|}{\cos 2\sigma'}\, y\left(\frac{\theta_1}{2}, \sigma''\right) \tag{5.36}$$

Equation 5.36 is the complete expression for the most significant constant, the coefficient of the growing exponential term. After a few cycles of oscillation before any saturation occurs the only term of consequence will be the growing term. (The decaying term is characterized by the exponent, $\mu_d$, which is much greater than the exponent of the growing term, i.e., $\mu_d >> \mu_g$.)

In the phase synchronization problem we are interested in "A"

under two conditions. The one is for the signal excitation, which in this specific instance is a current at a frequency of exactly $\omega_1$ radians per second. This is the completely degenerate case and is found from the foregoing expressions by letting $\zeta' = 0$, and noting that $|I_\ell| = |I_u| = |I_s|/2$ and $\theta_\ell = \theta_u$. This degenerate condition is equivalent to coincidence of equal side frequency source currents at identical phase positions. The other condition of interest is that of the value of A due to noise within the pass band where the source currents become Gaussian random variables whose mean values are zero and whose variances are identified with the circuit noise. In this study the noise energy will be assumed to be associated only with the resistance member of the load, that is, thermal noise, whose energy distribution within the band is uniform and whose phase angles are equally likely. The derivation of Eq. 5.36 where the source currents are explicit in $(v_+ - v_{ss+})$ and $(\dot{v}_+ - \dot{v}_{ss+})$, preserves the independent and explicit representation of the source currents. We will see that, for the signal alone, a coherence of phase position of these source currents can be specified and the value of A is strongly controlled by the particular phase chosen. For the noise sources no such phase coherence nor amplitude equality are possible and the input information must be handled differently.

## 5.5 Signal A

### 5.5.1 Degenerate Form.

In the degenerate case,

$$|I_\ell| = |I_u| = |I_s|/2$$

$$\alpha_\ell = \alpha_u = \alpha_s = \left(\theta_s - \frac{\theta}{2}1\right)$$

and Eq. 5.36 becomes

$$A_{deg} = \frac{|\Pi''|(1+|\Pi''|)g_m|I_s|}{\cos 2\sigma' G}\left[\sin\left(\theta_s - \frac{\theta}{2}1\right)\left(\cos\sigma'' - \frac{\delta|\Pi''|}{1+|\Pi''|}\sin\sigma''\right)\right.$$

$$\left. - \cos\left(\theta_s - \frac{\theta}{2}1\right)\frac{\delta|\Pi''|}{(1+|\Pi''|)}\cos\sigma''\right] + \frac{-2c|E_p|}{\cos 2\sigma'}\, y\left(\frac{\theta}{2}1, \sigma''\right)$$

The above is simplified significantly by noting that the general usage will be in the tuned or nearly-tuned case, i.e., for small $\delta$.

It is shown in Appendix VI that the term

$$\frac{\left(\cos\sigma'' - \frac{\delta|\Pi''|}{1+|\Pi''|}\sin\sigma''\right)^2 + \left(\frac{\delta|\Pi''|}{1+|\Pi''|}\cos\sigma''\right)^2}{\cos^2 2\sigma'} \cong 1$$

and

$$\frac{\frac{\delta|\Pi''|}{1+|\Pi''|}\cos\sigma''}{\cos\sigma'' - \frac{\delta|\Pi''|}{1+|\Pi''|}\sin\sigma''} \cong \frac{\delta}{2}$$

The assumptions made here are that the $Q_0 > 10$, that $g_m > 5$, and $\delta \leq 0.5$. Although the numbers chosen are somewhat arbitrary the approximation is of the order $\frac{\delta^4}{4}$ which is about 1-1/2 percent for the

worst case. Hence

$$A_{deg} \cong \frac{2\left(1 - \frac{3\delta^2}{4}\right) g_m |I_s|}{G} \sin\left[\theta_s - \frac{\theta_1}{2} - \tan^{-1}\frac{\delta}{2}\right] + \frac{-2c\,|E_p|}{\cos 2\sigma'}\, y\left(\frac{\theta_1}{2},\ \sigma''\right) \tag{5.37}$$

and for the tuned condition this reduces to

$$A_{\substack{deg \\ \delta = 0}} = \frac{2\, g_m |I_s|}{G} \sin\left(\theta_s - \frac{\theta_1}{2}\right) - 2ce\,|E_p|\, y\left(\frac{\theta_1}{2},\ \sigma''\right) . \tag{5.38}$$

It is convenient to relate the relative phase positions of $\theta_s$ and $\frac{\theta_1}{2}$ to the one which produces a maximum response. Accordingly let

$$\psi \equiv \theta_s - \frac{\theta_1}{2} - \frac{\pi}{2} \tag{5.39}$$

Using Eq. 5.39 in Eq. 5.38, and also that for high gains $|\Pi| \cong 1$,

$$A_{\substack{deg \\ \delta = 0}} = \frac{2\, g_m |I_s|}{G} \cos\psi - 2c\,|E_p|\, y\left(\frac{\theta_1}{2},\ \sigma''\right) \tag{5.40}$$

5.5.2 Signal Power. The signal power delivered to the tuned circuit ($\delta = 0$) is here defined as $P_s$.

$$P_s = \frac{|I_s|^2}{2G} \quad \text{from which} \quad \frac{|I_s|}{G} = \sqrt{\frac{2P_s}{G}}$$

When the passive circuit is detuned, the power, $P'_s$, is reduced, according to $\delta$

$$P'_s = \frac{|I_s|^2}{2G(1+\delta^2)} = \frac{P_s}{(1+\delta^2)} \tag{5.41}$$

Using Eq. 5.41 in Eq. 5.37,

$$A_{deg} = 2\left(1 - \frac{3\delta^2}{4}\right) g_m \sqrt{\frac{2P_s}{G}} \sin\left(\theta_s - \frac{\theta_1}{2} - \tan^{-1}\frac{\delta}{2}\right)$$

$$- \frac{2c|E_p|}{\cos 2\sigma'} \; y\left(\frac{\theta_1}{2}, \sigma''\right) \tag{5.42}$$

When $\delta = 0$, the tuned case,

$$A_{\substack{deg \\ \delta = 0}} = 2 g_m \sqrt{\frac{2P_s}{G}} \cos\psi - 2c|E_p| y\left(\frac{\theta_1}{2}, \sigma''\right)$$

## 5.6 Noise A

5.6.1 Excitation by Random Variables. The excitation sources, 4.1, and seen finally in Eq. 5.36 will now be considered to come from a thermal noise generator. For this situation $i_\ell$ and $i_\mu$ are identified as independent Gaussian random variables having phase angles $\alpha_\ell$ and $\alpha_\mu$, each of which has uniform probability of occurrence over the range $0 - 2\pi$. Over the narrowband of $\zeta$ to $(\zeta + d\zeta)$ both at the lower and upper side frequency position these sources will dissipate power characteristic

of a normal narrowband noise process. Such a process is described in detail by Middleton (Ref. 114) and in particular the independent components at each sideband are shown to have equal variances (mean-squared values). Thus:

$$\langle(|I_\ell| \sin \alpha_\ell)^2\rangle^* = \langle(|I_\ell| \cos \alpha_\ell)^2\rangle \qquad \begin{matrix} * \text{ read symbol } \langle\rangle \\ \text{as "the mean"} \end{matrix}$$

$$\langle(|I_u| \sin \alpha_\ell)^2\rangle = \langle(|I_u| \cos \alpha_u)^2\rangle \tag{5.43}$$

The components of $|I_\ell|$ and $|I_u|$ which appear together in Eq. 5.36 form a linear combination of independent Gaussian random variables and are here identified similarly:

$$\begin{aligned} |I_\ell| \sin \alpha_\ell + |I_u| \sin \alpha_u &= i_1 \\ |I_\ell| \cos \alpha_\ell + |I_u| \cos \alpha_u &= i_2 \end{aligned} \tag{5.44}$$

Writing the variances of $i_1$ and $i_2$ with the aid of Eq. 5.43,

$$\langle i_1^2\rangle = \langle(|I_\ell| \sin \alpha_\ell)^2\rangle + \langle(|I_u| \sin \alpha_u)^2\rangle$$

and

$$\langle i_2^2\rangle = \langle(|I_\ell| \cos \alpha_\ell)^2\rangle + \langle(|I_u| \cos \alpha_u)^2\rangle$$

$$\langle i_1^2\rangle = \langle i_2^2\rangle \equiv \langle i_N^2\rangle$$

which defines $i_N$.

We seek the statistical description of $A_\zeta$ due to the excitation sources of bandwidth $d_\zeta'$ at $\pm\zeta'$, and thus from Eq. 5.36:

$$\langle A_{\zeta'}{}^2 \rangle = \left[\frac{|\Pi''|(1+|\Pi''|)g_m}{\cos 2\sigma' \sqrt{1+\zeta'^2}\, G}\right]^2 \left[\langle i_N{}^2\rangle \left(\cos\sigma'' - \frac{\delta|\Pi''|}{1+|\Pi''|}\sin\sigma''\right)^2 + \langle i_N{}^2\rangle \left(\frac{\delta|\Pi''|}{1+|\Pi''|}\cos\sigma''\right)^2\right] \qquad (5.45)$$

5.6.2 Noise Power. We now identify $\langle i_N{}^2\rangle$ with the circuit thermal noise. First note that per Eq. 4.1, $i_N$ was derived from peak rather than effective value currents. Also each of the components of $i_1$ and $i_2$ (i.e., $|I_\ell| \sin\alpha_\ell$ and $|I_\ell| \cos\alpha_\ell$, etc.) are identified with just half of the noise energy within the band $d_\zeta'$. Thus if we allow dN to be the total thermal noise source power occurring within the $d_\zeta'$ bandwidth

$$\frac{dN}{2} = \frac{\langle(|I_\ell| \sin\alpha_\ell)^2\rangle}{2G} = \frac{\langle(|I_u| \sin\alpha_u)^2\rangle}{2G} \qquad (5.46)$$

from which $dN = \frac{1}{2G}\langle i_N{}^2\rangle$.

From the thermodynamical argument of Nyquist (Ref. 114)

$$dN = 4\,KT\,|df| \qquad (5.47)$$

Returning to Eqs. 4.6 and 4.14 we evaluate df.

$$f_\ell = \frac{\omega_0}{2\pi}\left(1 + \frac{\delta}{2Q_0} - \frac{\zeta'}{4g_m Q_0}(1+\delta^2)\right) \qquad (5.48)$$

$$|df_\ell| = \frac{\omega_0(1+\delta^2)}{8\pi g_m Q_0} d\zeta' \tag{5.49}$$

Exactly the same value of $|df|$ results from the upper side frequency, and thus

$$\langle i_N^2 \rangle = 2G\, dN = \frac{KT\,\omega_0 G(1+\delta^2)\, d\zeta'}{\pi Q_0 g_m} \tag{5.50}$$

It has been shown (Ref. 114 that the total thermal noise, N, associated with a passive resonant circuit is:

$$N = \frac{KT\,\omega_0}{Q_0} \tag{5.51}$$

Using this normalization Eq. 5.50 becomes

$$\langle i_N \rangle^2 = \frac{NG(1+\delta^2)}{\pi g_m} d\zeta' \tag{5.52}$$

The active circuit bandwidth is significantly narrowed as evidenced by the relationship between the descriptive parameters, $\xi$ for the passive bandwidth, and $\zeta'$ for the detuned active bandwidth. Accordingly let us further normalize Eq. 5.52 in terms of the noise, N', associated with the active band. Let

$$N' = \frac{N\, df_{\zeta'}}{df_\xi} = \frac{N(1+\delta^2)}{2 g_m} \tag{5.53}$$

from which

$$\langle i_N \rangle^2 = \frac{2N'G}{\pi} d\zeta' \tag{5.54}$$

Substituting Eq. 5.54 into Eq. 5.45 and again using the simplifications following Eq. 5.39,

$$\langle A_{\zeta'}{}^2 \rangle = \left[2\left(1 - \frac{3\delta^2}{4}\right) g_m\right]^2 \frac{2N'}{\pi G} \frac{d\zeta'}{(1+\zeta'^2)} \tag{5.55}$$

If each $A_{\zeta'}$ is treated as an independent Gaussian random variable which results from the currents $i_1$ and $i_2$ within the interval $\zeta'$ to $(\zeta' + d\zeta')$ the mean squared A which results from all the noise source currents over the whole band is simply the sum of the mean-squared components.

$$\langle A_N{}^2 \rangle = \left[2\left(1 - \frac{3}{4}\delta^2\right) g_m\right]^2 \frac{2N'}{G} \tag{5.56}$$

The integration has been carried out from $-\infty$ to $+\infty$ since noise within $d\zeta'$ at $+\zeta'$ is generated by source currents at $+\zeta'$ and $-\zeta'$ just as noise within $-d\zeta'$ is generated by source currents at $-\zeta'$ and $+\zeta'$.

It will be convenient to associate the value of $A_N$ with the normalized Gaussian random variable, $a_N$, having mean of zero and variance unity. Then (5.56) becomes:

$$\begin{aligned} A_N &= \sqrt{\langle A_N \rangle^2}\, a_N \\ &= 2\left(1 - \frac{3}{4}\delta^2\right) g_m \sqrt{\frac{2N'}{G}}\, a_N \end{aligned} \tag{5.57}$$

and for the tuned case ($\delta = 0$)

$$\underset{(\delta = 0)}{A_N} = 2\, g_m \sqrt{\frac{2N'}{G}}\, a_N$$

## 5.7 General Expression for B

The coefficient of the decaying transient term of the general solution 5.1 is now sought, primarily to demonstrate that this portion of the solution does not dominate observed effects during growing oscillations.

From Eq. 5.4

$$B = \frac{(v_+ - v_{ss+})(-\omega_1)\left[\cos\left(\frac{\theta_1}{2} - \sigma''\right) + \mu_g \sin\left(\frac{\theta_1}{2} - \sigma''\right)\right] + (\dot{v}_+ - \dot{v}_{ss+}) \sin\left(\frac{\theta_1}{2} - \sigma''\right)}{\omega_1\left[\cos 2\sigma' + \mu(\sin\theta_1'' - \sin 2\sigma')\right]} \tag{5.58}$$

Recalling Eqs. 5.23 and 5.27

$$\begin{aligned} B = {} & \frac{-\left[\cos\left(\frac{\theta_1}{2} - \sigma''\right) + \mu_g \sin\left(\frac{\theta_1}{2} - \sigma''\right)\right]}{\cos 2\sigma'} \left\{ \frac{|\Pi''|\, g_m}{G\sqrt{1+\zeta'^2}} \left[ |I_\ell| (-|\Pi'| \cos\alpha + \cos\beta) \right.\right. \\ & \left.\left. + |I_u| (-|\Pi'| \cos\gamma + \cos\phi)\right] - c|E_p| \sin\theta_1 \right\} \\ & + \frac{\sin\left(\frac{\theta_1}{2} - \sigma''\right)}{\cos 2\sigma'} \left\{ \frac{|\Pi'|\, g_m}{G\sqrt{1+\zeta'^2}} \left[ |I_\ell| \left( |\Pi'| \sin\alpha - \sin\beta - \frac{2\eta}{|\Pi'|\, g_m} \cos\theta_1 \cos\alpha \right) \right.\right. \\ & \left.\left. + |I_u| \left( |\Pi'| \sin\gamma - \sin\phi - \frac{2\eta}{|\Pi'|\, g_m} \cos\theta_1 \cos\gamma \right) \right] - 2c|E_p| \cos\theta_1 \right\} \end{aligned} \tag{5.59}$$

Equation 5.59 can be simplified considerably by using $\alpha_\ell$ and $\alpha_u$ as in Eq. 5.32 and by neglecting the terms arising from the factors $\mu_g$ and $\frac{2\eta}{|\Pi'|\, g_m}$. Both of these quantities are very much less than unity.

In this vein Eq. 5.59 becomes

$$B = \frac{|\Pi''|\, g_m}{G \cos 2\sigma' \sqrt{1+\zeta'^2}} \left\{ |I_\ell| \left[ |\Pi'| \cos(\alpha_\ell + \sigma'' - \tan^{-1}\delta) - \cos(\alpha_\ell - \sigma'') \right] + |I_u| \left[ |\Pi'| \cos(\alpha_u + \sigma'' - \tan^{-1}\delta) - \cos(\alpha_u - \sigma'') \right] \right\} + \frac{2c\,|E_p|}{\cos 2\sigma'} \left( \cos\sigma'' \sin^3 \frac{\theta_1}{2} + \sin\sigma'' \cos^3 \frac{\theta_1}{2} \right) \quad (5.60)$$

Performing the operations within the parentheses reveals the excitation components used in evaluating A.

$$B = \frac{|\Pi''| g_m (1+|\Pi''|}{G \cos 2\sigma' \sqrt{1+\zeta'^2}} \left\{ (|I_\ell| \cos\alpha_\ell + |I_u| \cos\alpha_u) \left[ \frac{(|\Pi''|-1)}{(1+|\Pi''|)} \cos\sigma'' + \frac{\delta|\Pi''|}{(1+|\Pi''|)} \sin\sigma'' \right] + (|I_\ell| \sin\alpha_\ell + |I_u| \sin\alpha_u) \left[ -\sin\sigma'' + \frac{\delta|\Pi''|}{(1+|\Pi''|)} \cos\sigma'' \right] \right\} + \frac{2c\,|E_p|}{\cos 2\sigma'} \left( \cos\sigma'' \sin^3 \frac{\theta_1}{2} + \sin\sigma'' \cos^3 \frac{\theta_1}{2} \right) \quad (5.61)$$

Equation 5.61 is very similar to the general expression for A. The major difference, and a highly significant one is the effect of detuning. When the circuit is tuned A is accentuated, whereas B is minimized. The converse is also true.

5.7.1 Signal B. Two special cases of B are of interest. The first is the degenerate or Signal B. When $\zeta$ is zero $B_{deg}$ becomes:

$$B_{deg} = \frac{|\Pi''|(1+|\Pi''|)\, g_m\, |I_s|}{G \cos 2\sigma'} \left\{ \cos\left(\theta_s - \frac{\theta_1}{2}\right) \left[ \frac{(|\Pi''|-1)}{(1+|\Pi''|)} \cos\sigma'' + \frac{\delta\,|\Pi''|}{(1+|\Pi''|)} \sin\sigma'' \right] \right.$$
$$\left. + \sin\left(\theta_s - \frac{\theta_1}{2}\right) \left[ -\sin\sigma'' + \frac{\delta\,|\Pi'|}{(1+|\Pi''|)} \cos\sigma'' \right] \right\}$$
$$+ \frac{2c\,|E_p|}{\cos 2\sigma'} \left( \cos\sigma'' \sin^3 \frac{\theta_1}{2} + \sin\sigma'' \cos^3 \frac{\theta_1}{2} \right) \tag{5.62}$$

When the circuit is tuned

$$B_{\substack{deg \\ (\delta=0)}} = \frac{|\Pi|(1+|\Pi|)}{G}\, g_m\, |I_s| \left[ \cos\left(\theta_s - \frac{\theta_1}{2}\right) \frac{(|\Pi|-1)}{(1+|\Pi|)} \right] + 2c\,|E_p| \sin^3 \frac{\theta_1}{2} \tag{5.63}$$

For the instances when the signal-pump phase difference is adjusted to give maximum growing component, (A), the value of B is negligible. The appearance of the $\frac{|\Pi|-1}{1+|\Pi|}$ term further makes the B term negligible under all but the adjustment of $\left(\theta_s - \frac{\theta_1}{2}\right)$ to $n\pi$ radians. Although both B and A will be very small under this particular condition they will be of comparable value.

5.7.2 Noise B. Proceeding as in Section 5.6.1 and introducing the random excitation currents $i_1$ and $i_2$ defined in 5.44 the mean-square value of B at a particular value of $\zeta'$ is:

$$\langle B_{\zeta'}\rangle^2 = \left[\frac{|\Pi''|(1+|\Pi''|\,g_m}{G\cos 2\sigma'\sqrt{1+\zeta'^2}}\right]^2 \left[\langle i_1\rangle^2 \left\{\frac{(|\Pi''|-1)}{(1+|\Pi''|)}\cos\sigma'' + \frac{\delta|\Pi''|}{1+|\Pi''|}\sin\sigma''\right\}^2 + \langle i_2\rangle^2 \left\{-\sin\sigma'' + \frac{\delta|\Pi''|}{1+|\Pi''|}\cos\sigma''\right\}^2\right] \quad (5.64)$$

Again identifying the excitation currents with the thermal noise in the passive and active circuits an expression for $\langle B_{\zeta'}\rangle^2$ identical with Eq. 5.55 but for one term is produced. The exceptional term is given below and is of the order of $\frac{\delta^4}{2}$ compared with the corresponding value of unity for the case of the A value. The term of the B expression and the relative value of $\langle B_{noise}\rangle^2/\langle A_{noise}\rangle^2$ is:

$$\frac{\langle B_N\rangle^2}{\langle A_N\rangle^2} = \left[\frac{(|\Pi''|-1)}{(1+|\Pi''|)}\cos\sigma'' + \frac{\delta|\Pi''|}{1+|\Pi''|}\sin\sigma''\right]^2 + \left[-\sin\sigma'' + \frac{\delta|\Pi''|}{(1+|\Pi''|)}\cos\sigma''\right]^2 \cong \frac{\delta^4}{2} \quad (5.65)$$

For the assumptions under Eq. 5.55 the $\frac{\delta^4}{2}$ is about 3 percent for the worst case. Thus the value of B produced by the noise is negligible compared with the value of A produced by the noise.

# CHAPTER VI

## BISTATE SIGNAL DETECTION BY SUBHARMONIC OSCILLATIONS

In this chapter we assume that the parametric device under study is connected to a signal source for the purpose of detecting and amplifying bistate phase information. That is, the signal frequency is assumed locked exactly to the pump source at half the pump frequency, and also that the information is being carried by the two stable phase states of the oscillation. We have seen how the growing oscillation of the device can have one of the two phases represented by either sign of the coefficient, A, of the growing term. Further we note that the signal is most effective in producing a value of A when it bears the same phase relation to the pump as the natural response of the system. In the absence of noise the growing oscillation will always be in phase with the signal. However, when a noise signal in the form of a thermal agitation current is superimposed on the signal there develops a probability that, at the instant of initiation of pumping, (the time the sign of A is determined) the noise exceeds the signal and the growing oscillation can become $\pi$ radians out of phase with the signal. When this does happen an error in detection occurs. The probability of error varies widely with the phase and magnitude of the signal relative to the noise occurring within the system. These effects are also related to system adjustments, and to the pecularities of the actual physical circuit construction.

## 6.1 Linear Superposition

We have seen in Chapter V (Eqs. 5.5, 5.6, 5.7) how coefficients of a growing and a decaying oscillation arise in a pumped resonant circuit. The exponents of growth and decay have been expressed in Eq. 5.1 as $\mu_g$ and $\mu_d$ and are the difference and sum of the natural circuit $\mu$ and loading parameter $\mu_L$. In moderate to high gain situations ($g_m > 5$) $\mu_g$ is very much less than $\mu_d$. Thus when an oscillation is observed for many cycles after initiation but before any saturation has occurred the effect of the decaying term is completely lost. The oscillation grows at the rate determined by $\mu_g$, and with the initial magnitude and phase determined by A. By Eq. 5.36 A is linearly dependent on the excitation current whether this current is signal or noise. Accordingly the principle of linear superposition is applied and the value of A due to both signal and noise is simply:

$$A = A_{deg.} + A_{noise} \tag{6.1}$$

When $A_{noise}$ as shown in Eq. 5.45 is a Gaussian random variable the noise can conceivably dominate the situation and determine the sign of A for any value of $A_{deg}$.

## 6.2 Detection Level - Superregeneration

We will find that the significance of the noise term is felt only for signal levels of the order of the noise. In moderate Q circuits like those constructed using present day varactor components these noise

levels can be at power levels as much as $10^{-12}$ of easily obtainable steady-state oscillation levels. This, in effect, means that the device can be considered an amplifier for signals of the order of the noise up to the level of the saturated oscillation. The general concept is known as superregeneration and is useful whenever very high gain per stage is the dominant design requirement. For the purpose of this study critical examination of waveforms, growing rates etc. have been limited to portions of the quench cycle well below saturation where the linear analytical treatment applies.

Using the principle of superregeneration only one bit of information (in the digital sense) is obtainable during each quench cycle, i.e., during the time between initiation of the pump and the final extraction of the information by phase detection at a high level.

Thus the information rate is directly proportional to the quench frequency. For a given gain this information rate is limited by the growth rate of the oscillation. Thus we see the familiar concept of gain-bandwidth arising. It is useful at this point to evaluate just what this quality factor is for the device when used in the detection of bistate phase information.

The amplitude of output voltage of the device at any time is related to the input voltage according to the growing exponential:

$$v_o = v_i \epsilon^{\mu_g \omega_1 t} \qquad (6.2)$$

where t is the time interval since the quench cycle started. If there is a maximum output voltage $v_{om}$ to which the oscillation is allowed to grow, the voltage gain is then related to the maximum input voltage $v_{im}$:

$$\frac{v_{om}}{v_{im}} = g_v = \epsilon^{\mu_g \omega_1 t_m} \tag{6.3}$$

$g_v$ is the same for all signal levels which are below $v_{im}$ and faithfully preserves both signal and noise levels during the growing process.

Information can be recovered if data is sampled over each half cycle (Ref. 115) and thus if T is the sampling period and the quench cycle is symmetrical in time the maximum frequency of the data is $f_m = \frac{1}{2T}$, i.e., the bandwidth. $t_m$ of Eq. 6.3 becomes T/2 and the gain-bandwidth figure of merit is:

$$M = \frac{1}{2T} \epsilon^{\mu_g \omega_1 T/2} \tag{6.4}$$

For the tuned case $\mu_g$ is related quite simply to circuit parameters and adjustments by Eqs. 5.1, 2.5, and 3.10

$$\mu_g = \frac{1}{2Q_o} \left( - \frac{1}{2g_m} \right) \tag{6.5}$$

(Recall that $g_m$ is negative in the oscillating region.)

When operating as a superregenerative amplifier Eqs. 6.4 and 6.5 show that as the steady-state gain ($g_m$) increases in magnitude

(due to pump adjustment) $\mu_g$ is smaller and the circuit gain $g_v$ is lower.

When the pump is turned off at the end of the firsthalf cycle of the quench the oscillation decays at the natural passive decay rate characterized by $Q_0$ and at the natural frequency $\omega_0$. By Eq. 3.10 $\mu_L >> \mu_g$ and the natural decay is rapid compared with the forced growth.

It should be noted in passing that because of the disparity between $\mu_g$ and $\mu_L$ the quench cycle need not be a symmetrical square waveform in time, but could be scaled to the relative values of $\mu_g$ and $\mu_L$. Thus the bandwidth could possibly be increased by a factor of nearly two. It will be shown that $v_{im}$, for bistate phase signals of the order of the thermal noise produce good probabilities of correct phase synchronization, and that only a few decibels of signal power over the active circuit noise power are required to produce excellent phase synchronization.

In addition to these properties the active bandwidth of the circuit is completely adjustable by electrical means, thereby providing a simple method for exploiting the full range of the gain-bandwidth figure of merit in either gain or bandwidth.

## 6.3 Error Probability

The result of the preceding is to allow the expression of the error probability during the detection of bistate phase information.

Using Eq. 6.1 (linear superposition), Eq. 5.42 ($A_{deg.}$), and Eq. 5.57 ($A_{noise}$)

$$A = \frac{2\left(1 - \frac{3\delta^2}{4}\right)}{\sqrt{G}}\, g_m \left[\sqrt{2P_s}\, \sin\left(\theta_s - \frac{\theta_1}{2} - \tan^{-1}\frac{\delta}{2}\right) + \sqrt{2N'}\, a_N - 2c|E_p|\sqrt{1+\delta^2}\, y\left(\frac{\theta_1}{2}, \sigma''\right)\right] \tag{6.6}$$

6.3.1 Signal and Noise. One case of particular interest will be that when the pump unbalance is zero and the detection is concerned only with signal and thermal noise. We will designate an error whenever the sign of A differs from the sign of $A_{deg}$, i.e., the sign of the signal. To facilitate this understanding assume that $A_{deg}$, is positive, i.e.,

$$\sin\left(\theta_s - \frac{\theta_1}{2} - \tan^{-1}\frac{\delta}{2}\right) > 0$$

There will now be an error if:

$$\sqrt{2P_s}\, \sin\left(\theta_s - \frac{\theta_1}{2} - \tan^{-1}\frac{\delta}{2}\right) + \sqrt{2N'}\, a_N < 0$$

or

$$\sqrt{\frac{P_s}{N'}}\, \sin\left(\theta_s - \frac{\theta_1}{2} - \tan^{-1}\frac{\delta}{2}\right) < -a_N \tag{6.7}$$

Recall that $a_N$ is the normalized Gaussian random variable, and has a symmetric probability density about zero. (See Fig. 6.1)

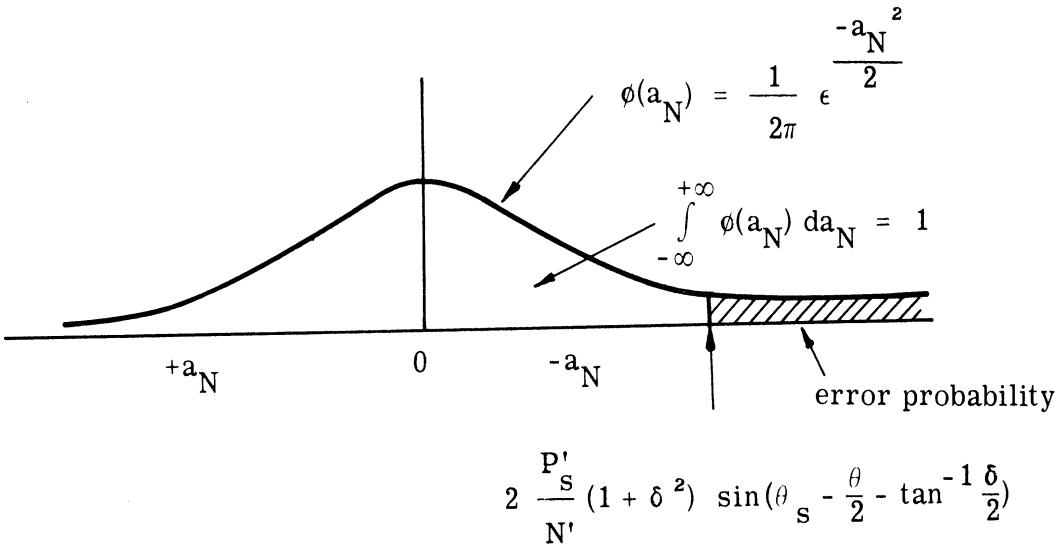


Fig. 6.1 Error probability density.

Thus when $a_N$ is positive there is no time when the left member of Eq. 6.7 (being positive) is less than $-(a_N)$. Accordingly the upper limit for the error probability which follows from these assumptions is 0.5. When $a_N$ is negative, $-(a_N)$ is positive and there is always a finite probability, as evidenced by the area under the probability density curve of the normalized variable $a_N$, that the value of $-(a_N)$ (i.e., the noise) is greater than the signal. This area is tabulated in publications on probability functions and when related to the actual signal-to-normalized noise ratio $(P_S/N')$ of Eq. 6.7 results in the curves of Fig. 6.2. The two cases shown demonstrate the effect the optimum adjustments, tuning and signal phase displacement, have on the error probability. From Eq. 6.7 it can be noted that detuning can be compensated by re-adjusting the relative phase position between the signal and the pump phase. The effect of serious departure from optimum signal-pump phase alignment is shown in Curve 2 of Fig. 6.2.

$$\sin\left(\theta_s - \frac{\theta_1}{2} - \tan^{-1}\frac{\delta}{2}\right) = \frac{1}{2}$$

6.3.2 Signal and Pump Unbalance. Another interesting case arises when the pump unbalance is the dominant effect masking the signal. Recall Eq. 6.6 for the pump unbalance terms

$$A_{pu} = -2c\,|E_p|\sqrt{1+\delta^2}\;\; y\left(\frac{\theta_1}{2},\ \sigma''\right) \qquad (6.8)$$

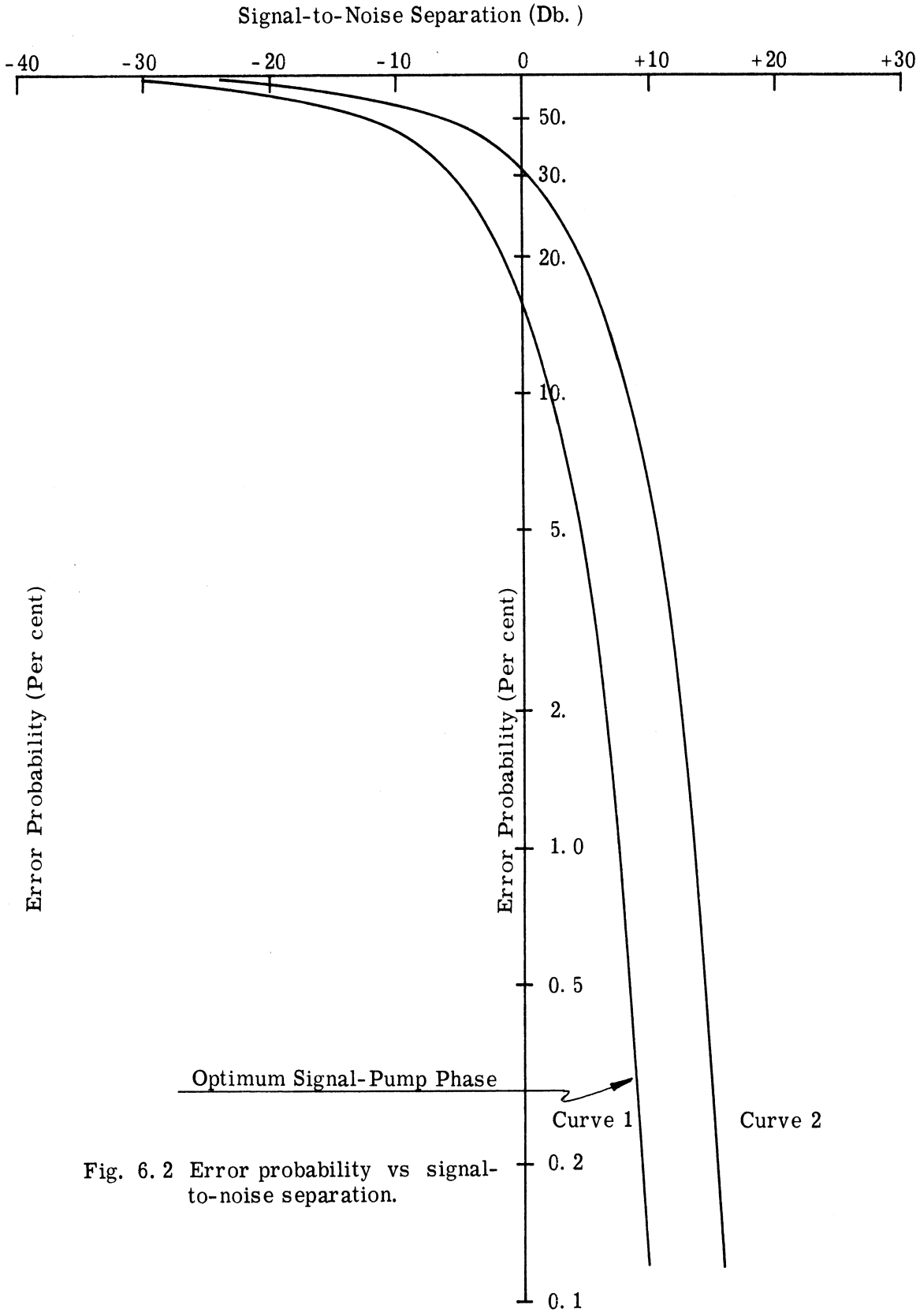


Fig. 6. 2 Error probability vs signal-to-noise separation.

The term of interest here is $y\left(\frac{\theta_1}{2}, \sigma''\right)$ which has been carried along in the development in this form in order to focus attention more simply on other effects. $y\left(\frac{\theta_1}{2}, \sigma''\right)$ was introduced in Eq. 5.32 of the general solution development and is:

$$y = \frac{\sin \theta_1}{2}\left[\sin\left(\frac{\theta_1}{2} + \sigma''\right) + \mu_d \cos\left(\frac{\theta_1}{2} + \sigma''\right)\right] + \cos \theta_1 \cos\left(\frac{\theta_1}{2} + \sigma''\right) \quad (6.9)$$

Following Eq. 5.31 a judgement was made regarding retention of terms involving $\mu_d$, and for the signal terms, these effects were deemed very small compared with more prominent effects. For pump unbalance consideration we will be attempting to minimize the effect and thus will need to retain second-order effects to improve that possibility. Doing so in Eq. 6.9 and using the cosine of difference angles identify:

$$y = \frac{1}{2}\left[\cos\left(\frac{\theta_1}{2} - \sigma'\right) + \cos \theta_1 \cos\left(\frac{\theta_1}{2} + \sigma''\right) + \mu_d \sin \theta_1 \cos\left(\frac{\theta_1}{2} + \sigma''\right)\right] \quad (6.10)$$

Separating out the effects of $\sigma''$ we find y dominated by cubic terms in $\frac{\theta_1}{2}$. Grouping in this fashion Eq. 6.10 becomes:

$$y = (\cos \sigma'' + \mu_d \sin \sigma'') \cos^3 \frac{\theta_1}{2} + (\sin \sigma'' - \mu_d \cos \sigma'') \sin^3 \frac{\theta_1}{2} + \mu_d \cos \sigma'' \sin \frac{\theta_1}{2} - \mu_d \sin \sigma'' \cos \frac{\theta_1}{2} \quad (6.11)$$

In the tuned and nearly-tuned situation both $\mu_d$ and $\sin\sigma''$ can be expressed in terms of $Q_0$, since by Eq. 5.30

$$\sin\sigma'' = \sin\left(\sigma + \frac{\pi}{4} + \frac{1}{2}\tan^{-1}\frac{1}{Q_0}\right) \cong \frac{1}{2Q_0}$$

$\sigma$ is the phase angle in the transient solution developed in Chapter III. Reference to Fig. 3.2 shows that in the tuned situation $\sigma$ is about $-\frac{\pi}{4}$ radians. Further, for reasonable values of steady-state gain, $g_m$, used in this study the departure of $\sigma$ from $\frac{\pi}{4}$, $(\sigma')$, within the region of oscillation allowed by the pump level, is a few degrees at the most. Thus for the tuned and nearly-tuned situation $\sin\sigma''$ is very small compared with unity and simply related to $Q_0$. By Eqs. 5.1 and 3.10,

$$\mu_d = (\mu + \mu_L)$$

and for moderate gains

$$\mu \cong \mu_L \cong \frac{1}{2Q_0}$$

$$\mu_d \cong \frac{1}{Q_0}$$

$$y = \cos^3\frac{\theta_1}{2} - \frac{1}{2Q_0}\sin^3\frac{\theta_1}{2} + \frac{1}{Q_0}\sin\frac{\theta_1}{2} \qquad (6.12)$$

(the terms neglected being of order $\frac{1}{2Q_0^2}$).

In order to discover the action of Eqs. 6.8 and 6.12 some observations must be made about the operating scheme of the device. Focusing attention on $\theta_1$, the initial pump phase angle, two situations can arise. If $\theta_1$ is to be a constant some means must be provided to initiate the quench cycle at exactly the same time in the pump cycle for each quench cycle. Recall that the signal which appears in the tank circuit during the time the pump voltage is disconnected from the SHO bears a fixed-phase relation to the pump. In a sense the pump is a master clock of the system which is always running. When these "means" are used the quench mode is described as coherent (CQM). The alternative is to allow complete phase freedom between pump and quench. This quench mode is described as incoherent (IQM). Each operating mode has its peculiarities as they affect signal detection properties. They are discussed in what follows.

6.3.2.1 Coherent Quench Mode (CQM). Assume $\theta_1$ is constrained to be a constant for each quench cycle in Eq. 6.12. The "means" used to accomplish this are incidental to the consideration and will be discussed in the next chapter on the experimental work. Under this condition A is determined in the absence of signal or noise, simply by system adjustments. If c, the fractional capacitance unbalance, is built into the system by combinations of varactor assymmetry and bias assymmetry the value of A is determined by the particular value of $\theta_1$ chosen. As various values of $\theta_1$ are chosen the variations of A are

demonstrated by what we will call here as "A Contours in $\frac{\theta_1}{2}$" (Fig. 6.3). The shape of these are determined by the factor y of Eq. 6.12. The primary effect is the large $\cos^3 \frac{\theta_1}{2}$ lobe at $\frac{\theta_1}{2} = n\pi$ radians and the gentle slope in the vicinity of $\frac{\theta_1}{2} = (2n + 1)\frac{\pi}{2}$ radians.

6.3.2.2 Errors in CQM. We can add signal information to the pump-imbalance using Eq. 6.6. To use a quantity similar to the noise power the pump-unbalance power, $P_{pu}$, is

$$P_{pu} = \frac{(c|E_p|)^2}{2} G \tag{6.13}$$

and for signal and pump-unbalance

$$A = 2\sqrt{\frac{2P_{pu}(1+\delta^2)}{G}}\left[\frac{(1 - \frac{3}{4}\delta^2)}{\sqrt{1+\delta^2}} g_m \sqrt{\frac{P_s}{P_{pu}}} \sin\left(\theta_s - \frac{\theta_1}{2} - \tan^{-1}\frac{\delta}{2}\right) - y\right] \tag{6.14}$$

Presumably the phase relationship between signal and pump can be maintained constant as $\theta_1$ of y is varied. Under these assumptions the sign of A is determined by the difference between y and the rest of the bracket quantity. The general effect is to offset the baseline of y by increments depending essentially on $P_s/P_{pu}$ for magnitude, and $\sin\left(\theta_s - \frac{\theta_1}{2}\right)$ for sign. Thus the sign of A is either all correct or all incorrect. The presence of noise confuses the situation if all effects are considered simultaneously. However, the adjustment of y to the value of zero by selecting the appropriate $\frac{\theta_1}{2}$ offers a means of separating these effects. Indeed, as we shall see in discussing experimental results,

the appearance of a spurious signal would have made limiting thresholds much more difficult to measure had it not been for this ability to inject a compensating condition by using the variation of $\theta_1$ in the coherent quenching mode.

6.3.2.3 Incoherent Quench Mode (IQM). When means for establishing each quench cycle the same value of $\theta_1$ in y of Eq. 6.8 are not provided in the system incoherent quenching prevails. This was the situation in the early experimental work before any understanding of the importance of the pump unbalance situation had been achieved. The treatment follows the analytical forms for coherent quenching when the angle $\theta_1$ is allowed to vary from quench cycle to cycle.

To visualize the variation of $\theta_1$, recall from Eq. 4.30 the pump voltage, $e_1$, for the first quench cycle.

$$e_1(1) = |E_p| \sin(2\omega_1 t + \theta_1) \tag{6.15}$$

where the parenthetical (1) denotes the first quench cycle. The quench angular frequency is $\omega_q$ and thus after a full quench period (i.e., $\frac{2\pi}{\omega_q}$ seconds) later the pump is turned on again,

$$e_1(2) = |E_p| \sin\left[2\omega_1\left(t + \frac{2\pi}{\omega_q}\right) + \theta_1\right]$$

where the initial phase angle is

$$\theta_1(2) = \left(\frac{2\omega_1}{\omega_q}\right) 2\pi + \theta_1$$

In general, the n-th quench cycle will have the initial phase angle.

$$\theta_1(n) = (n - 1)\, 2\pi \frac{2\,\omega_1}{\omega_q} + \theta_1 \qquad (6.16)$$

6.3.2.4 Error Probability in IQM. The effect of the pump unbalance in incoherent quenching is to mask the signal just as effectively as does the noise. Moreover, the pump unbalance effect can be considerably greater than the noise and as we shall see has characteristics which set it apart from the noise. Qualitatively one notes from Eq. 6.16 that when $\frac{2\,\omega_1}{\omega_q}$ is not an integer all values of the first term are possible. This is equivalent to sampling in time all the values of $\frac{\theta_1}{2}$ in Fig. 6.3. When no signal is present the sign of y is equally distributed between plus and minus. This 50-50 split is exactly the same as when thermal noise determines the phase in the absence of pump unbalance and signal.

We will now develop an expression for the error probability of signal detection for this incoherent quenching mode. Return to Eq. 6.14. Let us decide as was done in the case of noise that an error occurs when the sign of A differs from the sign of the signal term. In contrast to the noise situation the masking quantity, y, for pump unbalance has a maximum value. Thus there is a minimum value of $P_s/P_{pu}$ for which there is zero error. Identify this minimum value as $p_0$ and note that this must be just sufficient to make the left term of the bracket expression equal to unity, since $y_{max} \equiv 1$.

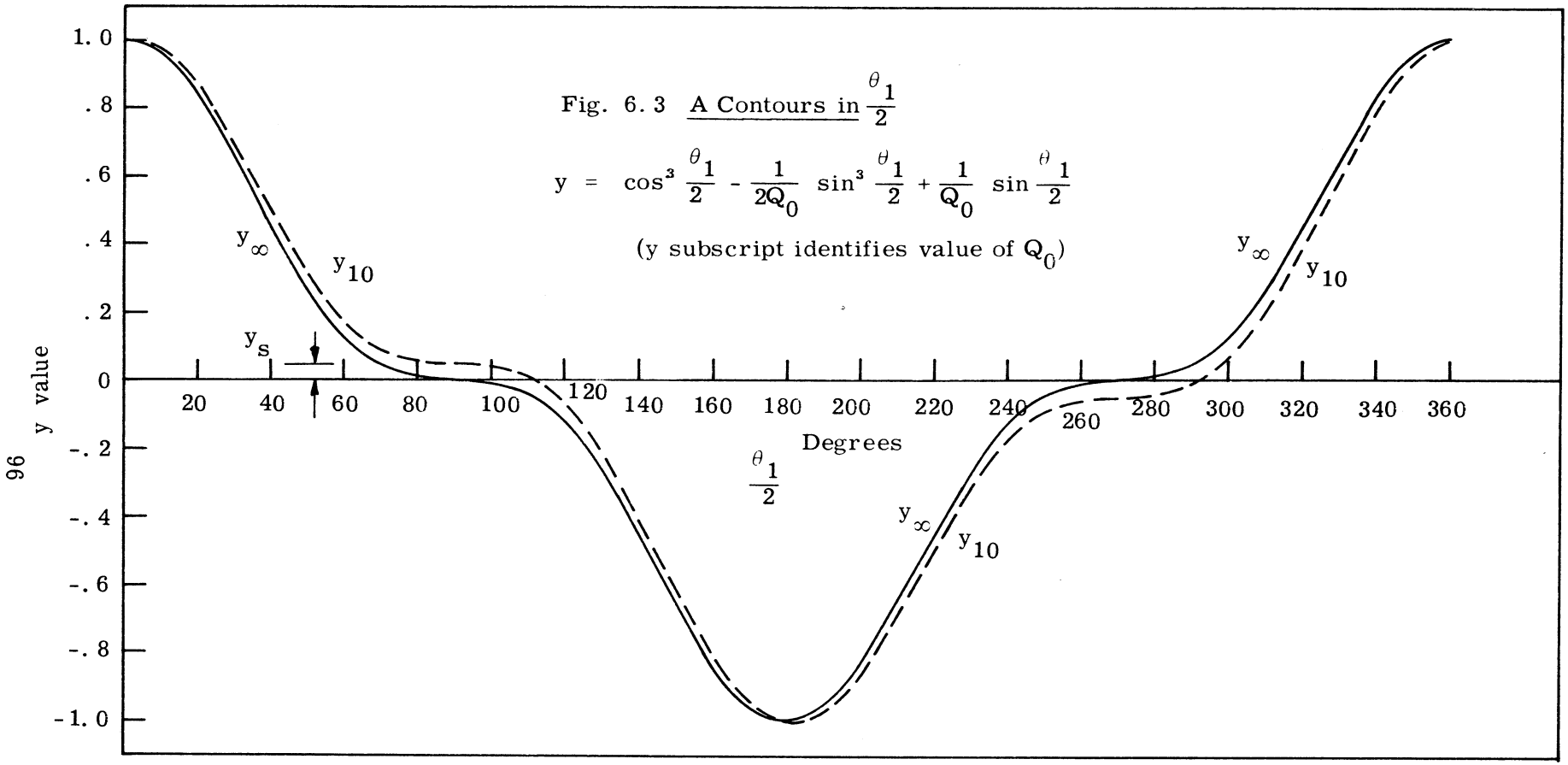


Fig. 6.3 A Contours in $\frac{\theta_1}{2}$

$$y = \cos^3 \frac{\theta_1}{2} - \frac{1}{2Q_0} \sin^3 \frac{\theta_1}{2} + \frac{1}{Q_0} \sin \frac{\theta_1}{2}$$

(y subscript identifies value of $Q_0$)

Accordingly

$$\frac{\left(1 - \frac{3}{4}\delta^2\right)}{\sqrt{1+\delta^2}} g_m \sqrt{p_o} \sin\left(\theta_s - \frac{\theta_1}{2} - \tan^{-1}\frac{\delta}{2}\right) = 1 \qquad (6.17)$$

Now assuming that the system adjustments (tuning, gain, $\left(\theta_s - \frac{\theta_1}{2}\right)$ are being held constant and that the signal terms are positive, an error will occur when:

$$\sqrt{\frac{P_s/P_{pu}}{p_o}} < y \qquad (6.18)$$

As $P_s/P_{pu}$ is reduced below $p_o$, decimal fractions are generated. When this is expressed in decibels the correspondence is given in Table 6.I below.

| $\frac{P_s/P_{pu}}{p_o}$ in db | $\sqrt{\frac{P_s/P_{pu}}{p_o}}$ |
|---|---|
| 0 | 1.000 |
| -0.1 | 0.989 |
| -0.2 | 0.977 |
| -0.5 | 0.943 |
| - 1 | 0.896 |
| - 2 | 0.796 |
| - 5 | 0.563 |
| -10 | 0.316 |
| -20 | 0.100 |
| -30 | 0.032 |
| -40 | 0.010 |

The error probability is obtained by applying the fraction of Table 6.I, and the criterion of Eq. 6.16 to the particular A contour of Fig. 6.3 applicable to the system construction and adjustment. Although the analytical form for y does not lend itself to this manipulation the graphical approach is very direct. For a particular ordinate $\left(\sqrt{\frac{P_s/P_{pu}}{p_o}}\right)$ the width of the A contour is measured in $\frac{\theta_1}{2}$ units and compared with $2\pi$ radians ($360^o$). The fraction is the error probability. Figure 6.4 presents these calculations based on the two contours given in Fig. 6.3 and a third one based on a spurious signal $y_s$ present in the $y_{10}$ contour. This latter represents the kind of situation which might be encountered in an operating situation.

Two significant differences separate the effects of thermal noise from pump unbalance as seen in incoherent quenching. The first is the slope of the error probability curve for low-error rates. The thermal noise, characterized by a Gaussian distribution presents a finite probability of error at increasing ratios of signal-to-noise. As evidenced by Eq. 6.15 the error probability for pump unbalance approaches a definite value of signal-to-pump unbalance as an asymptote. The other basic difference is the production of a jog in the curve of error probability vs. signal-to-pump unbalance due to the condition of zero slope at $\frac{\theta_1}{2} = \frac{\pi}{2}$ radians. Small increases in signal-to-pump unbalance cause large changes in error probability.

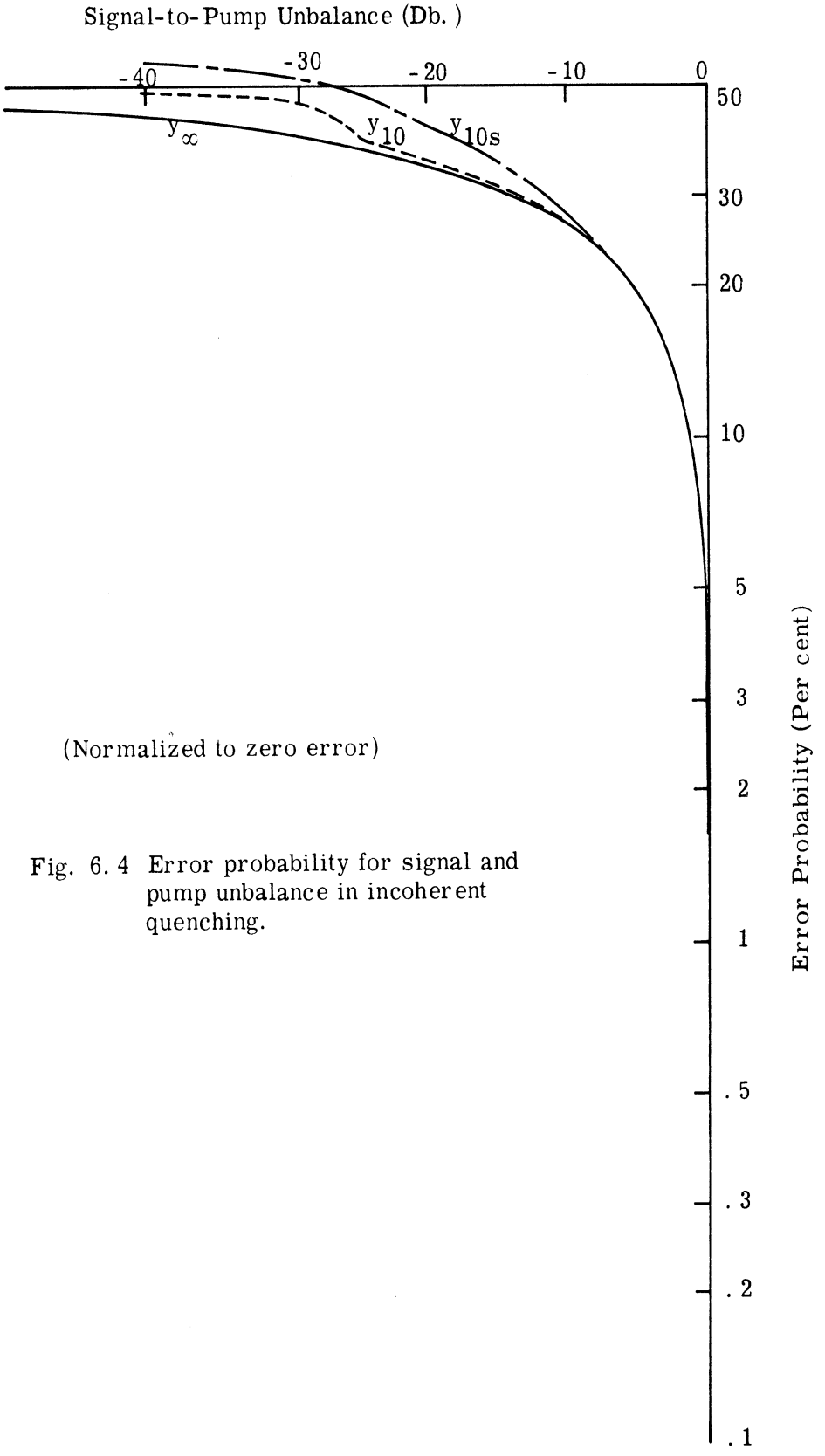


(Normalized to zero error)

Fig. 6.4 Error probability for signal and pump unbalance in incoherent quenching.

# CHAPTER VII

## EXPERIMENTAL WORK

### 7. 1 Objectives Related to Study

The objectives of the experimental phase of the study are summarized by the following four statements:

To demonstrate:

1. Basic properties of a parametric amplifier operating in the quasi-degenerate, and degenerate modes.

2. Properties of the associated parametric sub-harmonic oscillator.

3. Quantitative relationships of phase synchronization by a signal in the presence of thermal noise, including the error probability.

And to determine:

4. The effects of incoherent and coherent quenching as they relate to the phase synchronization process.

### 7. 2 Circuit Descriptions

7. 2. 1 General. The experimental layout for the study is shown in Fig. 7. 1. The sub-harmonic oscillator, SHO, in the center receives energy at angular frequency, $2\omega_1$, through the quench switch from the pump oscillator. The nominal pump frequency for the study was $10^6$ Hz. The quench switch, controlled by the quench oscillator allows periodic application of pump energy to the SHO. The pump oscillations are counted down; by 2 to provide a signal frequency; and then by 128 more to provide

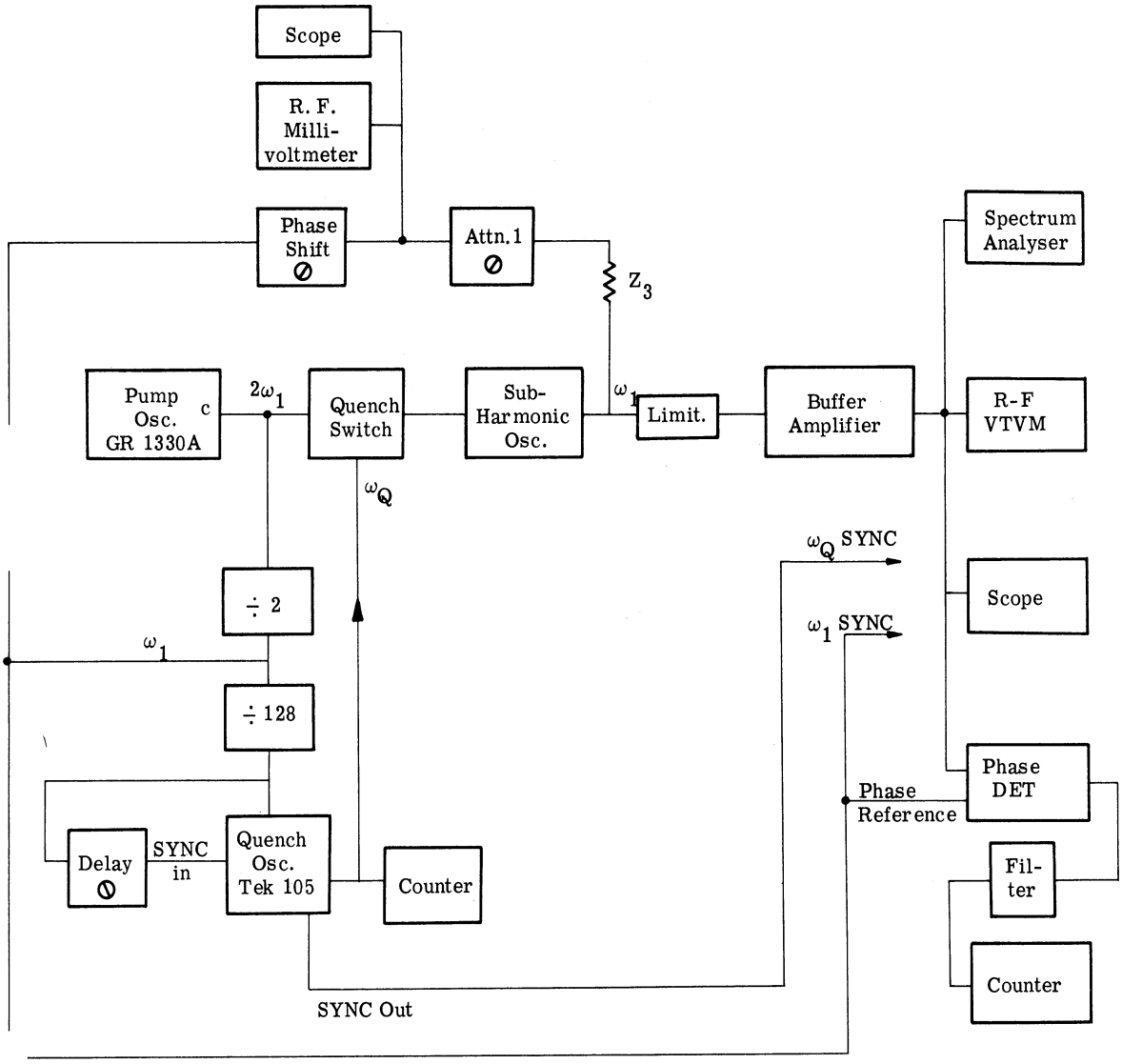


Fig. 7. 1 Block diagram of experimental layout for phase synchronization study.

a fixed time relationship between the start of the pump and the start of the quench. Attenuators and phase shift circuits in each line allow independent adjustment of the phase difference along the appropriate line.

The output of the SHO is fed through a limiting circuit and buffer amplifier and on to the various points of observation such as oscilloscope, VTVM, etc. It is interesting to note that the input and output are connected to the same point in the SHO circuit. The common point functions as the input before pumping starts and as the output after pumping starts. Time references for $\omega_1$ and $\omega_Q$ are taken from the pump and counting circuits.

Of particular significance in the entire circuitry is the flow of information to the right, through the SHO, and, because the ultimate signal levels are so low compared with the operating levels of the circuitry, the paths back to the SHO. The backward paths provide undesired signal coupling and tend to mask the final measurements.

Each block is discussed in detail below.

7. 2. 2 SHO Circuit. The two circuits tested in this study are given in Figs. 7. 2a and 7. 2b. The basic configuration is parallel resonant, being tuned approcimately to . 5 megacycles per second. The variable reactance elements are $D_1$ and $D_2$, which are Pacific Semiconductor Type 27E "Varicaps." This varactor has a nominal value of 27$\mu\mu$f at -4 volts and a range of 7-70$\mu\mu$f. The two circuits differ in the back-biasing technique. The original circuit uses Mallory RM1-R cells having a fixed output of about 1. 35 volts. The pump-unbalance study revealed

Fig. 7. 2 SHO Circuits.

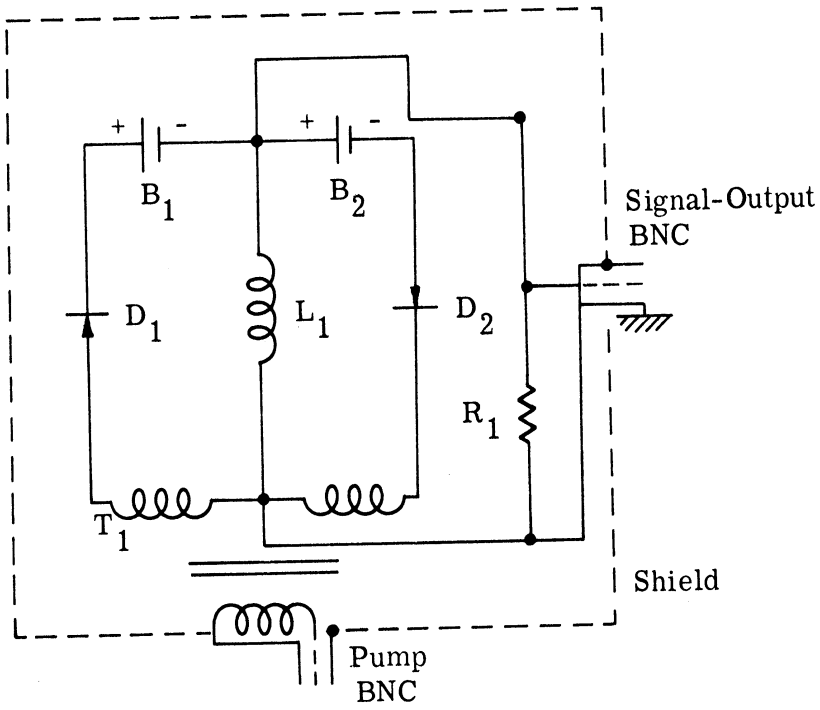


(a) Fixed Bias-initial design

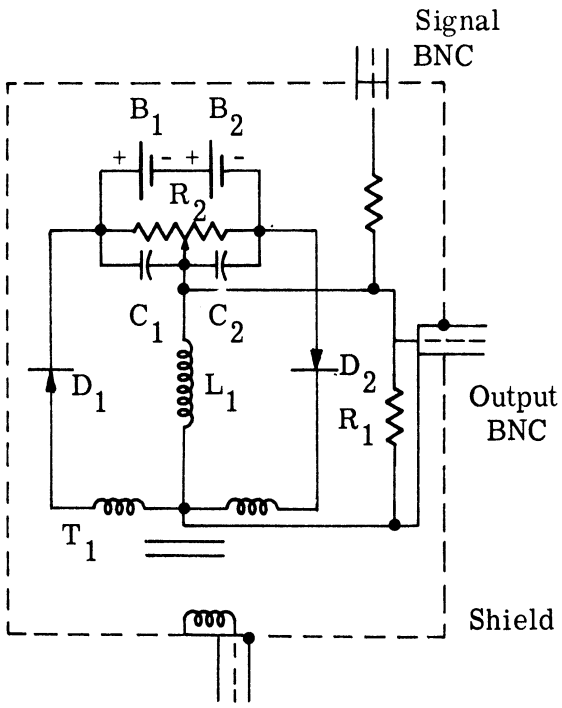


(b) Differential Bias, for variable pump unbalance.

small difference in $D_1$ and $D_2$ which are compensated by the differential bias circuit of Fig. 7. 2b. In this latter circuit it is possible by adjusting $R_2$ to balance out the pump voltage appearing across the circuit. $T_1$ is a small ferrite toroidal transformer designed to give a 1:1 "unbalanced-to-balanced" transformation. A separate signal BNC is incorporated in the circuit of Fig. 7. 3 in order to establish within the shield box the final attenuated signal level. The resistance $R_1$ is an arbitrarily applied load resistance. Its value is low enough to dominate the usual loads of high impedance measuring devices and to control the aggregate circuit Q.

Measurements made on the assembled circuit are given below:

| | |
|---|---|
| Resonant frequency | 482. 2 KHz |
| Loaded Q | 10. 8 |
| Equivalent circuit resistance | 14. 8 Kilohms (Conductance = 67. 6 $\mu$mhos) |
| Circuit inductance | . 45 mhy |
| Equivalent $Z_3$ | 565 Kilohms |

The complete assembly is enclosed in an aluminum shield box as shown in the closeup, Fig. 7. 3.

7. 2. 3 Quench Switch. The quench switch is designed to operate with the Tektronix Type 105 square-wave generator to produce electronic interruption of the 1 megacycle pump energy into the SHO. Fig. 7. 4 gives the details of the circuit. The transistor chosen is a 300 mc unit which is capable of shutting off the pump well within a single cycle. The external positive voltage provides the back bias necessary to assure $Q_1$ being "off" when the pump is to be "on. " The characteristic of the Type 105 square-wave generator provides essentially zero volts during part of the cycle, and an adjustable negative voltage during the alternate part of the cycle.

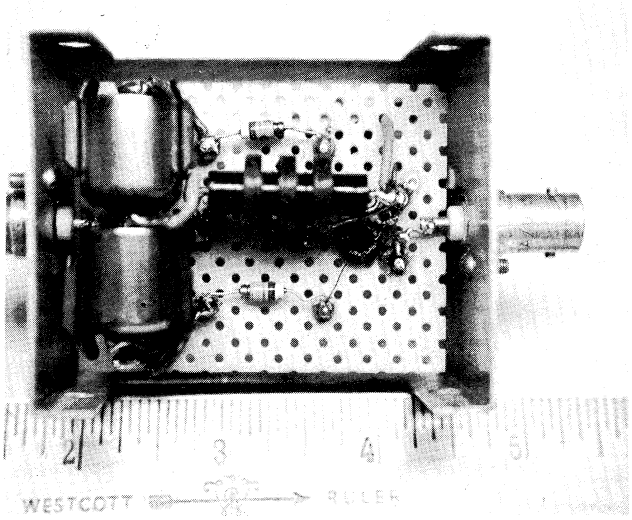


Fig. 7.3 Sub-Harmonic Oscillator Assembly

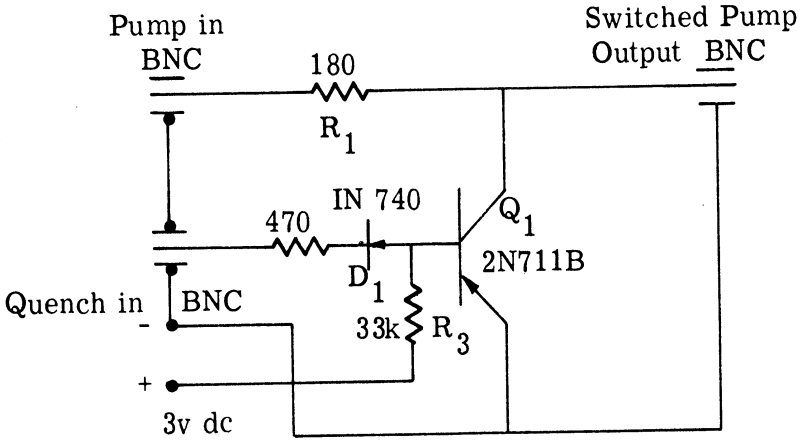


Fig. 7. 4 Quench Switch

7. 2. 4 Quench-Pump Synchronization. The need to provide fixed relationships between the start of the pump and the start of a quench cycle necessitated the use of a counting-down process to derive the quench trigger. The first scale-of-two provides the angular frequency $\omega_1$. Harvey-Wells modules provided this and the remainder of the flip-flops required to derive a trigger pulse every 256 pump cycles. In order to allow this trigger to start the quench cycle at any arbitrary point of the pump cycle a continuous delay of 0 to 2 microseconds is used (Harvey-Wells Delay C Module) between the counters and the external trigger point of the 105 square wave generator. In some parts of the experimental work extremely low quench frequencies were used, and it was found helpful to provide external trigger pulses less often. For example, the count of 256 provides about 3750 trigger pulses per second. If the desired quench frequency is 100 Hz there will be 37+ trigger pulses each quench cycle. This large number is sufficient to cause considerable difficulty in effecting the solid synchronization needed. An additional count of 2, 4, 8, or 16 was used for the very low quench frequencies so that, at most, only a few trigger pulses occurred each quench cycle.

7. 2. 5 Signal Generation. The seed signal is at exactly $\omega_1$ radians per second and is derived from the Harvey-Wells modules counting down the pump frequency of $2\omega_1$ radians per second. The phase relationship between pump and signal is a dominant parameter [$(\theta_S - \frac{\theta_1}{2})$ as per equation 5. 38] and is adjusted, in steps and continuously between steps, by the delay mechanisms shown in Fig. 7. 5. The various resistances

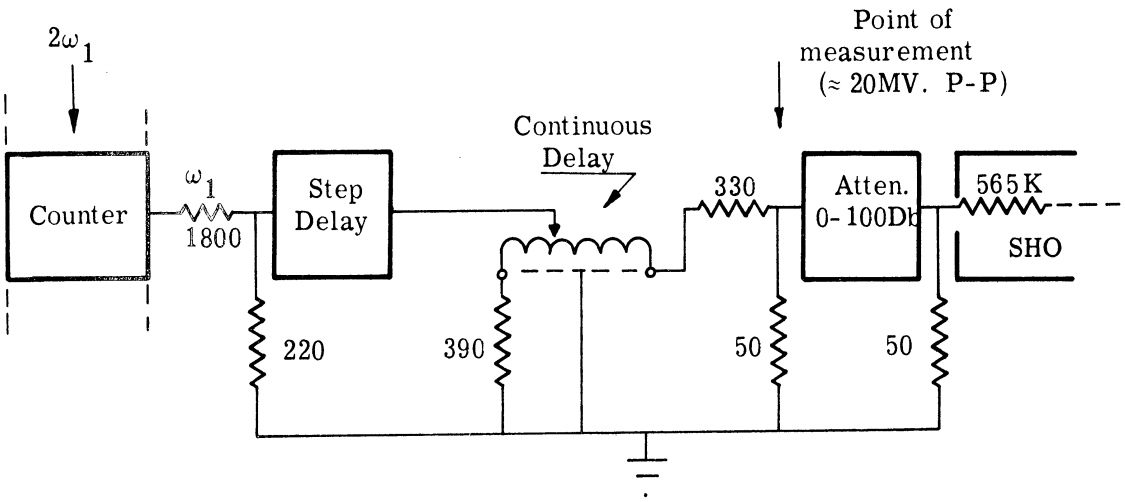


Fig. 7.5 Signal Attenuation and Delay.

used are to accomodate loading levels and impedance requirements of the counting and delay components. The step delay box is Type 602 from Advance Electronics Co., and provides .25 micro-second per step in 10 steps. This amounts to about $\pi/4$ radians of the signal frequency per step. The continuous delay is Type 509 also from Advance Electronics and has a full scale delay of 1 micro-second.

The signal level is monitored at the input to the 100 Db attenuator. At this point the square wave from the Harvey-Wells counter is reduced about 46 Db from the original 4 volt, peak-to-peak value. The value of signal at the output of the attenuator is reduced by the attenuator setting and considered further as a square wave entering the resonant circuit of the SHO via 565 Kohms located within the SHO box. Since the resonant impedance presented by the SHO is of the order of 15 Kohm ($<<$ 565K) the signal is injected essentially as a current. The resonant circuit develops a voltage at only $\omega_1$. The details of the calcuations follow later in paragraph 7.4.3.1.

7.2.6 Buffer Amplifier. The output of the SHO, also being the input, must be carefully isolated from all the measurement and observation circuits since these circuits use large signals having components at signal frequency as time references. The isolation device used was the Hewlett-Packard Model 450A amplifier operating in the 20 Db (x10) gain position. The output is limited to ± 10 volts. In order to insure that the input never exceed 1 volt a pair of silicon diodes was used across the SHO for some of the measurements.

7. 2. 7 Phase Detector. The final question during any one quench cycle is "which of the two possible phase states actually occurred?" During the initial stages of the investigation it was sufficient to answer this question by observing the SHO output on an oscilloscope which was externally triggered by a voltage at $\omega_1$ radians per second. As the number of trials required became greater and as the ability to make the trials rapidly was realized through the use of electronic quenching a new scheme was required. Thus the particular variety of phase detector suitable to this problem was developed. It is shown in block diagram form in Fig. 7. 6 and schematicly in Figs. 7. 7 and 7. 8. The input oscillation is isolated by an emitter follower, amplified and limited to a standard voltage form similar to that used in the Harvey- Wells modules. At the detector stage the signal voltage is compared through a simple "AND" logic circuit with a reference phase taken from the counter which supplies signal information . The output is isolated and inverted by a final stage. When the signal and reference disagree in phase the output is a 15 volt square wave at frequency $\omega_1$. When the signal and reference disagree in phase the output is zero volts. When filtered by two simple R-C stages the average output is -7. 5 volts for agreement, and zero volts for disagreement.

In the case of rapid quench cycles at frequency $f_q$ cycles per second, a counter observing the output of the filter will count successes, $f_s$. The errors are, of course, $f_q - f_s$. After a great many trials we see that the error probability will approach the average value of $\frac{f_q - f_s}{f_q}$.

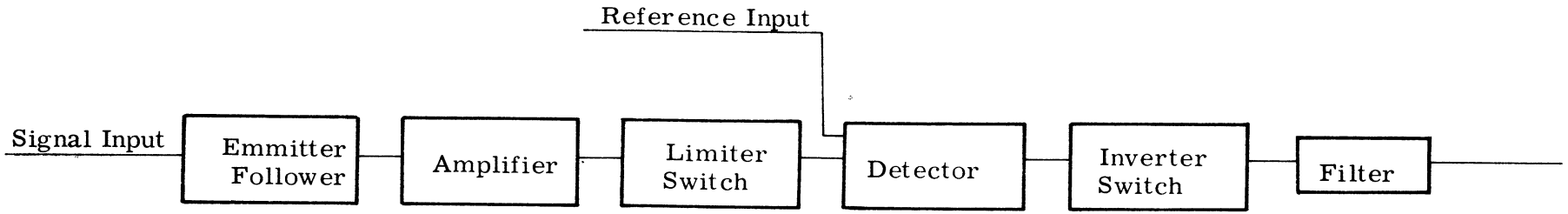


Fig. 7.6 Phase detector block diagram.

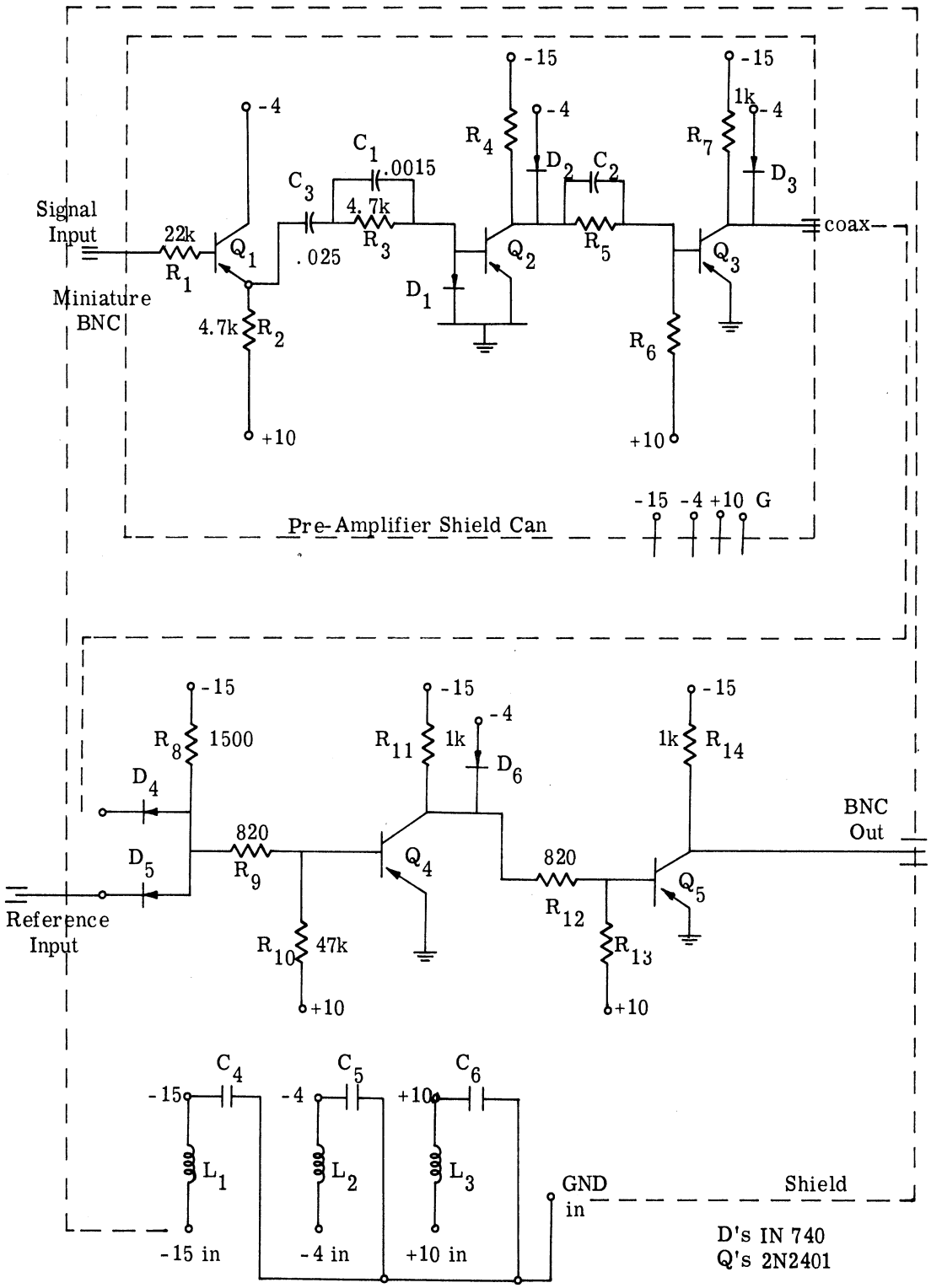


Fig. 7.7 Phase sensitive detector schematic.

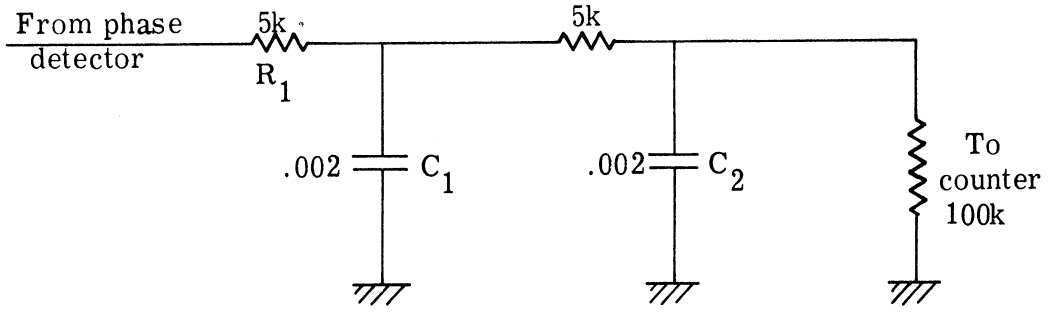


Fi. 7. 8 Detector filter.

## 7. 3 Laboratory Methods

7. 3. 1 Setting the Value of $g_m$ In all of the experimental work where quantitative measurements are made it is necessary to know the value of $g_m$ the steady state gain term. The method used exploits the appearance of the gain in the growing exponential. After the decaying exponential term has disappeared we note from equation 5. 1 that the envelope of the circuit voltage is:

$$V_{envelope} = A\epsilon^{\mu_g \omega_1 t} \tag{7.1}$$

If we make two observations of the envelope the ratio of their amplitudes at times $t_1$ and $t_2$ is:

$$\frac{V_2}{V_1} = \epsilon^{\mu_g \omega_1 (t_2 - t_1)} \tag{7.2}$$

Now arbitrarily select $V_2/V_1$ to be a simple value, 2, and solve 7. 2 for the spacing in time, $(t_2-t_1)$:

$$(t_2-t_1) = \frac{\log \frac{V_2}{V_1}}{\mu_g \omega_1 \log \epsilon} \tag{7.3}$$

$\mu_g$ contains the gain term and is found by noting:

$$\mu_g = \mu - \mu_L$$

For the tuned case

$$\mu = \frac{\eta}{4} \qquad \mu_L = \frac{1}{2Q_0}$$

$$\Pi = \frac{\eta Q_0}{2} \qquad g_m = \frac{1}{1 - \Pi^2} \tag{7.4.}$$

After appropriate substitutions

$$\mu_g = - \frac{1}{4Q_0 g_m}$$

(recall that $g_m$ is negative in the oscillating region), and (7.5)

$$(t_2 - t_1)_{x2} = - \frac{4Q_0 \log 2}{\omega_1 \log \epsilon} g_m$$

Using the parameters in 7.2.2 the value of the time interval $(t_2 - t_1)$ to <u>double</u> the envelope is:

$$(t_2 - t_1)_{x2} = (9.88 \cdot 10^{-6}) |g_m|$$

$$(t_2 - t_1)_{x2} \cong 10 |g_m| \text{micro-seconds.} \tag{7.6}$$

This is remarkably simple to perform in the laboratory. If a gain of 10 is desired the circuit is carefully tuned, and then the pump level is adjusted until 100 $\mu$ seconds are required to double the envelope. Care must be taken to insure that the measurement is made well below saturation. Fig. 7.9 showing the increasing waveform on a time scale of 20 $\mu$ sec / cm demonstrates the SHO with a steady state gain term of 10.

<u>7.3.2 Measurement of $\mu$.</u> Evaluation of $\mu$ follws from 7.4

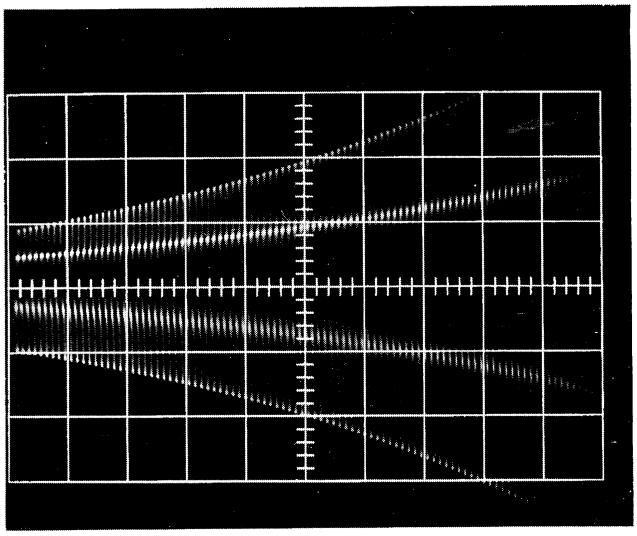

time base 20 $\mu$sec/major div.

Fig. 7.9 Evaluation of $G_m$

For the tuned case

$$\mu = \frac{\eta}{4} \qquad \mu_L = \frac{1}{2Q_0}$$

$$\Pi = \frac{\eta Q_0}{2} \qquad g_m = \frac{1}{1 - \Pi^2} \tag{7.4.}$$

After appropriate substitutions

$$\mu_g = - \frac{1}{4Q_0 g_m}$$

(recall that $g_m$ is negative in the oscillating region), and (7.5)

$$(t_2 - t_1)_{x2} = - \frac{4Q_0 \log 2}{\omega_1 \log \epsilon} g_m$$

Using the parameters in 7.2.2 the value of the time interval $(t_2 - t_1)$ to double the envelope is:

$$(t_2 - t_1)_{x2} = (9.88 \cdot 10^{-6}) |g_m|$$

$$(t_2 - t_1)_{x2} \cong 10 |g_m| \text{ micro-seconds.} \tag{7.6}$$

This is remarkably simple to perform in the laboratory. If a gain of 10 is desired the circuit is carefully tuned, and then the pump level is adjusted until 100 $\mu$ seconds are required to double the envelope. Care must be taken to insure that the measurement is made well below saturation. Fig. 7.9 showing the increasing waveform on a time scale of 20 $\mu$ sec / cm demonstrates the SHO with a steady state gain term of 10.

7.3.2 Measurement of $\mu$. Evaluation of $\mu$ follws from 7.4

$$\mu = \mu_g + \mu_L = \mu_L \left( 1 + \frac{1}{2g_m} \right)$$

$$\mu_L = \frac{1}{2(10.8)} = .0463 \qquad (7.7)$$

$$\mu = .0463\left(1 + \frac{1}{2g_m}\right)$$

The gain values used in the experimental work ranged from 5 to 100. Over this range $\mu$ varies only slightly from .051 to .0466

## 7.4 Results

The following paragraphs relate directly to the objectives of 7.1.

7.4.1 Basic Properties of Amplifier. When the configuration of Fig. 7.1 is pumped below the level of oscillation the seed signal is amplified. If the seed signal at $\omega_1$ radians/sec. is in the preferred phase position it will be amplified depending on the exact pump level. If the signal is $\frac{\pi}{2}$ radians from the preferred position the signal is attenuated. The theoretical description for the tuned degenerate case is obtained from Equ. 4.24 and is:

$$v_{ss}(t) = \frac{g_m}{G} |I_s| \left[ \cos(\omega_1 t + \theta_s) - \Pi \cos(\omega_1 t + \theta_1 - \theta_s) \right]$$
$$\delta = 0 \qquad (7.8)$$
$$\zeta' = 0$$

The preferred signal phase by inspection is where:

$$(\theta_1 - \theta_s) = \theta_s + \pi \qquad (7.9)$$

In this condition a maximum steady-state term results and is:

$$v_{ss}(t)_{max.} = \frac{g_m}{G} |I_s| (1 + \Pi) \cos(\omega_1 t + \theta_s)$$

$$\cong \frac{2g_m}{G} |I_s| \cos(\omega_1 t + \theta_s) \qquad (7.10)$$

(since $\Pi \approx 1$)

Recall from Eq. 4.1 that the degenerate signal is

$$i_s(t) = |I_s| \cos(\omega_1 t + \theta_s)$$

and that the pump voltage producing the capacitance variations from Eq. 4.3 is:

$$e_1 = |E_p| \sin 2(\omega_1 t + \theta_1)$$

Using the constraint for maximum response, i.e., (7.9)

$$e_{1_{\substack{resp. \\ max.}}} = |E_p| \sin 2(\omega_1 t + \theta_s + \frac{\pi}{2}) \qquad (7.11)$$

Fig. 7.10 demonstrates these time relationships. Note that the signal and steady-state response are in-phase and so related to the pump that the response nodes ($\omega_1 t + \theta_s = \frac{\pi}{2} + n\pi$) occur at positive slope nodes of the pump and the response peaks ($\omega_1 t + \theta_s = n\pi$) occur at negative slope nodes of the pump. Checking Eq. 7.11 for $(\omega_1 t + \theta_s) = (\frac{\pi}{2} + n\pi)$:

$$e_{1_{\text{response nodes}}} = |E_p| \sin 2(n+1)\pi = 0 \text{ (i.e. nodes)} \qquad (7.12)$$

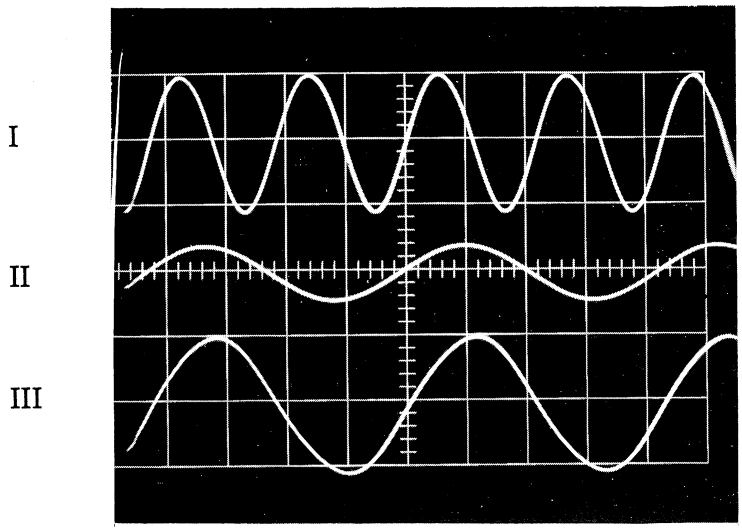


Fig. 7. 10 Maximum Steady State Response

I Pump . 5v / cm

II Signal . 05 v/ cm

III S.S. Response . 2 v/ cm voltage gain = 10 ($G_m$ = 5) time base . 5$\mu$ sec/ cm

$$\dot{e}_1 = 2\omega_1 |E_p| \cos 2(\omega_1 t + \theta_s + \frac{\pi}{2})$$

$$\dot{e}_1 = 2\omega_1 |E_p| \cos 2(n+1)\pi = 2\omega_1 |E_p| \text{ (i.e. positive slope)} \qquad (7.13)$$

and for $(\omega_1 t + \theta_s) = n\pi$

$$e_1 = |E_p| \sin (2n+1)\pi = 0 \text{ (i.e. nodes)} \qquad (7.14)$$

response peaks

$$\dot{e}_1 = 2\omega_1 |E_p| \cos (2n+1)\pi = -2\omega_1 |E_p| \text{ (i.e. negative slope)} \qquad (7.15)$$

response peaks

When the signal is adjusted $\frac{\pi}{2}$ signal radians with respect to the pump the output is a minimum. The theoretical condition by inspection of Eq. 7.8 is $(\theta_1 - \theta_s) = \theta_s$ (i.e. $\theta_1 = 2\theta_s$). Accordingly the steady-state response becomes

$$v_{ss}(t)_{\text{min.}} = \frac{g_m}{G} |I_s| (1 - \Pi) \cos (\omega_1 t + \theta_s)$$

and recalling Eq. 4.14

$$\cong \frac{|I_s|}{2G} \cos (\omega_1 t + \theta_s) \qquad (7.16)$$

With respect to the signal the pump has shifted so that

$$e_{1_{\text{resp.}}}_{\text{min.}} = |E_p| \sin 2(\omega_1 t + \theta_s)$$

Referring to Fig. 7.11 for this condition, response nodes ($\omega_1 t + \theta_s = \frac{\pi}{2} + \eta\pi$) correspond to negative slope nodes of the pump, and response peaks correspond to positive slope nodes of the pump.

The minimum condition here is actually a loss($g_m = 1/2$). Small departures from the minimum phase position present signals having a component in the preferred phase and thus experience the gain of the system. The phase shift of the response with respect to the pump is apparent only when the signal in the preferred position actually goes to zero. The degenerate amplifier acts like a phase selective amplifier, --amplifying the signal component in the preferred phase and attenuating the signal in the quadrature phase.

The ratio of the maximum to minimum responses due to signal phase change alone is of some interest. Using Eq. 7.10 and 7.16.

$$\frac{v_{ss_{max.}}}{v_{ss_{min.}}} = 4g_m$$

Since $g_m$ can be arbitrarily large, the signal phase has a profound effect on the steady state ouput of the device. *

Figs. 7.13 and 7.14 demonstrate the same properties described above using a much higher adjusted circuit gain. The device is on the threashold of oscillation and the effect of the phase position of the signal is very pronounced.

---

*In stark constrast with statements of Bura in Ref. 17 .

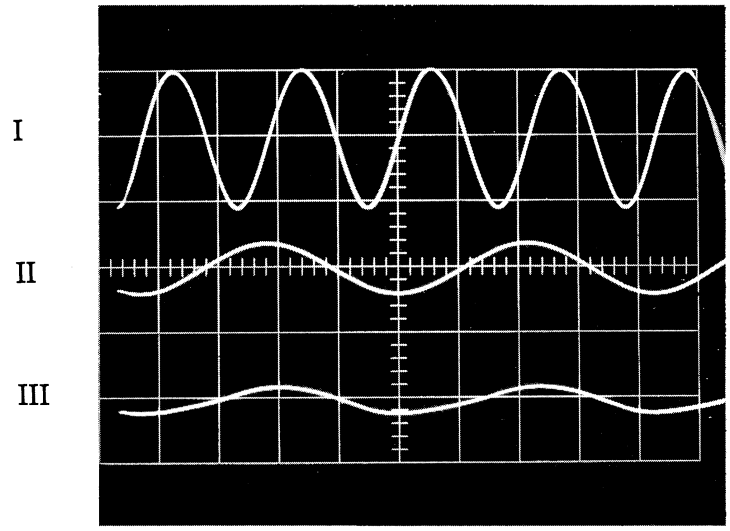


Fig. 7. 11 Minimum Steady State Response

I Pump . 5 v/ cm

II Signal . 05 v/ cm

III Response . 05 v/ cm voltage gain
Time-base . 5 $\mu$sec/cm = 1/2

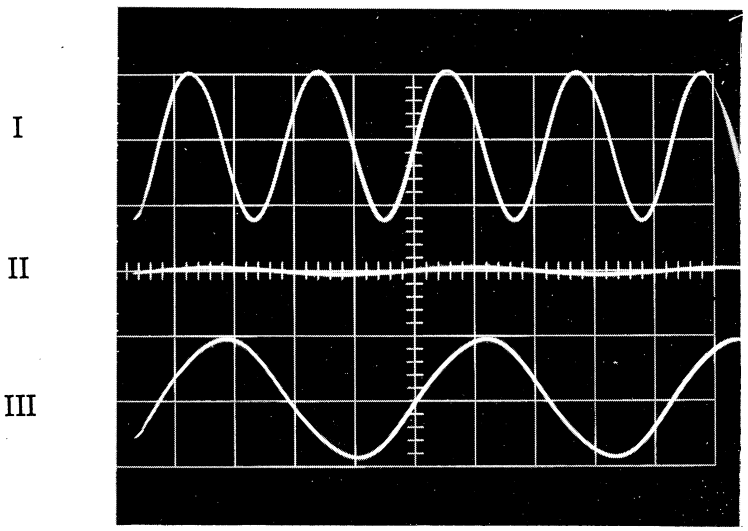


Fig. 7. 12 Maximum Steady State Response - High Gain

I Pump . 5 v/ cm

II Signal . 05 v/ cm

III Response . 2 v/ cm voltage gain 72 ($G_m$ = 36)
Time base . 5$\mu$ sec/ cm

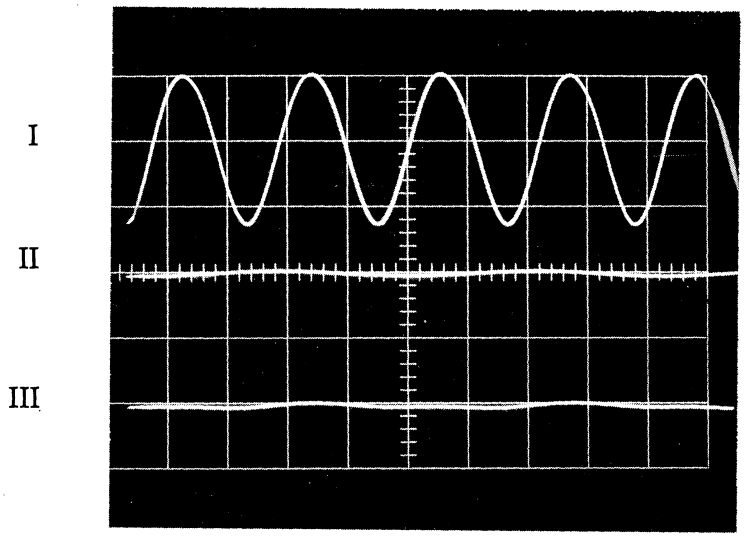


Fig. 7. 13 Minimum Steady State Response - High Gain

I Pump . 5v/ cm

II Signal . 05v/ cm

III Response . 2v/ cm
Time base . 5$\mu$ sec/cm

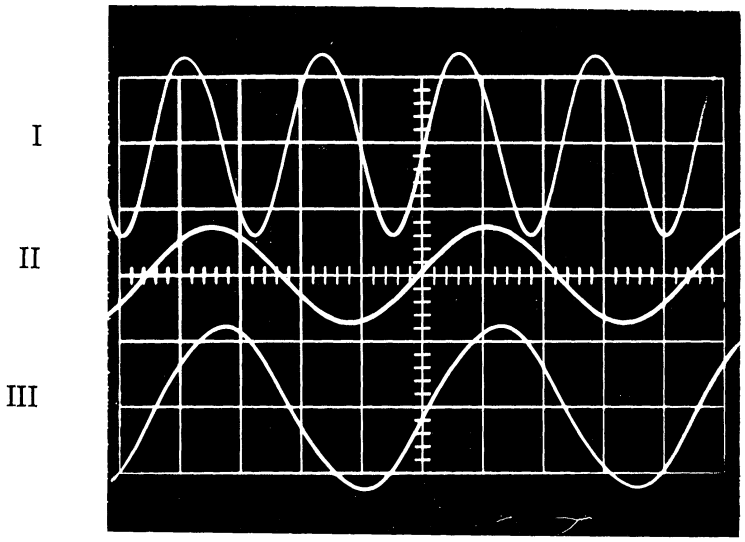


Fig. 7.14 Sub-Harmonic Oscillation in Growing Region

I Pump . 5 v/cm

II Signal . 01 v/cm

III Response . 5 v/cm, 1/3 saturation value

### 7. 4. 2 Properties of the Associated SHO

7. 4. 2. 1 General. As the pumping parameter $|\Pi'|$ increases toward unity the amplifier gain increases toward positive infinity. As the point 1 is passed $g_m$ becomes negative and decreases in absolute value as $|\Pi'|$ increases. As shown in Fig. 4. 2 the region beyond unity is the oscillating region, and the transient solution possesses a positive exponent. When a dominant signal is present in the circuit before the oscillation begins the oscillation will assume the phase of the signal. Fig. 7. 14 shows the signal and grown oscillation in phase and related to the pump exactly as was the steady-state response. The magnitude continues to grow until the conditions for growth are balanced by non-linearities in the system. The mechanisms for this large-signal behavior are amply treated in other works (Refs. 21, 25 and 46). It is sufficient to observe here that the final phase position slightly lags the transient portion of the oscillation. This will be evident in some of the oscilloscope pictures which follow.

7. 4. 2. 2 Bistate Phase Positions. Equation 5. 36 gives the coefficient, A, of the growing exponential. The sign of A is determined by the instantaneous sum of signal effects whether these effects are desired or undesired (noise). The magnitude observed at any point in the growth interval depends on the initial magnitude. A noise input, having a distribution of magnitudes and signs, will cause a cloud of rising exponentials. Each has its nodes at the same points relative to the pump waveform. This is pictured at three successively higher pump levels in Figs. 7. 15 to 7. 17.

I

II

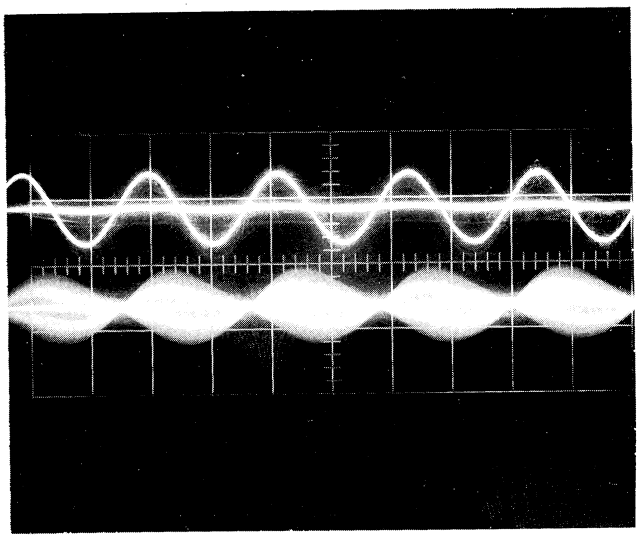

I Pump 1 v/ cm

II Output 10 mv/ cm

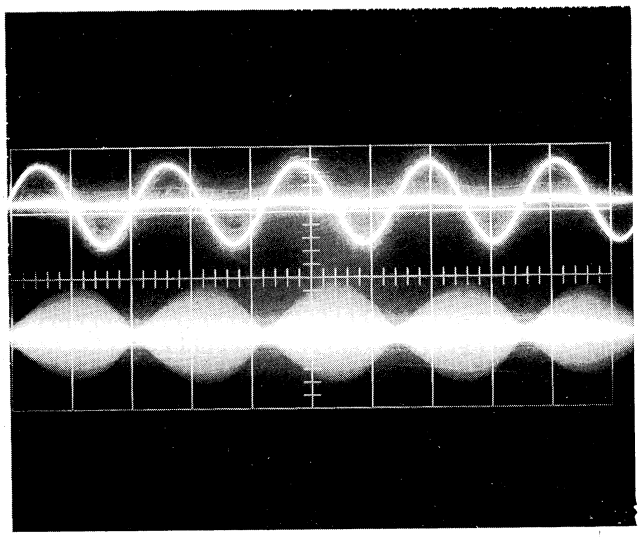


Fig. 7.16 Moderate level amplification of noise.

I Pump 1 v/cm

II Output .2 v/cm

I

II

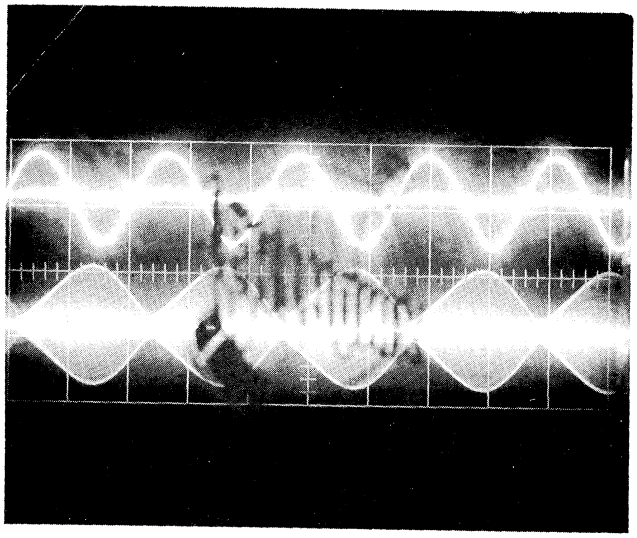

Fig. 7. 17 Sub-harmonic oscillation.

I Pump 1 v/ cm

II SHO 2 v/ cm time base . 5$\mu$ sec/ cm

Fig. 7. 15 trace I shows the pump in the two states controlled by the quench switch. Trace II shows the noise amplified only slightly, i. e. an oscillation is not occurring because the pump level is not quite high enough. The noise, occurring with random magnitude and phases experiences gain in only the preferred phase. However both signs appear. Fig. 7. 16 has a slightly higher pump level, and consequently higher gain. Fig. 7. 17 results when the pump level is increased just to the oscillation state. The darker extreme traces of the SHO trace show the oscillation has saturated. The background cloud includes all the rising exponentials of the superimposed traces.

7. 4. 2. 3 Effect of Pump Level on Output. For the tuned case the magnitude of the positive exponent in the growing portion of A is given by equation 7. 5. For small variations in pump level within the oscillating region the more pronounced effect is the inverse relation between pump and gain, and thus the direct relation between $\mu_g$ and pump. This is demonstrated by the waveforms in Fig. 7. 18.

7. 4. 2. 4 Effect of Tuning on $\mu_g$. Fig. 3. 3 for a constant pump level, $\eta$, shows the variation of $\mu$ with detuning. Recalling that a = 1 is the tuned situation, the approximate symmetry of the plot shows decreasing $\mu$ for detuning in either direction. For the experimental work the tuning was accomplished by varying the pump frequency to produce the fastest rise. This procedure is very sensitive to detuning and becomes very simple to perform.

7. 4. 2. 5 Effect of Signal Level on Output. When the signal level is significantly above the noise the major manifestation when viewing an

I

II

III

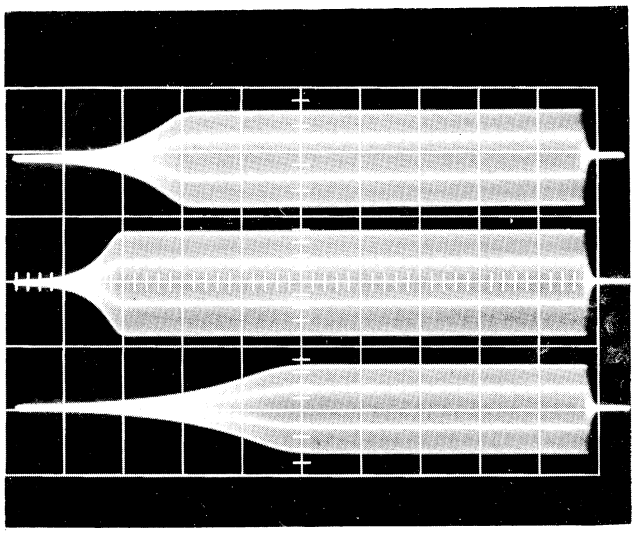

Fig. 7. 18 Gain Variation with pump level.

I Gain 10

II Gain 5

III Gain 20

entire quench cycle is the control of the location of the rising portion on the time axis. The value of A determines the initial value of the exponential, the rising shape being the same. If the oscillation is allowed to saturate a simple model (Ref. 11) shows the quench envelope to be proportional to the logarithm of the signal. Thus the term "logarithmic mode" of operation is understood. When the signal is varied over a 60 Db range in 10 Db steps a linear variation of the location of the rising portion results. Fig. 7.19 demonstrates this property. For a -60 Db signal, (below an arbitrary reference) noise influences the start of the exponential in a random manner as evidenced by the haze on the exponential.

7.4.2.6 Effect of Signal Phase on Output. We have seen in paragraph 7.4.1 how the steady state gain depends upon the phase relationship between pump and signal. Now we see the corresponding variation of the output of the sub-harmonic oscillator for signal phase variation. In Fig. 7.20 if we describe "0" phase as the phase adjustment to give maximum response (as per equation 5.40), variations to $\frac{\pi}{2}$ produce output variations as shown. Note the appearance of the noise when the signal phase is in quadrature to the preferred phase.

7.4.2.7 Coherent Quenching. A development of particular significance to this study has been the matter of coherent quenching. Coherent quenching is achieved when, on successive quench cycles, the pumping begins with exactly the same pump phase angle. For this case not only is the value of A determined, but also the instantaneous value of the growing oscillation is determined. Thus each cycle of the oscillation will track on

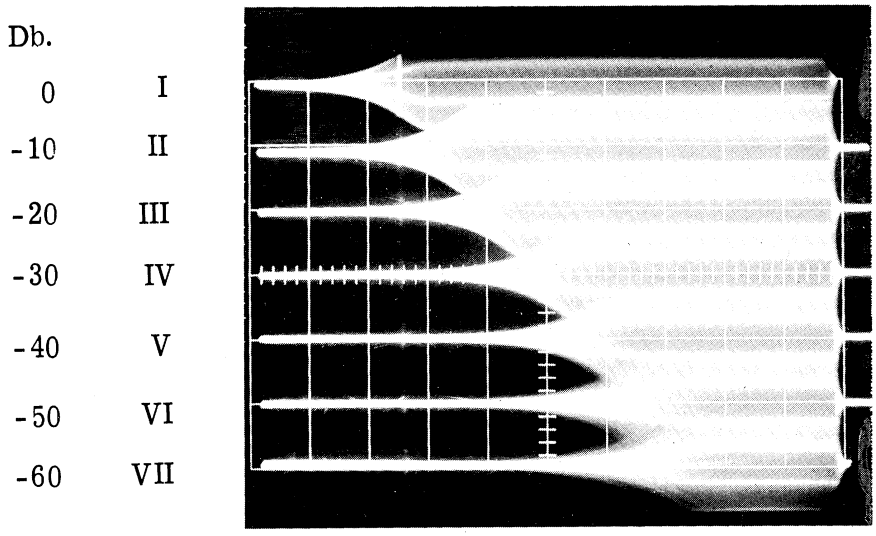


Fig. 7. 19 Output variation with signal level.

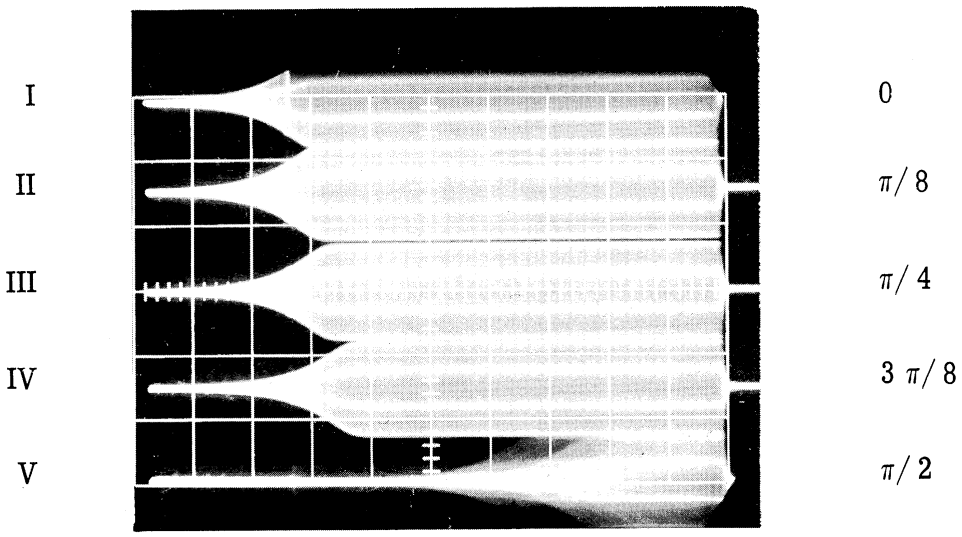


Fig. 7.20 Output variation with signal phase.

superimposed traces. The following series of traces demonstrates the phenomenon. Fig. 7. 21 (a) shows three entire quench cycles. The pump is not completely "off" during any of the cycle but is well below the level required for oscillation. The brightened interval at the start of the second burst of pump energy is selected for display in (b). This waveform is made on repetitive quench cycles and we note the identical pump initiative phase each time. The SHO trace immediately starts to show an oscillation. If the brightened portion of (a) is moved to the right to the saturated portion the resulting delayed trace, (c), is perfectly superimposed. Fig. 7. 21 (d) shows both stable states superimposed by making one exposure with a signal in one state, and a second exposure with the signal delayed $\pi$ radians.

When the oscilloscope is synchronized with the pump (not with the quench as in 7. 21) both pump states appear in the pump trace and the unusual superimposed trace of Fig. 7. 22 results. The growth of the oscillation is exactly related to the framing rate since the quench is ultimately tied to the pump, and thus the sync pulse. If this coherence is not established the saturated region has the same envelope as Fig. 7. 22, but instead of superimposed traces, the envelope is filled with the continuous range of possible values of the same phase. (much as in Fig. 7. 17)

7. 4. 3 Quantitative Relationships, Signal-to-noise. This section concerns the experimental demonstration of the relationships set forth in the theoretical derivation of paragraph 6. 3. 1. Here the error probability

Fig. 7. 21 Coherent Quenching

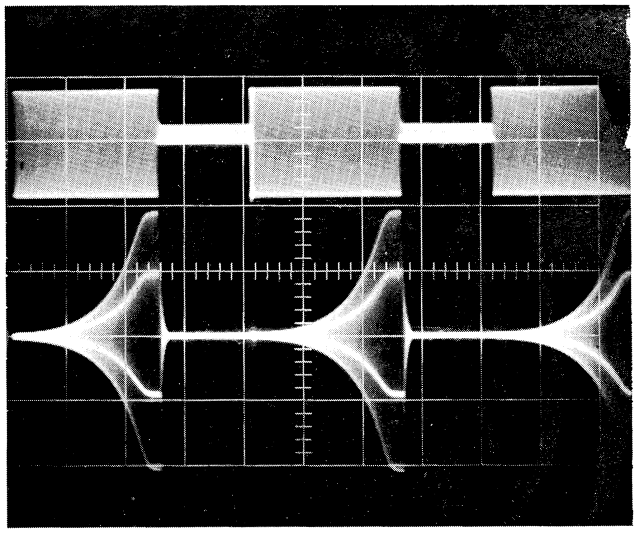


(a)

Entire quench cycle

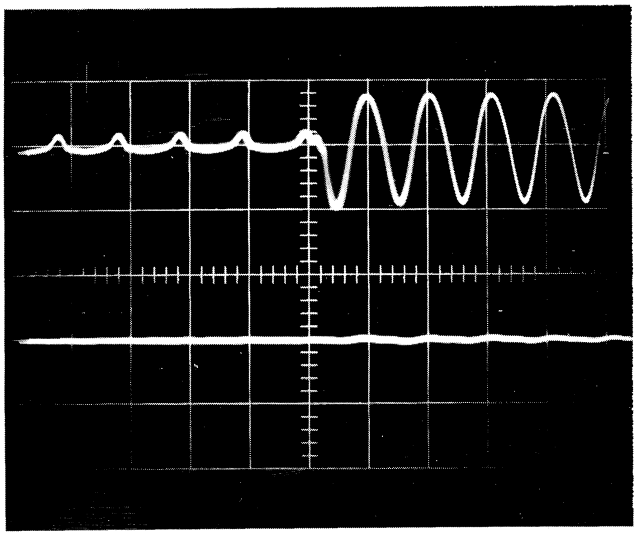


(b)

Pump initiation

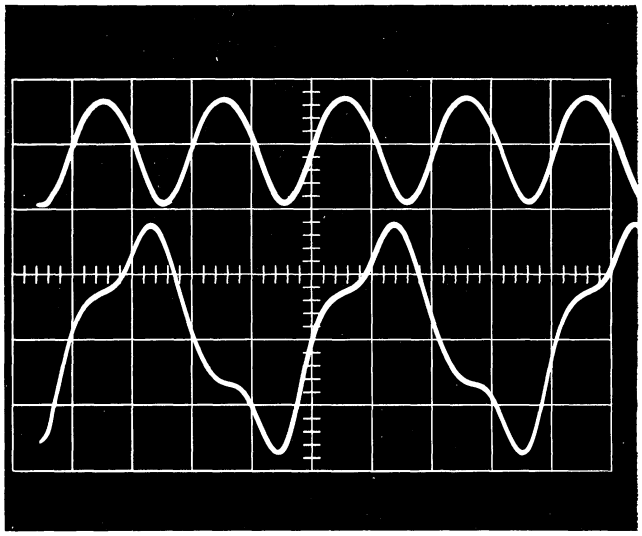


(c)

Oscillation saturation

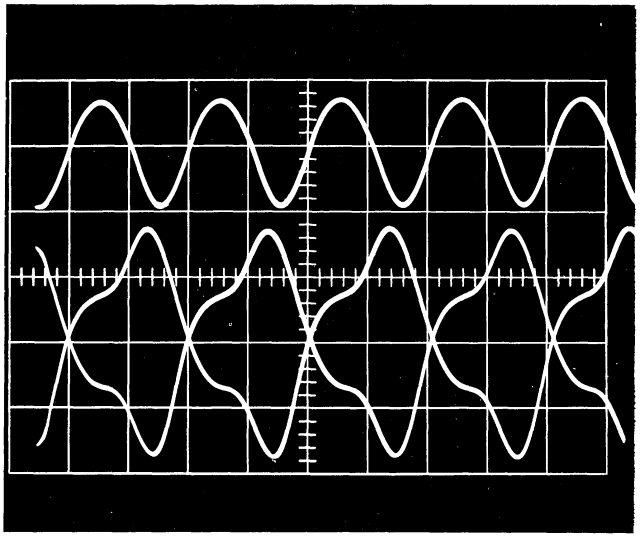


(d)

Two stable states

Fig. 7.21 (cont.)

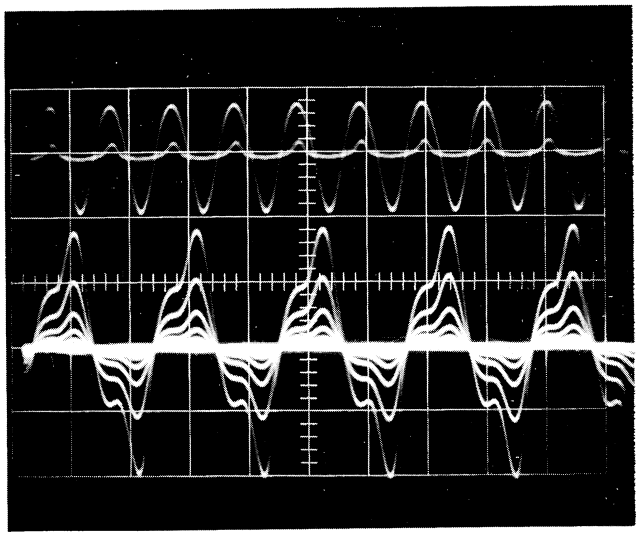


Fig. 7.22 Saturated State-Coherent Quenching

for phase synchronization of the oscillation in the presence of thermal noise is related to the normalized signal-to-noise ratio, or as is more commonly used, the signal-to-noise separation in decibels. Looking at Fig. 7. 1 we see that the experimental problem is to measure the signal-to-noise ratio and then to measure the error probability as evidenced by sufficient trials to give statistical confidence to the result. Each phase presents particular problems of absolute measurement (accuracy) and repeatability (precision). Illustrative of these problems, a sample data point will be carried along.

7. 4. 3. 1 Signal power measurement. The signal power delivered to the oscillator circuit is simply $\overline{E}_S{}^2 G$ where $\overline{E}_S$ is the effective signal voltage across the resonant circuit and G is the circuit conductance. Examining the signal path on Figs. 7. 1 and 7. 5, and the measurement problem we note:

1. Lowest level of absolute measurement is made by the oscilloscope at the input to attenuator 1.

2. 0-100 Db attenuator feeds SHO assembly.

3. A series resistor (with associated shunt capacitance) feeds the final SHO circuit described by measurements in paragraph 7. 2. 2.

Examining each of these in detail:

1 a. The lowest level of actual observation was the attenuated and phase shifted square-wave output of the first Harvey-Wells count-down circuit. This measurement was made using the Tehtronix oscilloscope on a 50 mv/ cm dual trace preamplifier unit, and was the peak-to-peak value. The initial reading for the sample data point was 28 mv, peak-to-peak. The effective value of the signal power is developed only from the fundamental component of the input square wave since the higher harmonics are rejected by the

tuned oscillator circuit. A simple Fourier description of the square wave reveals that the effective value of the fundamental is $\sqrt{2}/\pi$ (i. e. .45) times the peak-to-peak value of the square wave. Thus the lowest level observed was 12. 6 mv (effective). Estimated errors, --less than . 6 Db.

2a. The signal next was attenuated by a 0-100 Db step attenuator. This is the only variable link. The particular unit used had a 50 ohm characteristic impedance and estimated accuracy of . 5 Db. The particular data point being followed here is typified by a 50 Db setting.

3a. The series resistor (nominal value 1 megohm) $Z_3$ forms a fixed attenuator with the conductance of the loaded oscillator circuit. The voltage ratio of this attenuator measured at the resonant frequency of the SHO circuit (approx. 482KC), was found to be 39. 2/ 1. This is almost exactly 32 decibels. The attenuation is sensitive to frequency since the element shunting the one megohm resistor is the lead-to-lead capacitance (about . 5 $\mu\mu$f). However, over the narrow range of frequencies of interest the variation of attenuation is less than . 2 Db.

From these figures the signal voltage across the SHO circuit for the data point in question is 82 decibels below the measured value of 12. 6 mv. This is coincidently almost exactly 1 microvolt. (i. e. $10^{-6}$V) The signal power then is $.68 \cdot 10^{-16}$ watts.

7. 4. 3. 2 Noise Power Measurement. The noise power was not measured directly but rather taken from the theoretical value depending on the circuit parameters. It was stated in Eq. 5. 51 that the passive resonant circuit noise power is $KT\,\omega_0/Q_0$. Using the numbers of paragraph 7. 2. 2 the passive noise power is $1.16 \cdot 10^{-15}$ watts. The power used in the expression 6. 7 is normalized by the steady-state gain factor $2g_m$. (c. f. Eq. 5. 53) In the data point being examined here, the gain as determined by the procedure of paragraph 7. 3. 1 is 10. The active band power is

$$N' = \frac{N}{2g_m} = .580 \cdot 10^{-16} \text{ watts}$$

7. 4. 3. 3 Signal-to-Active Band Noise. The signal to active band noise ratio is

$$\frac{.68 \cdot 10^{-16}}{.580 \cdot 10^{-16}} = 1.17$$

or a positive separation of . 67 Decibels

7. 4. 3. 4 Error Probability Determination-Noise. Knowing the signal phase, and as described in 7. 2. 7,having a phase detector device to measure correct phase identification or errors, it is a matter of accurately counting the number of trials and the number of times the oscillation grew with the correct phase over a selected period of time. Since the noise as used in 6. 7 is normalized for the actual steady-state gain factor, $g_m$, by equation 5. 53 the value of $g_m$ must be known. This is pre-set by the method described in 7. 3. 1. Now both the quench oscillator frequency (the trials) and the phase detector filtered output (the successes) are counted over a preselected interval of time. It was convenient to count over a 1second interval and repeat the counting procedure at least five times. Thus for a quench frequency of about 200 Hz at least 1000 trials were made. For 1 % error probability, this means only 10 errors in the total run. This number is marginal to obtain good confidence in the result but was sufficient to locate the trend. For higher error rates correspondingly better statistics result. For no signal entering the system, the theoretical error probability is . 5 or 50 %.

Because the passive thermal noise is over 100 Db below the normal saturation levels, and because the active circuit noise is further depressed by the gain, it became extremely difficult to insure that there was no signal leakage into the tank circuit. After all available measures were taken to isolate the tank from extraneous signal, it was amply evident that the phase was not being determined by thermal noise. The method used to check this was to shift the phase of the signal by $\pi$ radians. The output phase, if determined by a control signal,will shift phase. If determined by noise, primarily both phases occur and signal phase shifting only alters the density of one phase position compared with the other.

The final method used to make the very lowest level measurements was to provide an auxiliary signal balancing the leakage exactly equal in magnitude but opposite in phase in order to allow the residual noise to be the final phase determining quantity. A convenient method for doing this was to use coherent quenching, and to phase shift the pump slightly to make use of the arbitrarily small controlled signals available through the action of the $\frac{\theta_1}{2}$ quantity of equation 5.42.

Fig. 7.2 3 (a, b, and c) illustrates the appearance of oscilloscope waveforms of the error situation for various signal levels. These traces are delayed sweep traces showing a short section of the growing oscillation and the presence of oscillation of both possible phases. The decibel notation is that of the variable attenuator setting. For -100 Db both output phases occur, and the lines of the two phases appear nearly equal. Increasing the signal (-80 Db, etc.) decreases the error phase trace

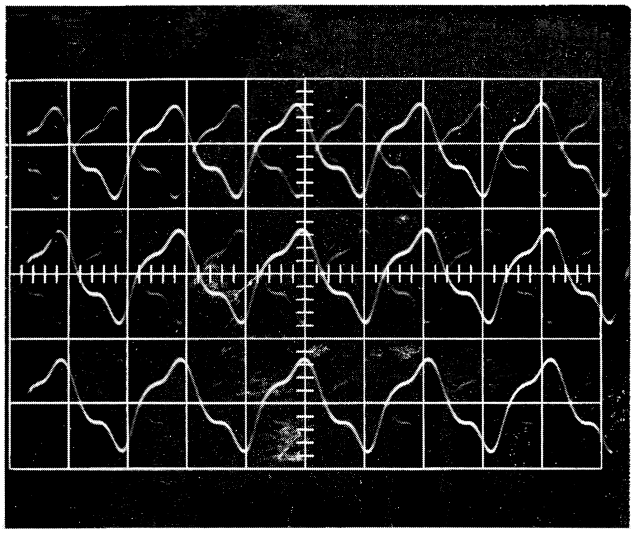


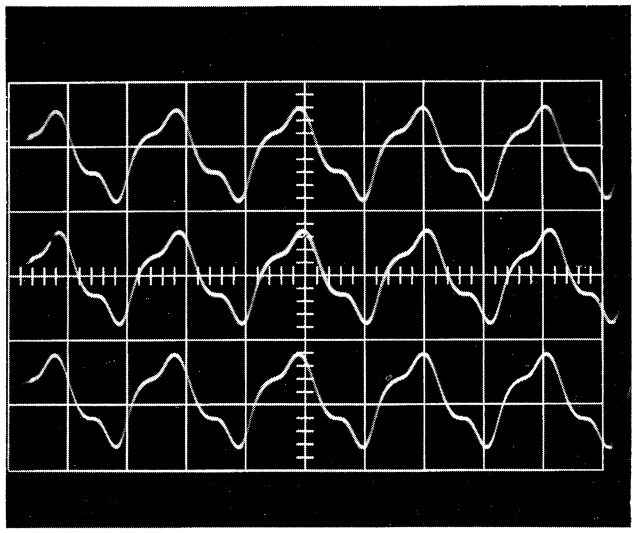


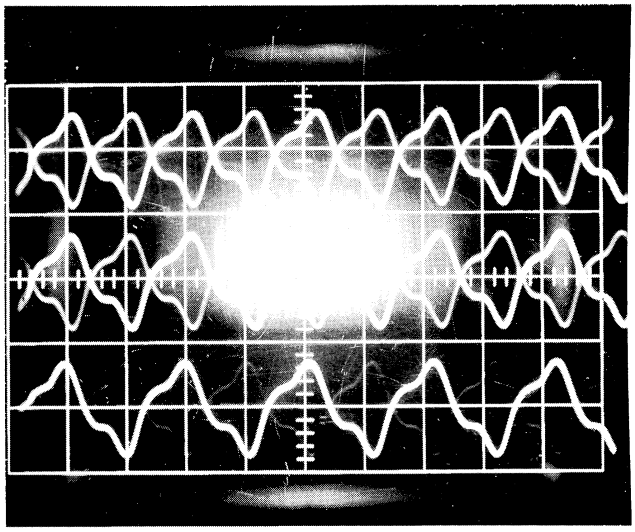


Fig. 7.23 Output phases for various signal input levels.

density, and increases the signal phase density. This proceeds through the signal levels to -45 Db. At this point it appears that there is no error phase. However, if the oscilloscope camera is allowed to integrate the effect over a period ten times the original period, Fig. 7.23 c shows the appearance of the error phase. Even the -45 Db signal generates significant error.

The sample data point under discussion in the previous paragraphs resulted from the following data

QUENCH FREQUENCY 185.0 hertz

| ATTEN. SETTING | ERROR COUNTS | AVE. | PERCENT ERROR |
|---|---|---|---|
| -50 Db | 32, 39, 29, 38 | 34.5 | 18.65 |
| -100 Db | (MIN. SIGNAL) 95, 96, 92, 88 | 92.75 | 50.1 |

For each point it was found necessary to establish that the minimum signal (-100 Db attenuator setting) actually produced an error probability of nearly 50%. If it did not, the balancing signal was readjusted to produce the 50% error probability, the actual signal inserted, the run made, and then an additional run was made with the minimum signal again. The adjustment of phase of $\frac{\theta_1}{2}$ was difficult and tended to drift during a run. The normal run consisted of a series of 5, 1 second counts, interspersed with reading times of about 2 seconds. Thus the total run time was about 15 to 20 seconds.

7.4.3.5 Theory and Experimental Correlation-Noise. Fig. 7.24 shows the sample data point and other data points with respect to the

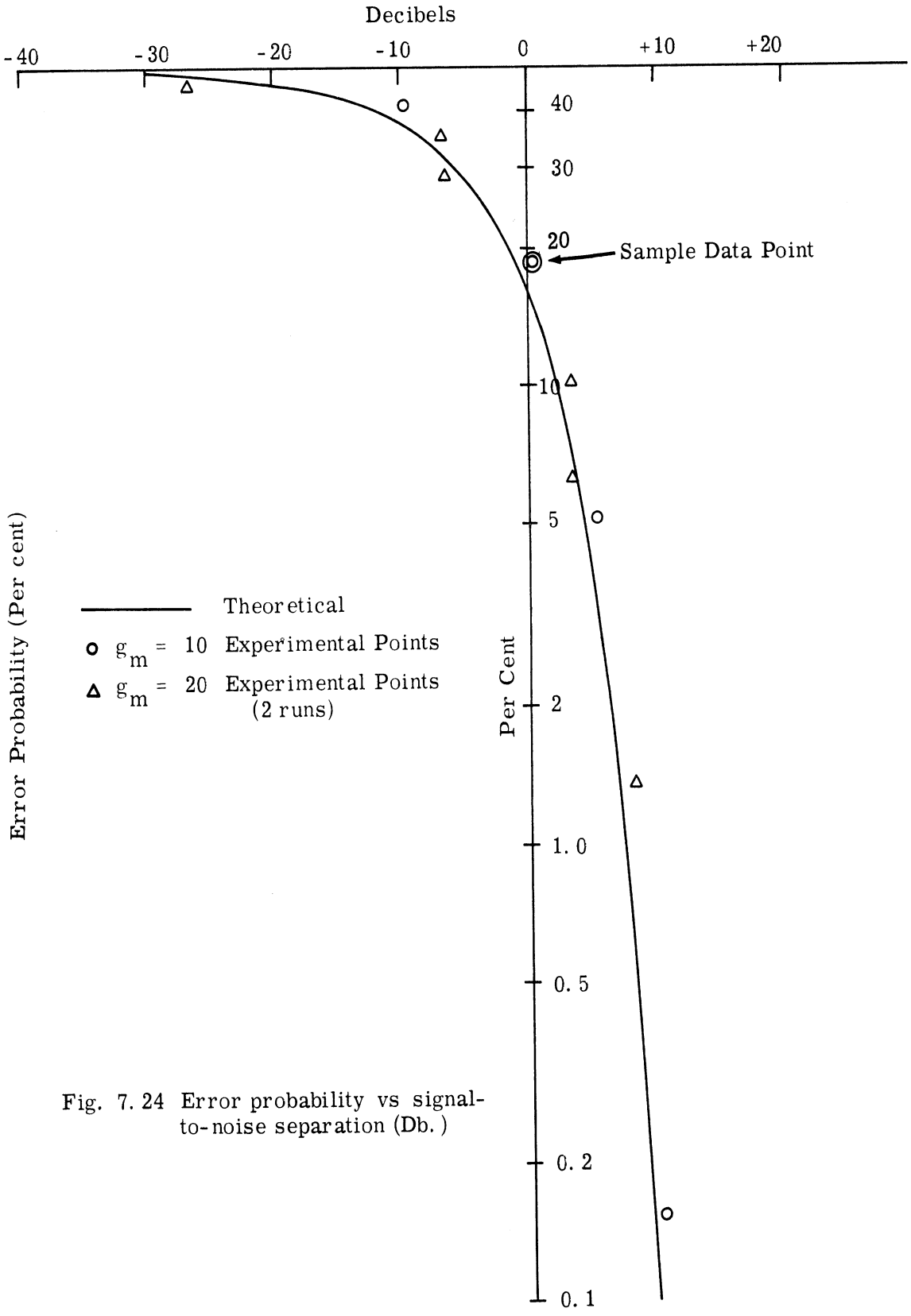


Fig. 7.24 Error probability vs signal-to-noise separation (Db.)

theoretical curve. Considering the range of well over 100 Decibels through which the oscillation moves the deviations shown are remarkably small. Both the curve shape and level are significant in judging the harmony between theory and experiment. The shape is determined by the spectral distribution of the masking signal, while the level relates to absolute values and basic accuracy of measurement. As we shall see in the following section, when the masking signal is caused by a different phenomena the shape of the ensuing error probability curve is quite different.

7. 4. 4 Signal to Pump-Unbalance

7. 4. 4. 1 Experimental A Contours. As pointed out in Chapter VI for coherent quenching (CQM), variation of $\frac{\theta_1}{2}$ produces a phase determining constraint. This has been used in the previous paragraph to inject a controlled signal to balance a spurious signal arising in the apparatus. The phase determining constraint produces what was called an A contour. Theoretical A contours were plotted in Fig. 6. 3. In the course of the experimental work a number of these A contours were measured as given in Fig. 7. 25. Particularly worthy of note is the variety of experimental contours achieved with various system adjustments. Curve #1 is that achieved on the original SHO (paragraph 7.2.2 with no special attempt to insure absence of spurious signals. Curve #2 is the same device having a balance signal so adjusted in magnitude and phase to cause zero A at the expected zero point of curve $y_{10}$ of Fig. 6. 3. Finally curve #3 is of a later SHO having a passive $Q_0$ of 30.

Fig. 7.25. Experimental A contours
in coherent quenching

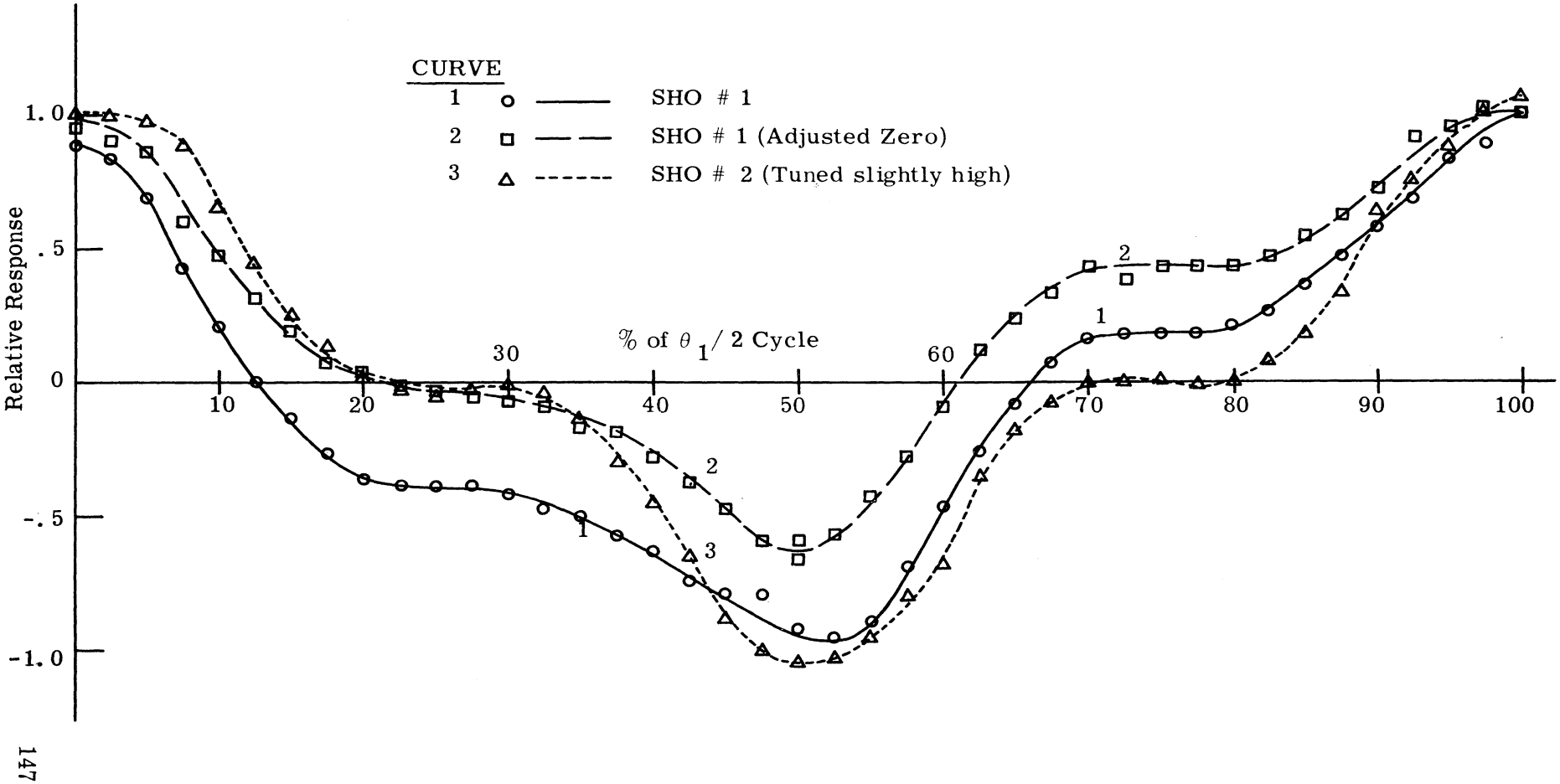

Each of the above curves demonstrates the sharp major lobe and flat portions of the curve characteristic of the $\cos^3 \frac{\theta}{2}$. The departure of the zero slope portion from the axis is dependent on a combination of things. They are listed below and have varying degrees of importance depending on the particular effect predominating.

1. Spurious signal present
2. Minor detuning
3. Removed spurious signal by amplitudes and phase adjustment
4. Removed spurious signal by phase only adjustment
5. $Q_0$ of the SHO
6. Pumping level

It is worthy of comment here that it has been singularly difficult to isolate each of the above effects because of the serious interaction and the extremely low signal levels which are effective in the active circuit.

7. 4. 4. 2 Experimental Error Probabilities. A group of experimental error probability curves vs signal-to-pump unbalance were run during the course of the investigation. It was determined early in the study that the amount of signal unbalance present in the sample SHO produced a curve about 30 decibels above the expected signal-to-noise curve. The curves in Fig. 7. 26 have been normalized at the point of zero error. They each show the trends of the pump unbalance interference. That is, the asymptote at zero error, the relatively sharper break toward higher errors and the jog in the curve due to the displaced zero slope of

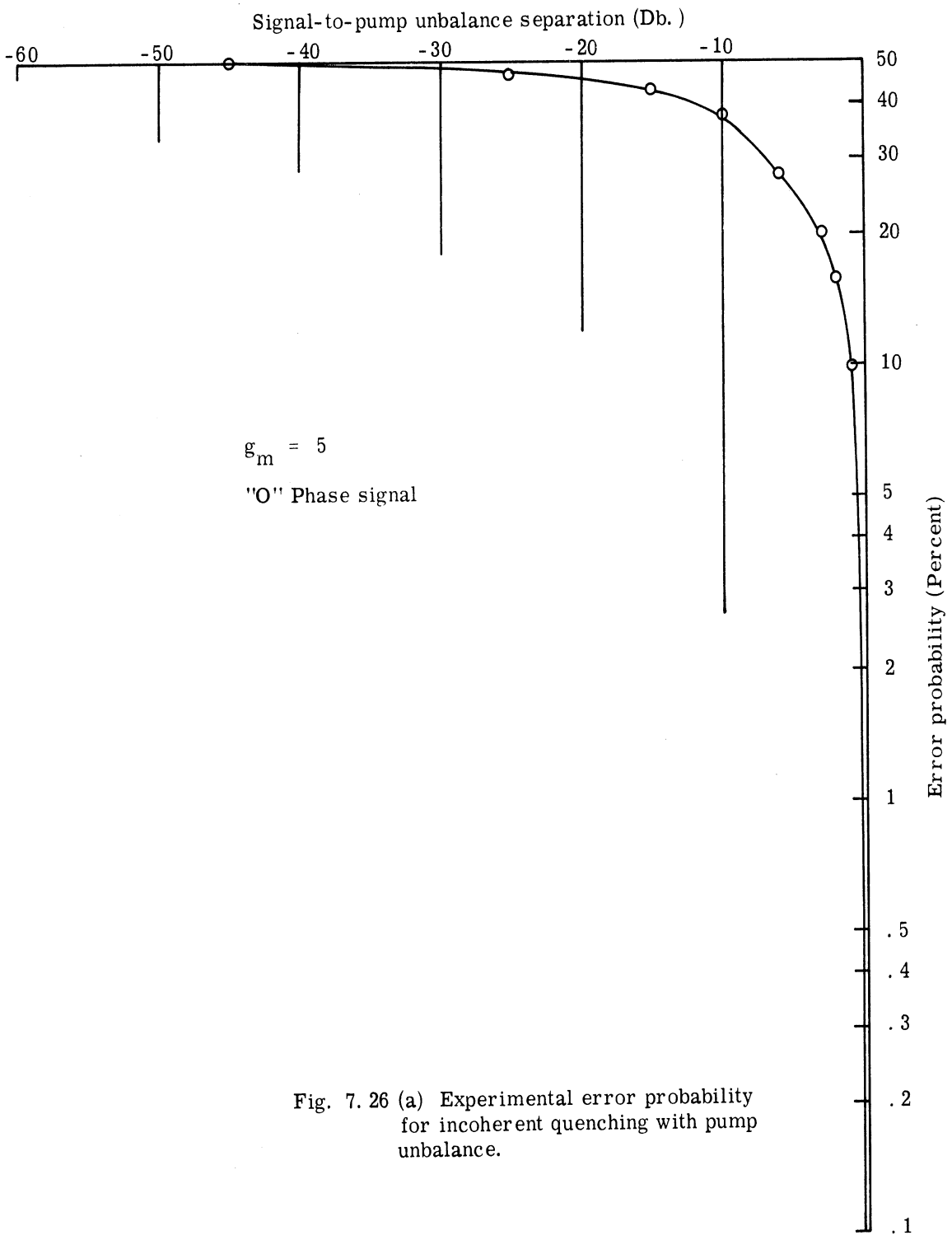


Fig. 7.26 (a) Experimental error probability for incoherent quenching with pump unbalance.

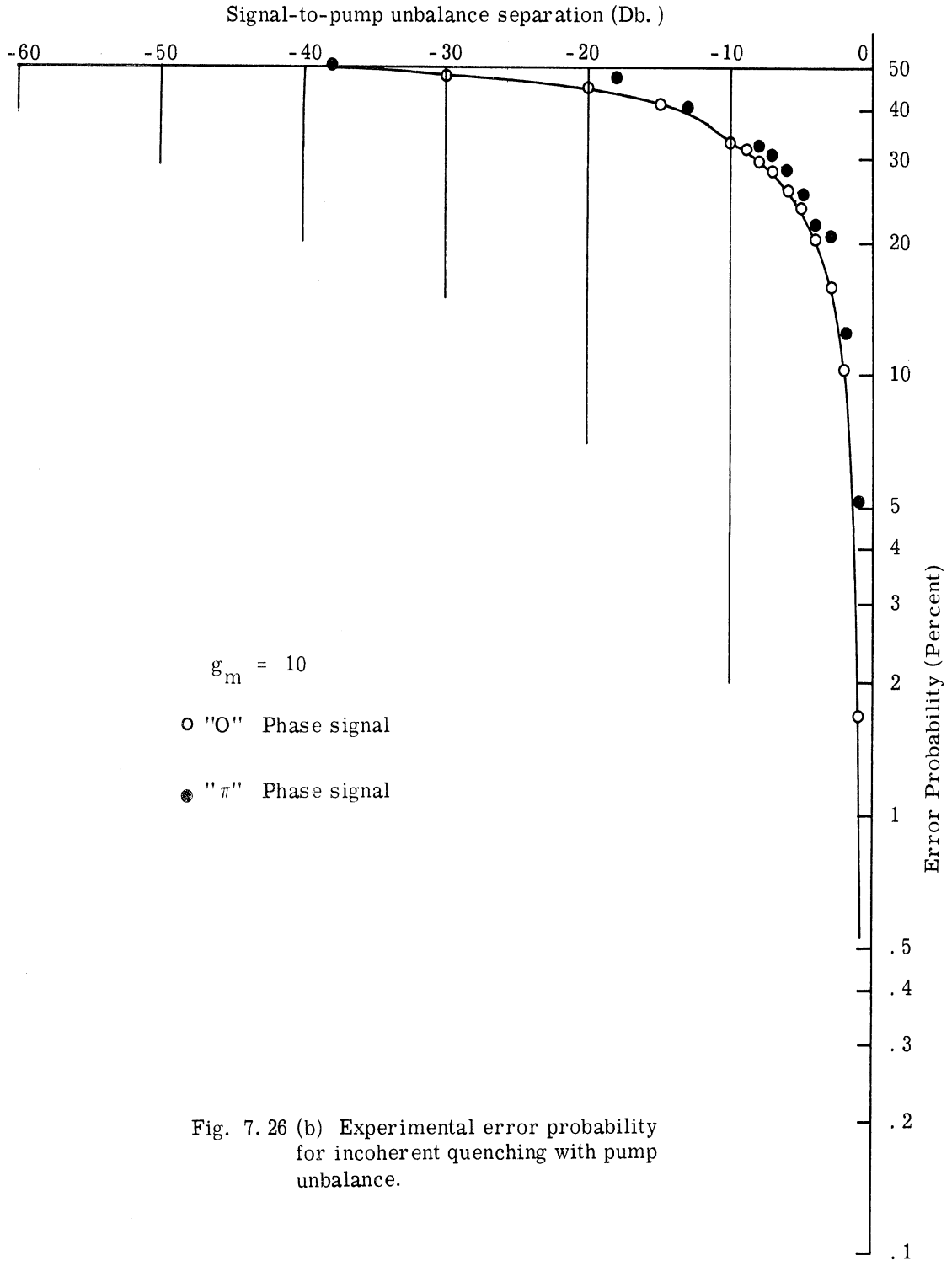


Fig. 7. 26 (b) Experimental error probability for incoherent quenching with pump unbalance.

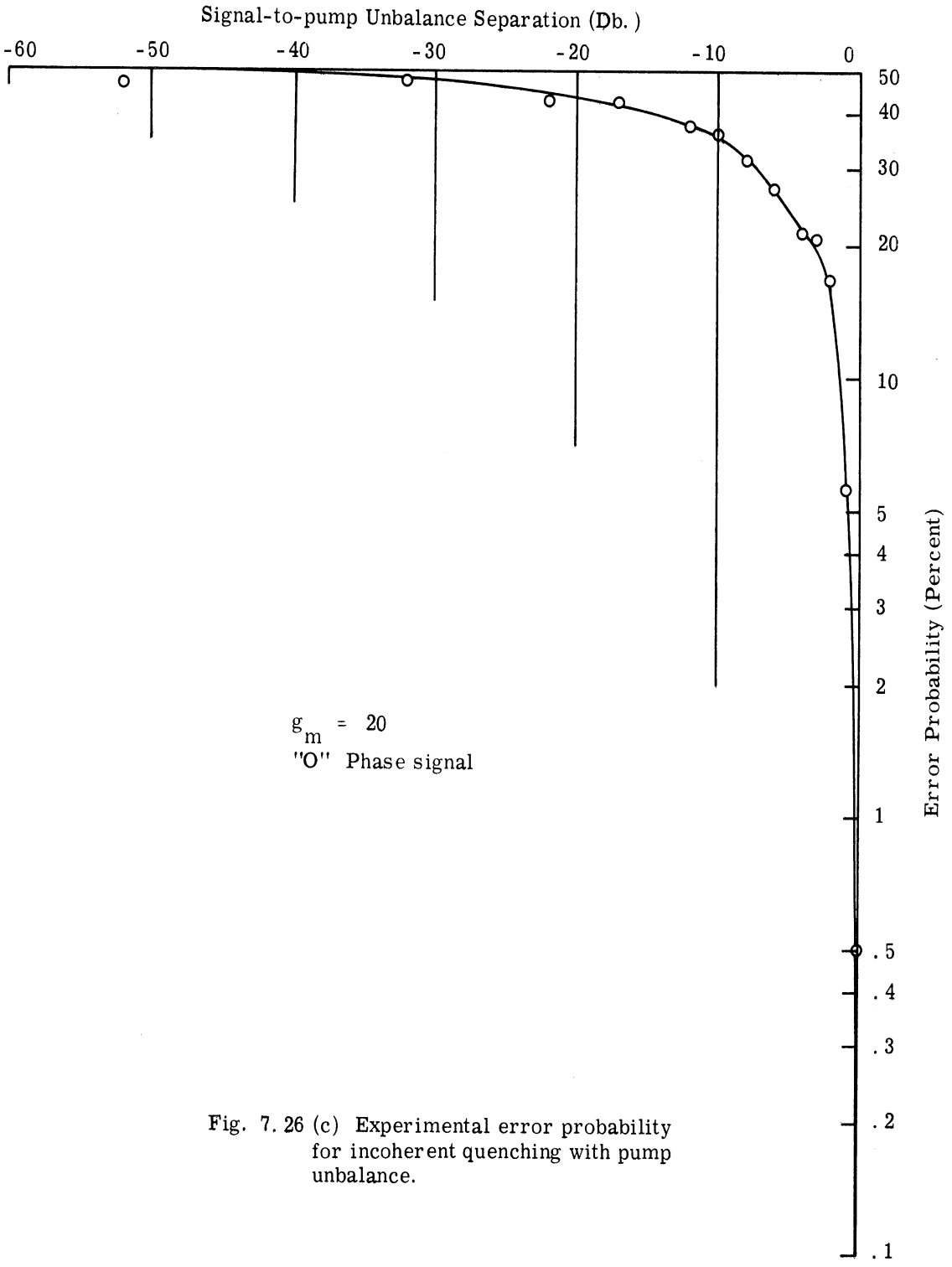


Fig. 7.26 (c) Experimental error probability for incoherent quenching with pump unbalance.

the $\text{Cos}^3 \frac{\theta_1}{2}$ curve.

7. 4. 5. Higher Order Subharmonic Oscillations. In the course of the experimentation the question was asked, "could higher order sub-harmonics be demonstrated with the particular experimental apparatus used in this study?" Fig. 3. 1 showing the stability regions for Mathieu equation solutions provides fuel for the inquiry. We note the increasingly narrow approach of the unstable regions to the g axis as the higher orders are sought. However the refinement of construction and adjustability of a second sub-harmonic oscillator, along with an electronic counter for precision location of pumping and tuned frequencies made possible the location of higher order harmonics. The procedure was to tune the passive circuit exactly to 0. 5 Mhz which now represents the frequency at which sub-harmonics will occur. Pumping was then performed at 500 Khz for the second sub-harmonic oscillation, and at 250 Khz and 125 Khz for the third and fourth. By the balanced pump provided in the construction, the pump voltage does not appear directly across the resonant circuit. The higher order sub-harmonics are shown in Fig. 7. 27 along with the pump trace in each case.

7. 4. 6. Magnetic SHO. In order to demonstrate some of the same properties as shown for the parallel-resonant, pumped capacitance device a series-resonant, pumped inductor SHO was built. The magnetic couplings from pump to SHO and from signal source to SHO offer some advantages to the varactor device studied intensively. The particular torroidal ferrites used were essentially square-loop materials and exhibited

the $\text{Cos}^3 \frac{\theta_1}{2}$ curve.

7. 4. 5. Higher Order Subharmonic Oscillations. In the course of the experimentation the question was asked, "could higher order sub-harmonics be demonstrated with the particular experimental apparatus used in this study?" Fig. 3. 1 showing the stability regions for Mathieu equation solutions provides fuel for the inquiry. We note the increasingly narrow approach of the unstable regions to the g axis as the higher orders are sought. However the refinement of construction and adjustability of a second sub-harmonic oscillator, along with an electronic counter for precision location of pumping and tuned frequencies made possible the location of higher order harmonics. The procedure was to tune the passive circuit exactly to 0. 5 Mhz which now represents the frequency at which sub-harmonics will occur. Pumping was then performed at 500 Khz for the second sub-harmonic oscillation, and at 250 Khz and 125 Khz for the third and fourth. By the balanced pump provided in the construction, the pump voltage does not appear directly across the resonant circuit. The higher order sub-harmonics are shown in Fig. 7. 27 along with the pump trace in each case.

7. 4. 6. Magnetic SHO. In order to demonstrate some of the same properties as shown for the parallel-resonant, pumped capacitance device a series-resonant, pumped inductor SHO was built. The magnetic couplings from pump to SHO and from signal source to SHO offer some advantages to the varactor device studied intensively. The particular torroidal ferrites used were essentially square-loop materials and exhibited

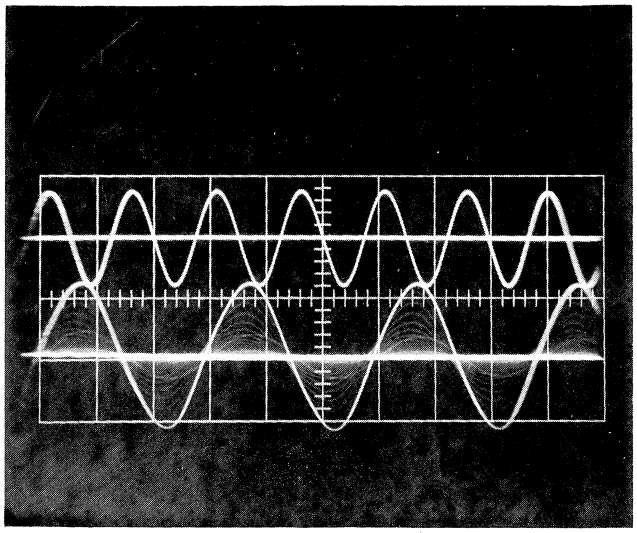

$f_p$ = 1300 Hz . 5v/ cm

$f_{SHO}$ = 650 Hz 1. 0v/ cm

(a)

1st. Sub-Harmonic

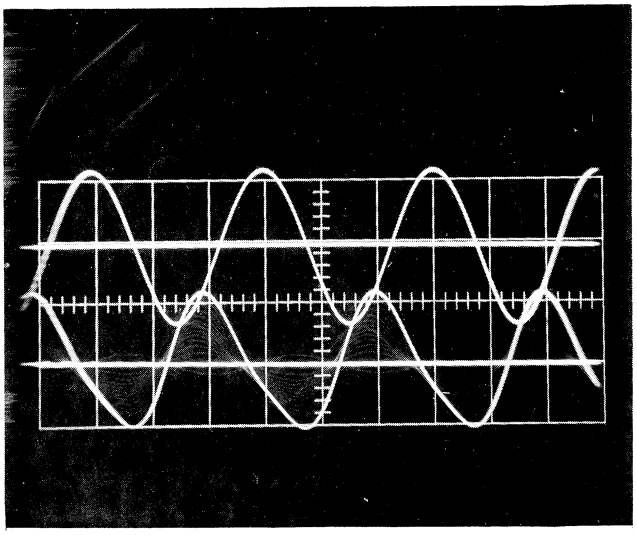

$f_p$ = 635. 13 Hz 1v/ cm

$f_{SHO}$ = 635. 13 Hz 1v/ cm

(b)

2nd. Sub-Harmonic

Fig. 7. 27 Higher Order Sub-Harmonic Oscillations

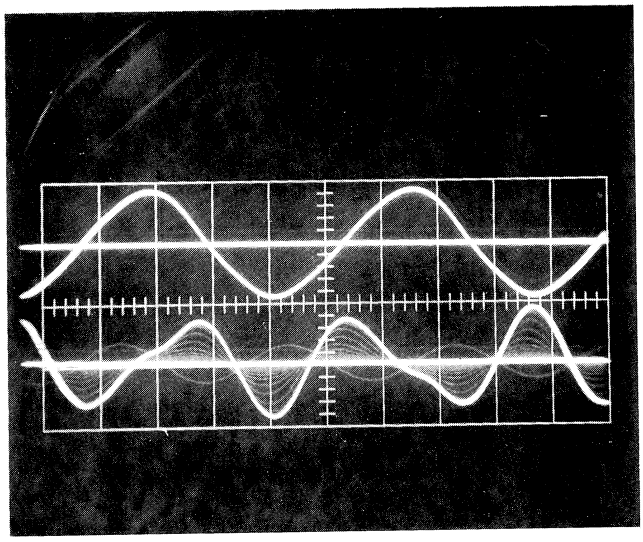

$f_p$ = 416.3 Hz 2v/cm

$f_{SHO}$ = 624.2 Hz 1v/cm

(c)

3rd. Sub-Harmonic

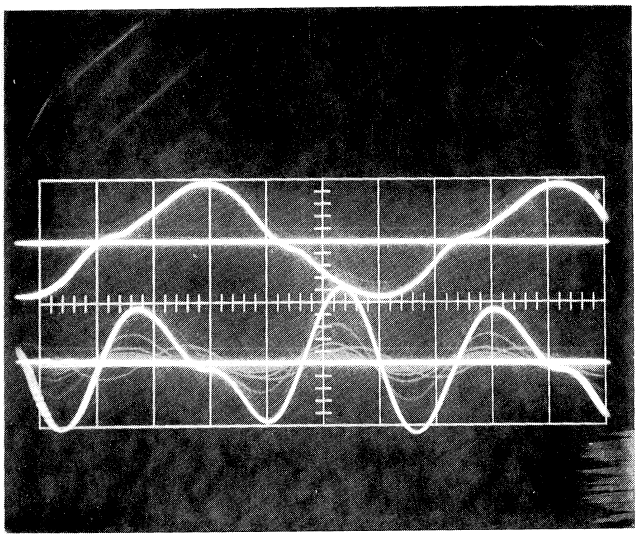

$f_p$ = 314.3 Hz 2v/cm

$f_{SHO}$ = 608.6 1v/cm

(d)

4th. Sub-Harmonic

Fig. 7.27 Higher Order Sub-Harmonic Oscillations (Cont.)

marked hysteresis. In this latter respect, they were difficult to use. The Japanese in their Musasino-I (Ref. 37) computer have evolved ferrite devices as the basic pumped element and have demonstrated the remarkable reliability possible using such active elements.

# CHAPTER VIII

# SUMMARY OF RESULTS

## 8. 1 Novel Features of the Research

Although the parametric subharmonic oscillator has been the subject of quite a body of authors, a number of facets of the study presented here are novel and represent new analyses and new understanding. These will be summarized here and then discussed briefly. Since no study is an isolated affair, nor complete in comprehension, these aspects will be mentioned. Finally an application of particular interest to the writer will be presented and discussed in conceptual form.

In any study which treats a specific problem and draws on a body of prior literature for its starting place,the problem of notation and analytical forms to be used must be faced. In this study the usual amount of new forms are introduced and at times they may appear to be confusing. However, from the author's viewpoint there are reasons for the progression of forms as they relate to comprehension, sophistication, and elegance. Indeed, in reviewing the possible direction the presentation might have taken at various junctures it would have been possible to avoid some of the pain of the development. But comprehension usually is a painful process, and so some of the pain is evident in the rational used.

The specific features of the research which are novel are listed below:

1. Treatment of the statistical problem of phase synchronization of the parametric sub-harmonic oscillator in the presence of signal and thermal noise.
2. Involvement of pump unbalance in the solution for synchronization statistics in the presence of signal.
3. Presentation of the quantitative significance of coherent and incoherent quenching in realizing minimum signal power for phase synchronization.
4. Treatment of detuned transient solution of the active resonant circuit by detailed graphical plot relating differential equation parameters to form of solution.
5. Treatment of the steady-state solution of the quasi-degenerate amplifier-oscillator (where signal frequency, circuit passive resonant frequency, and half-pump frequency do not coincide).
6. Experimental demonstration of the theoretical work of points 1 through 5, with particular emphasis on:
   - 6.1 Arbitrarily low level signal recognition in the presence of noise. Quantitative data on penetration of passive circuit noise level.
   - 6.2 Practical aspects of building parametric oscillator circuits for noncoherent quenching.

6.3 Superiority of coherent quenching to achieve maximum dynamic range between signal level and final oscillator output level.

8.1.1 The treatment of the statistical problem of the phase synchronation of the parametric subharmonic oscillator was the basic objective of the study. To do this two developments were made. The first was the degenerate solution, for the signal at exactly half the pump frequency. Although the development had been made in the prior art by Bura(Ref.17) it contained a number of errors significantly affecting the result. These were corrected and verified experimentally. The second development was the quasi-degenerate solution, posed in such a form to be applicable to random noise signal and then unified with the first development. These were combined with the transient solution and initial conditions to form the general solution. The results are typified by the curve of Fig. 7.24 which displays the theoretical and analytical work together.

By way of using numbers, it has been shown here that at least 120 decibels of signal gain are possible in the presence of thermal noise using the device under discussion for detection of binary phase signals. This is significantly higher than any statement found in the literature.

8.1.2 The involvement of the pump unbalance in the solution for the synchronization statistics was not an original objective of the study. It became a necessary part of fulfilling the basic objective, however, as the original error statistics suggested a noise level about 30 decibels

higher than thermal noise. As the phenomenon became more understandable and as the equipment to demonstrate pump unbalance and coherent quenching was assembled, this whole shubject became an integral part of the study and its understanding. The concept of "A Contour" as presented in Fig. 6.3 as a basis for understanding coherent quenching, and as a basis for error probability determination of incoherent quenching is new. So far as the writer knows there is no mention of this aspect of dynamic range limiting anywhere in the literature. The functional form developed and the demonstration of experimental A contours having these general characteristics as shown in Fig. 7.25 are essentially in harmony.

8.1.3 In presenting the quantitative significance of coherent and incoherent quenching in realizing minimum signal power for phase synchronization, alternatives for design are offered. It was shown, for example, that the ultimate limit for dynamic range is the active-band noise. The masking effects of pump unbalance can be minimized either by extremely careful construction and matching procedures if incoherent quenching is used, or by the use of coherent quenching and appropriate selection of initial pump phase angle. Of course, another alternative is to do both, which was done in the experimental procedures discussed.

8.1.4 At the inception of the study there were no detailed graphical presentations of the Mathieu solutions in the vicinity of the a-g plane occupied by this problem. Since then, Phillips (Ref.104) presented the concept

of iso-u curves in the vicinity of the first unstable Mathieu region. Included in the present study are terms neglected by Phillips which distort his iso-u curves and give improved prediction for criteria for oscillation. Also in the present study the phase angle of the transient terms are shown on the graphical representation as iso-$\sigma$ curves. This makes quite simple the complete visualization of the Floquet solution to the differential equation with time varying parameters used here. By this graphical form, for example, it is possible to show that for a particular steady state gain used (i. e. a particular pump level$\eta$) the phase angle of the growing term is constrained to lie between particular values close to $-\pi/4$, and what the angles will be when oscillation ceases due to detuning.

8. 1. 5 The quasi-degenerate amplifier is one where signals are expected within a small band about the half-pump frequency. Bura (Ref.17) treated this problem for discrete signals. Where many signals are present simultaneously (noise) the signal is conceived rather differently because of the expected interaction about the half-pump frequency. Using a signal form suggested by D. K. Adams the analysis produced a solution form which could be used equally for signal or noise by choosing appropriate constraints on amplitude and phase. By retaining departures from ideal centering of pump frequency, and passive resonant frequency the effect of these departures are expressed quantitatively right through the final analysis. Although these departures were not

used extensively, the forms are believed adequate and they provide a resource for further work in this particular vein.

## 8.2 Incomplete Aspects

Work such as presented in this study has many natural extensions. It appears to the writer that they will be worthy of investigation as the need for particular performance arises or as the state of-the-art in some aspect changes significantly to open up some new dimension.

As the picture of pump unbalance became clearer it was also obvious that many aspects of quench initiation had not been studied. The abrupt initiation used here was limited to the relative abruptness of a transistor turning on or off. More or less drastic initiation may have other consequences and these could be studied as a means of answering more exhaustively the question of what to do about unavoidable pump unbalance.

The subject of noise on the pump excitation was discussed in formulating the problem. This has not been discussed in this study although the forms used are generally amenable to this consideration. Similarly noise in amplitude or phase of the quench input, particularly for coherent quenching, is suitable for further study.

Application of the details of this study to the magnetic SHO would be of interest. Certainly there are properties particular to such circuits that would bear further investigation.

Finally, the study of the higher order sub-harmonic solutions would be fascinating just for the sake of knowing more about the function and performance in these relatively little known regions.

## 8.3 Suggested Application

Although not a direct part of the study, it is interesting to speculate just how the fruits of such a study might be used. The following is a description of such an application, actually conceived before the study, and for whose realization the subject study was an integral part.

The problem area is instrumentation of low-level transducers such as may be found in a great many distributed processes where a large number of sample points must be measured against known limits or set-points. A high pressure steam boiler or large nuclear reactor would be cases in point. Such processes normally operate close to limits in several parameters and must be monitored closely for satisfactory compromise between efficiency, safety, and destructive damage. A number of schemes for performing these measurements are being used currently, each having problems in one or more areas such as:

1. Low level metallic commutating contacts
2. Multiple precision amplifiers
3. Commutated low level amplifiers having long settling times

The scheme proposed uses the combination of two solid-state devices; the second-harmonic magnetic modulator (SHMM), and the parametric subharmonic oscillator (SHO). For one data sampling

point Fig. 8. 1 shows the proposed layout.

The operating scheme is this. The SHMM, pumped at frequency f, generates frequency 2f, proportional in amplitude and phase to the magnitude and polarity of the difference between the d-c levels of two currents, the signal, $S_1$, and the set point, $S_2$. This transducer principle is applicable to limiting d-c power levels of the order of $10^{-19}$ watts/hz and is singularly free of temperature dependence (Ref. 116). The SHO, pumped at frequency 4f, oscillates at 2f having a phase dependent on the phase of the received information from the SHMM, and whose amplitude, short of saturation, depends on the magnitude of the received information.

Two basic questions can be asked of the signal:

1. What is the value of the variable?
2. Is it above a set-point?

In answering 1, the SHO would be quenched at such a rate to place it in the linear operating mode, where average envelope carries amplitude information. In answering 2 the system need only decide which phase is present in the output.

The primary reason for offering such a hybrid system for commutation problems is that the equipment which would have to be duplicated for each point sampled is:

1. solid state
2. not temperature sensitive in basic mode of operation
3. inexpensive
4. simple and highly reliable

The rest of the equipment needed for such a system as shown in Fig. 8. 1 would not need to be duplicated at each point, and could be engineered for design reliability by normal practices.

In this application the unique properties of two devices have been married, one for low level d-c. transduction and conversion to low level a-c, and the other for extremely large stage gain to levels easily transmitted to and understood by a computer.

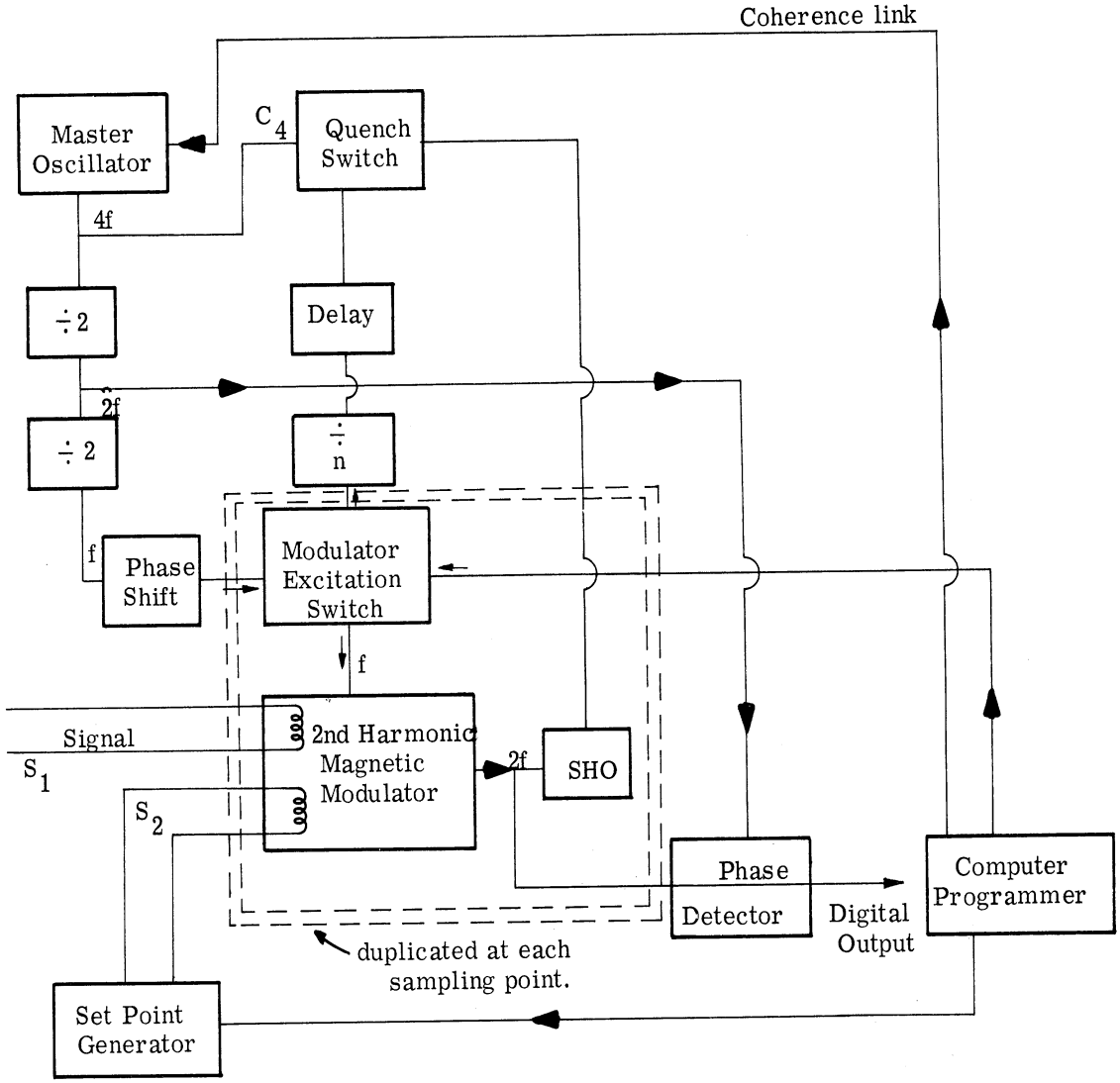


Fig. 8.1 Digital commutating scheme for analog system.

## APPENDIX I

## REMOVAL OF FIRST DERIVATIVE IN A GENERAL SECOND-ORDER DIFFERENTIAL EQUATION [1]

Given

$$\ddot{y} + K\dot{y} + My = f \tag{I. 1}$$

where K, M, f, and y are functions of the independent variable t. It is desirable in some instances to re-express this relation in terms of a new variable, a, such that the resulting equation has no first derivative.

Let

$$y \equiv ab \tag{I. 2}$$

$$\dot{y} = \dot{a}b + a\dot{b}$$

$$\ddot{y} = \ddot{a}b + 2\dot{a}\dot{b} + a\ddot{b}$$

where a is the new variable with the above constraint and b is a function to be determined.

Substitute (I. 2) in (I. 1) and collect terms in orders of a:

$$\ddot{a}b + \dot{a}(2\dot{b} + Kb) + a(\ddot{b} + K\dot{b} + Mb) = f \tag{I. 3}$$

now imposing the desired constraint that the first derivative vanish

$$2\dot{b} + Kb = 0 \tag{I. 4}$$

---

[1] As per Kaplan, (Ref. 60) and presented here for completeness.

and

$$b = \epsilon^{-\frac{1}{2}\int K\,dt}$$

$$\dot{b} = -\frac{K}{2}\,b$$

$$\ddot{b} = \left(\frac{K^2}{4} - \frac{\dot{K}}{2}\right) b$$

(I. 3) now becomes

$$\ddot{a} + \left(-\frac{K^2}{4} - \frac{\dot{K}}{2} + M\right) a = f\,\epsilon^{\frac{1}{2}\int K\,dt} \qquad \text{(I. 5)}$$

and when K is a constant (I. 5) simplifies further to

$$\ddot{a} + \left(-\frac{K^2}{4} + M\right) a = f\,\epsilon^{\frac{K}{2}t} \qquad \text{(I. 6)}$$

## APPENDIX II

## DETAILED PLOT OF A-G PLANE IN THE FIRST UNSTABLE ZONE

This appendix concerns the solution of the canonical homogeneous Mathieu equation

$$y'' + (a - 2g \cos 2z)\, y = 0 \qquad \text{(II. 1)}$$

The solution according to Floque's theorem is of the form:

$$y = A\, \epsilon^{\mu z}\, \phi(z) + B\, \epsilon^{-\mu z}\, \psi(z) \quad (\phi \text{ and } \psi \text{ periodic in } z) \qquad \text{(II. 2)}$$

$\mu$, $\phi$ and $\psi$ are very difficult to express in terms of "a" and "g" alone. Whittaker (Ref. 106) and McLachlan, using a slightly different form (Ref. 103) expressed "a" and "$\mu$" in terms of power series in "g", the coefficients of terms being functions of a new dependent variable, $\sigma$. Also the coefficients of the series:

$$\phi(z, \sigma) = \sin(z-\sigma) + s_3 \sin(3z-\sigma) + s_5 \sin(5z-\sigma) \ldots .$$

$$+ c_3 \cos(3z-\sigma) + c_5 \cos(5z-\sigma) \ldots . \qquad \text{(II. 3)}$$

(i.e., the s's and c's) are shown to be power series in g, the coefficients of the $g^n$ terms being functions of the new variable, $\sigma$. The term $\cos(z-\sigma)$ is missing as a consequence of the periodicity requirement on $\phi$.

In the notation of McLachlan the representations of $\mu$, a, s's and c's are:

$$a = 1\text{-}g\cos 2\sigma + \frac{g^2}{4}(-1 + \frac{1}{2}\cos 4\sigma) + \frac{g^3}{64}\cos 2\sigma + \frac{1}{16}g^4(\frac{1}{3} - \frac{11}{32}\cos 4\sigma) \ldots . \qquad \text{(II. 4)}$$

or

$$a = 1 - g\cos 2\sigma - \mu^2 + g\,s_3$$

$$\mu = -\frac{1}{2}g\sin 2\sigma + \frac{3}{128}g^3\sin 2\sigma - \frac{3}{1024}g^4\sin 4\sigma - \ldots \qquad \text{(II. 5)}$$

or

$$\mu = \frac{1}{2}g(-\sin 2\sigma + c_3)$$

$$s_3 = -\frac{1}{8}g + \frac{1}{64}g^2\cos 2\sigma - \frac{1}{512}g^3(-\frac{14}{3} + 5\cos 4\sigma) + \ldots$$

$$c_3 = \frac{3}{64}g^2\sin 2\sigma - \frac{3}{512}g^3\sin 4\sigma + \ldots$$

$$s_5 = \frac{1}{192}g^2 - \frac{1}{1152}g^3\cos 2\sigma + \ldots$$

$$c_5 = -\frac{7}{2304}g^3\sin 2\sigma + \ldots \qquad \text{(II. 6)}$$

. . . . .

. . . . .

All the basic information is given in II. 4 to II. 6. On the a-g plane two sets of curves are needed, namely iso-$\sigma$ (constant value of $\sigma$) and iso-$\mu$ (constant value of $\mu$).

Iso-$\sigma$

The iso-$\sigma$ curves are the most directly obtained since for a chosen value of $\sigma$ the a-g is a simple numerical relation according to II. 4.

A family of iso-$\sigma$ curves results when $\sigma$ is specified in discrete values over the total range $-90^{\circ} \leqq \sigma \leqq 0$. The boundary of the region is defined by the relation

$$a = 1 \mp g - \frac{g^2}{8} \pm g\frac{3}{64} + \frac{g^4}{1536} \quad \cdots\cdots \qquad \text{(II. 7)}$$

the upper signs corresponding to $\sigma = 0$

the lower signs corresponding to $\sigma = -90^{\circ}$

Errors

Within the region shown on Fig. 3. 2 the ordinates are values of the departure from the value of a = 1, i. e., (a-1). The maximum contribution of each term is given in Table II. 1.

Table II. 1

| Term | Absolute Value Maximum Contribution | Fraction of Principal Value, g | % g = .2 |
|---|---|---|---|
| 1 | g | 1 | 100. |
| 2 | $3/8\, g^2$ | $3/8\, g$ | 7.5 |
| 3 | $g^3/64$ | $g^2/64$ | .06 |
| 4 | $g^4\ 65/(96)(16)$ | $g^3\ 65/(96)(16)$ | .034 |
| ⋮ | | | ⋮ |

Retaining only 2 terms assures that the value of (a- 1) is within . 1 percent.

Iso-$\mu$

Equation (II. 5) is not suitable as it stands for determining an iso-$\mu$ curve since particular values of $\mu$ cannot be designated in terms of a and g. The procedure chosen is to select the number of terms in (II. 4) and (II. 5) to assure a desired accuracy, and then eliminate the variable $\sigma$ between them. Table II. 2 shows the rate of convergence of Eq. II. 5.

Table II. 2

| Term | Absolute Value (Maximum) | Fraction of Principal Value | Max % for $g \leq .2$ |
|---|---|---|---|
| 1 | $g/2$ | 1 | 100. |
| 2 | $3/128\ g^3$ | $3/64\ g^2$ | . 19 |
| 3 | $3/1024\ g^4$ | $3/512\ g^3$ | .0047 |

The problem is simplified by the very fast convergence of (II. 5). Thus we shall use:

$$\mu = -\frac{g}{2} \sin 2\sigma \qquad \text{(correct to better than . 2\%)} \qquad \text{(II. 8)}$$

$$a-1 = -g \cos 2\sigma - \frac{3}{8} g^2 + \frac{g^2}{4} \cos^2 2\sigma$$

$$\text{(correct to better than . 1\%)} \qquad \text{(II. 9)}$$

from which

$$(a-1) = \pm\, g \sqrt{1 - \frac{4\mu^2}{g^2}} - \frac{g^2}{8} - \mu^2 \qquad \text{(II. 10)}$$

For each value of $\mu$ and g chosen there are two values of (a-1), but note they are not symmetrical with respect to (a = 1). Referring back to Fig. II. 1 shows the extent of the asymmetry for large values of g. For the region chosen ($0 \leq g \leq .2$) the departure from symmetry is 2 to 10 percent at the large g values.

The data for Eqs. II. 9 and II. 10 were accumulated with the aid of the IBM 7090 and are presented in Fig. 3. 2.

## APPENDIX III

### The Steady-State Conversion Matrix

Consider a time varying capacitance

$$C = \sum_{n=-\infty}^{n=+\infty} C_n \epsilon^{j2n\omega_1 t} \qquad \text{III. 1}$$

The fundamental pumping frequency is $2\omega_1$. This notation is used to simplify consideration of the degenerate parametric amplifier. Due to charges flowing in and out of C there will be a voltage produced having the general form:

$$V = \sum_{n=-\infty}^{n=+\infty} V_k \epsilon^{j\omega_k t} \qquad \text{III. 2}$$

where $V_k = V^*_{-k}$ (condition for real voltage; * is the complex conjugate).

The general charge description is given in terms of the product of III. 1 and III. 2

$$q = \sum_{n=-\infty}^{+\infty} \sum_{k=-\infty}^{+\infty} C_n V_k \epsilon^{j(2n\omega_1 + \omega_k)t} \qquad \text{III. 3}$$

$$C_n = C^*_{-n} \text{ (condition for real capacitance)}$$

In the restricted instance of a resonant circuit, where the frequency components are limited to a small band, the number of significant terms in III. 3 is small. Specifically if the discussion is centered about those frequencies in the vicinity of $\omega_1$ the only combinations of indices can can produce these are:

| $\omega_\ell$ (lower side frequency) | | $\omega_u$ (upper side frequency) | | |
|---|---|---|---|---|
| n = 0 | $\omega_k = \omega_\ell$ | n = 1 | $\omega_k = \omega_{-\ell}$ | III. 4 |
| n = 1 | $\omega_k = \omega_{-u}$ | n = 0 | $\omega_k = \omega_u$ | |

If the terms of III. 3 represented by III. 4 are summed and the time derivative taken the capacitive currents results.

$$I_c = j\omega_1 C_o V_\ell \epsilon^{j\omega_\ell t} + j\omega_u C_i V^*_\ell \epsilon^{j\omega_u t} + j\omega_\ell C_1 V^*_u \epsilon^{j\omega_\ell t} + j\omega_u C_o V_u \epsilon^{j\omega_u t} \qquad \text{III. 5}$$

and in matrix form where row 1 is at the lower side frequency, and row two at the upper side frequency:

$$\begin{bmatrix} I_\ell \\ I^*_u \end{bmatrix} = \begin{bmatrix} j\omega_\ell C_o & j\omega_\ell C_1 \\ -j\omega_u C^*_1 & -j\omega_u C_o \end{bmatrix} \begin{bmatrix} V_\ell \\ V^*_u \end{bmatrix} C \qquad \text{III. 6}$$

For a general monochromatic sine pump:

$$C = C_o[1 + \eta \sin(2\omega_1 t + \theta_1)]$$
$$C_1 = \frac{\eta C_o}{2}(\sin\theta_1 - j\cos\theta_1) \qquad \text{III. 7}$$

and III. 6 becomes

$$\begin{bmatrix} I_\ell \\ I^*_u \end{bmatrix} = \begin{bmatrix} j\omega_\ell C_o & \omega_\ell \frac{\eta}{2} C_o \epsilon^{j\theta_1} \\ \omega_u \frac{\eta}{2} C_o \epsilon^{-j\theta_1} & -j\omega_u C_o \end{bmatrix} \begin{bmatrix} V_\ell \\ V^*_u \end{bmatrix} C \qquad \text{III. 8}$$

Since the introduction of the angle $\theta_1$ is tantamount to an arbitray choice of the origin of the time axis, t, a new time axis, t', can be chosen such that

$\theta_1$ will now be zero.

$$\begin{bmatrix} I_\ell \\ I^*_u \end{bmatrix} = \begin{bmatrix} j\omega_\ell C_o & \omega_\ell \frac{\eta}{2} C_o \\ \omega_u \frac{\eta}{2} C_o & -j\omega_u C_o \end{bmatrix} \begin{bmatrix} V_\ell \\ V^*_u \end{bmatrix} C \qquad \text{III. 9}$$

where the time variable has been chosen such that $2\omega_1 t' = (2\omega_1 t + \theta_1)$.

## APPENDIX IV

### Gain Function in Oscillation Region

The gain function, Eq. 4.12, is repeated here and examined in detail for the specific region of interest, the region of oscillation.

$$g_\xi \equiv \frac{1}{1 - \frac{|\Pi|^2}{1+(\delta^2 - \xi^2) - j2\xi}} \qquad \text{IV. 1}$$

where $\delta$ = fractional detuning

$\xi$ = fractional signal departure from half-pump frequency, $\omega_1$

$$\Pi = \frac{\eta Q_o}{2} \epsilon^{j\theta_1}$$

The conditions for g to be in the oscillating region are seen from IV. 1 to be:

$$\xi = 0$$

$$\frac{|\Pi|^2}{1+\delta^2} \geq 1 \qquad \text{IV. 2}$$

It will be convenient to think of a new variable $\Pi'$, the detuned pumping factor where

$$\Pi' = \frac{\Pi}{\sqrt{1+\delta^2}}$$

Simplifying IV. 1 produces

$$g_\xi = \frac{(1 + \delta^2 - \xi^2) - j2\xi}{(1 + \delta^2 - |\Pi|^2 - \xi^2) - j2\xi} \qquad \text{IV. 3}$$

And now if we actually factor out the detuning parameter $(1 + \delta^2)$ from numerator and denominator and use the detuned pumping parameter $\Pi'$

$$g_\xi = \frac{1 - \frac{\xi^2}{1+\delta^2} - j\,\frac{2j}{1+\delta^2}}{1 - |\Pi'|^2 - \frac{\xi^2}{1+\delta^2} - j\,\frac{2j}{1+\delta^2}} \qquad \text{IV. 4}$$

When $\xi = 0$, $g_\xi = g_m$

$$g_m = \frac{1}{1 - |\Pi'|^2} \qquad \text{IV. 5}$$

from which

$$g_\xi = g_m \frac{1 - \frac{\xi^2}{1+\delta^2} - j\,\frac{2\xi}{1+\delta^2}}{1 - \frac{g_m \xi^2}{1+\delta^2} - j\,\frac{2g_m \xi}{1+\delta^2}} \qquad \text{IV. 6}$$

For small values of $\xi$, where $\frac{2g_m\xi}{1+\delta^2}$ is of the order of unity IV. 6 becomes much simpler and recognizable as a simple resonance form:

$$g_\xi \cong g_m \quad \frac{1}{1 - j\zeta'} = g_m \frac{1}{\sqrt{1 + (\zeta')^2}} \; \epsilon^{\,j \tan^{-1} \zeta'} \qquad \text{IV. 7}$$

where

$$\zeta' = \frac{\zeta}{1+\delta^2} = \frac{2g_m \zeta}{1+\delta^2}$$

Here $\zeta$ is to the active circuit what $\xi$ is to the passive circuit, and $\zeta'$ to the active detuned circuit what $\frac{\xi}{1+\delta^2}$ is to the passive detuned circuit.

Since $g_\xi$ and $g_m$ are voltage gain expressions, a relative power gain form is achieved by the ratio of the squares of $f_\xi$ and $g_m$, thus:

$$\left(\frac{|g_\xi|}{|g_m|}\right)^2 = k = \frac{1}{1+\zeta'^2} = \frac{1}{1+\dfrac{\zeta^2}{(1+\delta^2)^2}} \qquad \text{IV. 8}$$

Solving IV. 8 for $\zeta$ in order to relate relative bandwidth to detuning yields

$$\zeta = \pm\sqrt{(\frac{1}{k} - 1)(1+\delta^2)} \qquad \text{IV. 9}$$

For a chosen fractional response, k, the bandwidth increases with detuning, and from IV. 5 the band center gain, $g_m$, decreases.

## APPENDIX V

### Relation between $\sigma'$ and $\delta$

$\sigma'$, introduced in equation 5. 29, is the departure of the Mathieu solution phase angle from $\frac{\pi}{4}$ radians. ($\frac{\pi}{4}$ radians being very nearly the tuned phase angle.) $\delta$ is introduced in Chapter 2 in connection with detuning the passive circuit from half the pump frequency. (cf equation 2. 24)

Combining 2. 20 and 2. 25 we note that

$$a \cong 1 - \frac{\delta}{Q_0} \qquad \text{V. 1}$$

From Appendix II for small values of $\mu$ II. 5 is written:

$$\begin{aligned} a - 1 &= -g \cos 2\sigma \\ &= -g \sin 2\sigma' \end{aligned} \qquad \text{V. 2}$$

From 2. 22 $2g' \equiv \eta$

$$2g \equiv \eta(1 - \frac{\delta}{Q_0}) \qquad \text{V. 3}$$

$$\frac{-\delta}{Q_0} = \frac{-\eta}{2} (1 - \frac{\delta}{Q_0}) \sin 2\sigma' \qquad \text{V. 4}$$

$$\sin 2\sigma' = \frac{2\delta}{\eta Q_0 (1 - \frac{\delta}{Q_0})} \cong \frac{\delta}{|\Pi|} \cong \frac{\delta}{1 + \delta^2} \qquad \text{V. 5}$$

$$\cos 2\sigma' \cong \sqrt{1 - \left(\frac{\delta}{|\Pi|}\right)^2} \cong \sqrt{1 - \frac{\delta^2}{1 + \delta^2}} \cong \frac{1}{\sqrt{1 + \delta^2}} \qquad \text{V.6}$$

## APPENDIX VI

### Phase-Shift Detuning Factor

In the development of A for both the signal and the noise a factor arises that will be evaluated here. This factor appears first in component form in (5. 37) and is:

$$\frac{1}{\cos 2\sigma'}\sqrt{\left(\cos\sigma'' + \frac{-\delta|\Pi''|}{1+\Pi''}\sin\sigma''\right)^2 + \left(\frac{\delta|\Pi''|}{1+|\Pi''|}\cos\sigma''\right)^2} \qquad \text{VI. 1}$$

The evaluation proceeds on the basis of some simplifying assumptions. Since $\frac{1}{2Q_0} << 1$ in all practical cases, we will neglect this small phase angle $\tan^{-1}\frac{1}{2Q_0}$.

1. $\sigma'' \cong \sigma' + \tan^{-1}\frac{1}{2Q_0}$

and use $\sigma'' \cong \sigma'$.

2. For $\delta = .5$ we use $\cos 2\sigma' = \frac{\delta}{\sqrt{1+\delta^2}}$ from Appendix V

$$\sin 2\sigma' = \frac{\delta}{\sqrt{1+\delta^2}}$$

Performing the operations indicated in VI. 1 the factor becomes

$$\frac{1}{\cos 2\sigma'}\sqrt{\cos^2\sigma' - \frac{2\delta|\Pi''|}{1+|\Pi''|}\cos\sigma'\sin\sigma' + \left(\frac{\delta|\Pi''|}{1+|\Pi''|}\right)^2} \qquad \text{VI. 2}$$

using the double angle identities

$$\cos^2 \sigma' \cong 1 - \frac{\delta^2}{4}$$

VI. 3

$$2 \cos \sigma' \sin \sigma' \cong \delta\left(1 - \frac{\delta^2}{2}\right)$$

and the relations for a medium to high gain system

$$\Pi' = \frac{\Pi}{\sqrt{1+\delta^2}} \cong 1 \qquad |\Pi''| \cong 1 - \frac{\delta^2}{2}$$

VI. 4

$$\frac{|\Pi''|}{1 + |\Pi''|} \cong \frac{1}{2}\left(1 - \frac{\delta^2}{4} \ldots\right)$$

VI. 2 now becomes

$$\sqrt{\frac{1 - \frac{\delta^2}{2}}{\frac{1}{1+\delta^2}}} \cong \sqrt{1 - \frac{\delta^4}{4}} \cong 1$$

VI. 5

In addition the ratio of the two factors of VI. 1 are used for an inverse tangent function.

$$\frac{\frac{\delta|\Pi''|}{1 + |\Pi''|} \cos \sigma''}{\cos \sigma'' + \frac{-\delta|\Pi''|}{1 + |\Pi''|} \sin \sigma''} = \frac{\delta\left[\frac{1}{2}\left(1 - \frac{\delta^2}{4}\right)\right]\sqrt{1 - \frac{\delta^2}{4}}}{\sqrt{1 - \frac{\delta^2}{4}} - \delta\left[\frac{1}{2}\left(1 - \frac{\delta^2}{4}\right)\right]\frac{\delta}{2}} \cong \frac{\delta}{2}$$

VI. 6

## REFERENCES

Superregenerative Devices


1. E. H. Armstrong, "Some Recent Developments in Regenerative Circuits," Proc. IRE, Vol. 10, August 1922, p. 244.

2. B. B. Bossard, "Superregenerative Reactance Amplifier," Proc. IRE, Vol. 47, No. 7, July 1959, 1. 1269.

3. B. B. Bossard, E. Frost, and W. Fishbein, "X Band Superregenerative Parametric Amplifier," Proc. IRE, (Corresp), Vol. 48, July 1960, pp. 1329-1330.

4. H. A. Glucksman, "Superregeneration," Proc. IRE, Vol. 37, May 1949.

5. A. G. Jordan and R. Elco, "Esaki Diodes as Superregenerative Detectors," Proc. IRE, Vol. 48, No. 11, November 1960, p. 1902.

6. J. K. Pulfer (Radio and E. E. Div., Nat. Research Council, Ottawa), "Microwave Superregenerative Amplifier," The Microwave Journal, Vol. 4, No. 2, February 1961, p. 61-p. 66.

7. H. E. Stockman, "Tunnel Diode Superregenerative Parametric Motor," Proc. IRE, Vol. 49, October 1961, p. 1586 (Corresp).

8. D. N. Thomson, "Microwave Superregenerative Amplifiers," Proc. NEC, Vol. 16, 1960, p. 753.

9. C. P. Wang, "Superregeneration in a Cavity-Type Parametric Amplifier," Tech. Report No. 318-1, April 24, 1961, Electron Devices Lab., Stanford Electronics Laboratory.

10. C. P. Wang and G. Wade, "Noise Figure and Sensitivity of a Superregenerative Parametric Amplifier," IRE Trans. on Circuit Theory, Vol. CT-9, December 1962, No. 4, p. 320.

11. J. R. Whitehead, "Superregenerative Receivers," (Book) Cambridge U. Press, 1950.

12. J. J. Younger, A. G. Little, H. Heffner, G. Wade, "Parametric Amplifiers as Superregenerative Detectors," Proc. IRE, Vol. 47, July 1959, pp. 1271-72.

Subharmonic Oscillators


13. I. Ageyta, F. Borgini, D. R. Crosby, "A Computer Sub-system using Kilomegacycle Subharmonic Oscillators," Proc. IRE, Vol. 49, January 1961, p. 128.

14. I. Abeyta, F. Borgini, D. R. Crosby, "A Computer Subsystem using Kilomegacycle Subharmonic Oscillators," Proc. IRE, Vol. 49, No. 1, January 1961, p. 128.

15. D. K. Adams, "A Study of Double-Sideband Reactive Mixers," Technical Report No. 134, Cooley Electronics Laboratory, Dept. of Electrical Engineering, The University of Michigan, Dec. 1962.

16. A. T. Bolint (U. of Buffalo), "An Improved Magnetic Modulator for Satic Subharmonic Generators," 1959 Proceedings Spec. Tech. Fonf. on Nonlinear Magnetics and Magnetic Amplifiers; p. 167.

17. P. Bura, "The Degenerate and Quasi-Degenerate Mode of Parametric Amplification," IRE Transactions on Circuit Theory, September 1960, pp. 200-210.

18. W. J. Cunningham, "Nonlinear Analysis," McGraw-Hill Book Co., Inc., New York, N. Y., 1958, pp. 245-280.

19. R. W. Damon and J. R. Eshbach, "Theoretical Limitations to Ferromagnetic Parametric Amplifier Performance," IRE Trans, Vol. 1077-8, January 1960, pp. 409.

20. R. A. Elco, J. Nee, "The Reactance Tube as a Parametric Frequency Divider and Amplifier," (EE Dept., Carnegie Inst. of Tech.), Proc. IRE, Vol. 49, March 1961, p. 624.

21. E. Goto, "The Parametron, A digital Computing Element which Utilizes Parametric Oscillations," Proc. IRE, Vol. 47, August 1959, pp. 1304-1316.

22. E. Goto, "On the Application of Parametrically Excited Nonlinear Resonators," J. Institute of Electrical Communication Engineers (Japan), Vol. 38, October 1955, pp. 770-775.

23. J. C. Greene and W. D. White (Airborne Instruments Lab., Melville, N. Y.), "Radar Sensitivity with Degenerate Parametric Amplifier Front End," Proc. IRE, Vol. 49, April 1961, pp. 804-807.

24. J. Hilibrand, C. W. Mueller, C. F. Stocker, R. D. Gold (RCA, Princeton), "Semiconductor Parametric Diodes in Microwave Computers," IRE Trans. on Electronic Computers, September 1959, pp. 287-297.

25. A. Lavi, L. A. Finzi, "An Analysis of the Magnetic Second Subharmonic Oscillator," Proc. IRE, Vol. 49, April, 1961, p. 779-787.

26. A. Lavi, "Large Signal Analysis of Parametric Subharmonic Oscillators," Magnetic Amplifiers, Techn. Report No. 28, Carnegie Inst. of Tech., Dept. of Electrical Engineering, Pittsburgh, Pa., September 1959.

27. D. L. Hedderly, "An Exact Analysis of a Parametric Subharmonic Oscillator," IEEE Trans. on Electron Devices, Vol. ED-10, May 1963, No. 3, p. 134.

28. R. V. L. Hartley, "Oscillations in Systems with Nonlinear Reactance," BSTJ, Vol. 15, pp. 424-440, July 1936.

30. C. Hayashi, Y. Nishikawa, and M. Able, "Subharmonic Oscillations of Order One-Half," IRE Trans. on C. T., Vol. CT-7, pp. 102-111, June 1960.

31. J. Hilibrand and W. R. Beam, "Seminconductor Diodes in Parametric Subharmonic Oscillators," RCA Review, Vol. 20, pp. 229-253, June 1959.

32. D. S. Leeson, "Subharmonic Generation with Nonlinear Reactance - A Circuit Analysis," Proc. IRE, Vol. 49, January 1961, p. 351.

33. H. T. McAleer, "A New Look at the Phase-Locked Oscillator," Proc. IRE, Vol. 47, June 1959, p. 1137.

34. N. Minorsky, "Parametric Excitation," Journal of Applied Physics, Vol. 22, No. 1, January 1951, pp. 49-54.

35. E. Mount and G. Begg, "Parametric Devices and Masers: An Annotated Bibliography," IRE Trans. of MT and T, 8-9, p. 222, 1960-61.

36. S. Muroga, "Elementary Principles of Parametron and Its Applications to Digital Computers," Datamation, Vol. 1, October 1958, pp. 31-34.

37. Muroga and Takashima, "The Parametron Digital Computer, MUSASINO-1," IRE Transactions on Electronic Computers, Vol. EC-8, September 1959.

38. S. Onyshkevych, W. F. Kosonocky, A. W. Lo, "Parametric Phase-Locked Oscillator Characteristics and Applications to Digital Systems," IRE Trans. on Electronic Computers, Vol. EC-8, September 1959, pp. 277-286.

39. S. Oshima, H. Enomoto, S. Watanabe, Y. Koseki, "Analysis of Parametrically Excited Networks," Committee on Electric Computers, I. E. C. J., September 1955.

40. N. S. Psywes, "Relaxation Oscillations at Multiple Frequencies of Even Subharmonics," 1960 Proceedings of Special Tech. Conf. on Nonlinear Magnetics and Magnetic Amplifiers, Phil., Pa., October 26-28, 1960, p. 181.

41. N. Rouche (Lovanium U., Leopoldville, Rep. of Congo, Africa), "Oscillations of Parametric Subharmonic Oscillator, IRE Trans. on C. T., Vol. CT-9, March 1962.

42. F. Sterzer (RCA), "Microwave Parametric Subharmonic Oscillators for Digital Computing," Proc. IRE, Vol. 47, August 1959, pp. 1301-1412.

43. F. Sterzer and W. R. Beam, "Parametric Subharmonic Oscillators," IRE-AIEE - U. of Pennsylvania Solid-State Circuits Conference, Phil., Pa., February 13, 1959.

44. H. Takahashi, "The Parametron," J. Inst. Elec. Commun. Engr. (Japan), Vol. 39, June 1956, pp. 586-590.

45. J. Von Neumann, "Nonlinear Capacitance or Inductance Switching, Amplifying, and Memory Organs," U. S. Pat. No. 2,815,488 assig. to IBM, December 3, 1957.

46. C. P. Wang, "The Transient Build-Up and Phase Synchronization of Thin Magnetic Film Parametrons," Proceedings of the 1963 Intermag. Conference, April 17, 18, 19, 1963, IEEE Com. on Nonlinear Magnetics, PTG on I Electronics and Electron Computers, pp. 2-6-1 - 2-6-8.

47. R. L. Wigington, "A New Concept in Computing," Proc. IRE, Vol. 47, April 1959, pp. 516-523.

Time Varying Systems

49. W. R. Bennett, "New Results in the Calculation of Modulation Products," BSTJ Vol. 12, pp. 228-243, April 1933.

50. S. Darlington, "An Introduction to Time-Variable Networks," Proc. of Midwest Symp. on Circuit Analysis, U. of Ill., 1955, pp. 5-1 to 5-25.

51. B. Henning, "Flow Graph Analysis for Variable Parametric Networks," IRE Trans. of C. T., CT-9, No. 3, September 1962, p. 283 (Corresp.).

52. R. E. Kalman, "On the Stability of Time-Varying Linear Systems," IRE Trans. on Circuit Theory, Vol. CT-9, December 1962, No. 4, p. 420 (Corresp.).

53. B. K. Kinariwala, "Analysis of Time-Varying Networks," IRE Convention Record 9, Part 4, 1961, pp. 268-276.

54. J. R. Macdonald, D. E. Edmonson, "Exact Solution of a Time-Varying Capacitance Problem, Proc. IRE, Fegruary 1961, p. 453.

55. H. E. Meadows, "Solution of Systems of Linear Ordinary Differential Equations with Periodic Coefficients," BSTJ, July 1962, Vol. 41, No. 4, p. 1275-94.

56. L. A. Pipes, "Matrix Solution of Equations of the Mathiew-Hill Type," Journal of Applied Physics, Vol. 24, pp. 902-910 (1953).

57. L. A. Pipes, "Matrix Analysis of Linear Time-Varying Circuits," IRE Transactions on Circuit Theory, Vol. CT-2, December 1953, pp. 91-105.

58. C. Sato, "Stability Conditions for Resonant Circuits with Time-Variable Parameters," IRE Transactions on Circuit Theory, Vol. CT-9, December 1962, No. 4, p. 340.

59. R. G. Smart, "Steady-State Analysis of Power-Frequency Relations in Time-Varying Systems," Proc. IRE, June 1961, p. 1051.

60. W. Kaplan, "Operational Methods for Linear Systems," (Book), Addison-Wesley Publishing Co., Inc., 1962, pp. 481-482.

Parametric Devices

61. 1960 Abstracts IRE, Oscillators - parametric, -using point contact diodes, 1525, June, p. 1197; Amplifiers - superregenerative parametric (88), February, p. 274 -.

62. D. K. Adams, "An Analysis of Four-Frequency Nonlinear Reactance Circuits," IRE Trans. on Microwave Theory and Techniques, Vol. MTT-8, No. 3, May 1960, pp. 274-283.

63. E. Ahlstrom, W. G. Matthei, W. W. Gartner, "Use of Surface-Barrier Photodiodes as Fast Response Photocapacitors," Rice Scientific Inst., Vol. 30, July 1959, pp. 592-3.

64. J. T. DeJager and B. J. Robinson, "Sensitivity of the Degenerate Parametric Amplifier," Proc. IRE, Vol. 49, July 1961.

65. E. P. Felch, V. E. Legg, F. G. Merrill, "Magnetic Modulators," Electronics, Vol. 25, February 1952, pp. 113-117.

66. L. J. Giacoletto, "Fundamental Limiting Noise of Depletion Layer Capacitance," IRE Int. Convention Record, Vol. 98t3, 3-9, 1961.

67. J. C. Greene, W. D. White and R. Adler, "Radar Sensitivity with Degenerate Parametric Amplifier Front End," Proc. IRE (Corresp.), Vol. 49, pp. 804-807, April 1961.

68. W. T. Hatley, Jr., "Simulating Parametric Amplifiers," IRE Trans. on Electron Devices, Vol. ED-8, No. 2, March 1961, p. 116-123.

69. H. Heffner, "Capacitive Definitions for Parametric Operation," IRE Trans. Microwave Theory and Techniques, Vol. MTT-9, January 1961, pp. 98-9.

70. H. Heffner and G. Wade, "Gain, Bandwidth, and Noise Characteristics of the Variable-Parametric Amplifier," Journal of Applied Physics, Vol. 29, No. 9, September 1958, pp. 1321-1331.

71. C. R. Hurtig, "Dielectric Modulators Using the Space-Charge Capacitance of Junction Diodes," IRE-AIEE-UP Transistor and Solid-State Circuits Conf., Phil., 1958.

72. F. V. Hyde and D. G. Tucker, "Parametric Amplifiers; Static and Dynamic Inductance and Capacitance and Their Significance in the Nonlinear and Time-Varying Approaches," British Institution of Radio Engineers, Journal, Vol. 25, April 1963, pp. 353-55.

73. E. T. Jaynes "Nonlinear Dielectric Materials," Proc. IRE, Vol. 43, 1955, p. 1733.

74. J. M. Manley, "Some General Properties of Magnetic Amplifiers," Proc. IRE, Vol. 39, March 1951, pp. 242-251.

75. J. M. Manley and E. Peterson, "Negative Resistance Effects in Saturable Reactor Circuits," Trans. Am. Inst. Elec. Eng., Vol. 56, December 1946, pp. 870-881.

76. W. P. Mason and R. F. Wick, "Ferroelectrics and the Dielectric Amplifier," Proc. IRE, Vol. 42, November 1954, pp. 1606-1620.

77. G. Sherane, F. Jona, R. Pepensky, "Some Aspects of Ferroelectricity," Proc. IRE, Vol. 43, 1955, pp. 1738.

78. D. J. Soltz, "Low Level Parametric Amplifier, J. of Franklin Inst., Vol. 275, No. 2, February 1963, p. 79-87.

79. G. C. Spacek (G-M, Santa Barbara, Calif.), "Double Pumped X Band Parametric Amp. with Extremely Large Gain-Bandwidth Products," Proc. IRE, Vol. 50, June 1962, pp. 1534-35.

80. H. Suhl, "Proposal for a Ferromagnetic Amplifier in the Microwave Range," Phys. Rev., Vol. 106, pp. 384-385, April 15, 1957.

81. A. M. Vincent, "Dielectric Amplifier Fundamentals," Electronics, Vol. 24, December 1951, p. 84.

82. M. T. Weiss, "A Solid-State Microwave Amplifier and Oscillator Using Ferrites," Phys. Rev., Vol. 107, p. 317, July 1957.

83. L. A. Zadeh (U. of Calif., Berkeley), "Time Varying Networks I," Proc. IRE, Vol. 49, October 1961, pp. 1488-1503.

84. "A Study of Microwave Superregenerative Amplifiers for Lightweight Radars," Atronics Report 761 - 196-6, 13 June 1960, ASTIA No. AD 318-865.

85. D. N. Thompson (General Atronics Corp.), "Microwave Superregenerative Amplifiers," Proceedings of the NEC, 1960, Vol. 16.

86. D. N. Thomson (General Atronics Corp., W. Conshohocken, Pa.), "Maximum Sampling Rate for Superregenerative Amplifiers," 1962 IRE Convention Record, Part 2 (Automatic Control and Circuit Theory), p. 77-87.

87. "A Study of Microwave Superregenerative Amplifiers for Lightweight Radars," Atronics Report 761-196-6, 13 June 1960, ASTIA No. AD 318-865.

88. P. Bura and D. M. Tombs, "Resonant Circuit with Periodically Varying Parameters," Wireless Engineer, pp. 120-125, April 1952, May 1952.

89. S. V. Yadavalli (Stanford Research Inst.), "Detection of a Sinusoid Immersed in Noise-Finite Integration Time and Linewidth," IEEE Proc., Vol. 51, May 1963, p. 865.

91. B. A. Kaufman, W. Pfieffer "On the Characteristics of Cylindrical Thin-Film Parametrons Pumped to Saturation," Proceedings of IEEE, Vol. 51, May 1963, pp. 855.

92. E. R. Peressini, Et. al., "Experimental Study of Parallel Pumped Ferromagnetic Amplifier," J. Applied Phys., Vol. 33: 329-5, November 1962.

93. E. D. Banta, "Transient Analysis of a Parametric Oscillator," 1962 IRE International Convention Record, Part 2 (Automatic Control and Circuit Theory), 1962, p. 70-76.

94. K. W. Beer, "An Experimental Investigation into the Operation of the Parametric Phase-Locked Oscillator," Radio Electronic Engineering, Vol. 25, No. 5, May 1963, p. 432-40.

95. Y. H. Ku, T. T. Yank, "Analysis of Parametrically Excited Systems," Franklin Inst. Journal, V. 274, No. 6, December 1962, p. 452-74.

96. A. R. Saha (Jadavpur University, Dept. of Telecom. Eng., Calcutta), "Transistor Parametric Subharmonic Generator," Journal of Electronics and Control, July 1963, p. 21-39.

98. C. A. Desoer, "Linear Time-Varying G-C Networks: Stable and Unstable," IEEE Transactions on Circuit Theory, Vol. CT-10, June 1963, No. 2, p. 180.

99. A. P. Bekasov and O. G. Smolianoff, "Transient Characteristics of Resonance-Type Parametric Amplifiers and Converters," Radiotechnica i Electronika, Vol. 8, February 1963, p. 241-247 (Russian).

100. R. Spence and A. R. Boothroyd, "Discriminating Properties of the Synchronized Oscillator," Inst. EE Proc., 110:481-92, March 1963.

101. A. J. Viterbi, "On Coded Phase Coherent Communications," JPL Technical Report No. 32-25, JPL Laboratory, California Institute of Technology, August 15, 1960.

102. P. N. Zanedvorov, "Transient Processes of Oscillator Phase Stabilization in an Oscillator Locked by a Weak Signal," Radiotekhnika (USSR), Vol. 18, No. 4, p. 31-9, April 1963.

103. N. W. McLachlan, "Theory and Application of Mathieu Functions," (Book) Oxford, 1947.

104. R. F. Phillips, "Parametric Oscillation in a Damped Resonant System," IEEE Transactions on Circuit Theory, December 1963, p. 512-515.

105. E. D Banta, "Transient Analysis of a Parametric Oscillator," General Atronics Corporation report, Sponsored by Rome Air Development Center under Contract AF 30(602)-2283.

106. E. T. Whittaker, "Proceedings of the Edinburgh Mathematical Society," July 1914.

107. L. A. Blackwell and K. L. Kotzebue, "Semiconductor-Diode Parametric Amplifiers," (Book) Prentice-Hall 1961.

108. P. Penfield, Jr. and R. P. Rafuse, "Varactor Applications" (Book) The MIT Press, 1962.

109. F. E. Melde, Pogg., Annalen 108, 508 (1859).

110. Lord Rayleigh, "On Maintained Vibrations," Phil. Mag. 15, p. 229-235 Fifth Series, (April 1883).

111. L. Mandelstam, N. Papalexi, A. Andronov, A. Witt, and S. Chaikin, "Exposé des recherches recentes sur les Oscillations Nonlineaires, J. Techn. Phys. (USSR), 2, 81-134 (1934).

112. W. W. Mumford, "Some Notes of the History of Parametric Transducers," Proc. IRE, Vol. 48, May 1960, p. 848-854.

113. A. Stephenson, Proc. Manchester Phil. Soc. 52, No. 8, (1908).

Noise

114. Middleton, "Introduction to Statistical Communication Theory," McGraw-Hill, 1960, pp. 348, 472, 476.

115. Ragazzine & Franklin, "Sampled-Data Control Systems," McGraw-Hill Book Company, New York, 1958.

116. Williams, F. C., and Noble, SW, "The Fundamental Limitations of the Second-Harmonic Type of Magnetic Modulator as Applied to the Amplification of Small D. C. Signals," Proc. IEE, Part II, Vol. 97, 1950, p. 445.

## DISTRIBUTION LIST

| No. of Copies | |
|---|---|
| 20 | Defense Documentation Center<br>Attn: DDC-IRS<br>Cameron Station (Bldg. 5)<br>Alexandria, Virginia 22314 |
| 1 | Office of Assistant Secretary of Defense<br>(Research and Engineering)<br>Attn: Technical Library, Rm. 3E1065<br>Washington, D. C. 20301 |
| 1 | Bureau of Ships Technical Library<br>Attn: Code 312<br>Main Navy Building, Rm. 1528<br>Washington, D. C. 20325 |
| 1 | Chief, Bureau of Ships<br>Attn: Code 454<br>Department of the Navy<br>Washington, D. C. 20360 |
| 2 | Director<br>U. S. Naval Research Laboratory<br>Attn: Code 2027<br>Washington, D. C. 20390 |
| 1 | Commanding Officer and Director<br>U. S. Navy Electronics Laboratory<br>Attn: Library<br>San Diego, California 92101 |
| 1 | Commander<br>U. S. Naval Ordnance Laboratory<br>Attn: Technical Library<br>White Oak, Silver Spring, Maryland 20910 |
| 1 | Rome Air Development Center (EMTLD)<br>Attn: Documents Library<br>Griffiss Air Force Base<br>New York 13440 |

DISTRIBUTION LIST (Cont.)

| No. of Copies | |
|---|---|
| 1 | Systems Engineering Group (SEPIR)<br>Wright-Patterson Air Force Base<br>Ohio 45433 |
| 2 | Electronic Systems Division (ESTI)<br>L. G. Hanscom Field<br>Bedford, Massachusetts 01731 |
| 2 | Chief of Research and Development<br>Department of the Army<br>Washington, D. C. 20315 |
| 2 | Commanding General<br>U. S. Army Materiel Command<br>Attn: R&D Directorate<br>Washington, D. C. 20315 |
| 3 | Commanding Officer<br>U. S. Army Combat Developments Command<br>Communications - Electronics Agency<br>Fort Monmouth, New Jersey 07703 |
| 1 | Commanding Officer<br>U. S. Army Sec Agcy Combat Dev Actv<br>Arlington Hall Station<br>Arlington, Virginia 22212 |
| 1 | Harry Diamond Laboratories<br>Att: Library<br>Connecticut Avenue and Van Ness Street<br>Washington, D. C. 20438 |
| 2 | Commanding General, U. S. Army<br>Security Agency, Arlington Hall Station<br>Arlington, Virginia 22207<br>Attn: IALOG and IARD |
| 1 | Chief, Mountain View Office<br>Electronic Warfare Lab., USAECOM<br>P. O. Box 205<br>Mountain View, California 94042 |

DISTRIBUTION LIST (Cont.)

| No. of Copies | |
|---|---|
| 1 | Chief, Intelligence Materiel Dev Office<br>Electronic Warfare Lab., USAECOM<br>Fort Holabird, Maryland 21219 |
| 1 | Chief<br>Missile Electronic Warfare Tech Area<br>EW Lab, USA Electronics Command<br>White Sands Missile Range, N. M. 88002 |
| 1 | Chief, Willow Run Office<br>CSTA Lab. USAECOM<br>P. O. Box 618<br>Ann Arbor, Michigan 48107 |
| 1 | USAECOM Liaison Officer<br>MIT, Bldg. 26, Rm. 131<br>77 Massachusetts Avenue<br>Cambridge, Massachusetts 02139 |
| 1 | USAECOM Liaison Officer<br>Aeronautical Systems Division<br>Attn: ASDL-9<br>Wright-Patterson AF Base, Ohio 45433 |
| 1 | USAECOM Liaison Officer<br>Rome Air Development Center<br>Attn: EMPL<br>Griffiss Air Force Base, New York 13440 |
| 1 | USAECOM Liaison Office<br>U. S. Army Electronic Proving Ground<br>Fort Huachuca, Arizona 85613 |
| 1 | Stanford Electronics Laboratories<br>Stanford University<br>Stanford, California<br>Attn: Dr. D. G. Grace |

DISTRIBUTION LIST (Cont.)

| No. of Copies | |
|---|---|
| 16 | Commanding General<br>U. S. Army Electronics Command<br>Ft. Monmouth, New Jersey 07703<br>Attn: AMSEL-EW<br>AMSEL-WL-D<br>AMSEL-WL-S (3 copies)<br>AMSEL-WL-N<br>AMSEL-WL-C<br>AMSEL-WL-E<br>AMSEL-HL-CT-DD<br>AMSEL-RD-MAT<br>AMSEL-RD-MAF<br>AMSEL-RD-MAF-2<br>AMSEL-RD-GFR<br>AMSEL-XL-D<br>AMSEL-RD-LNA<br>AMSEL-KL-TM |
| 1 | Dr. T. W. Butler, Director<br>Cooley Electronics Laboratory<br>The University of Michigan<br>Ann Arbor, Michigan 48105 |
| 10 | Cooley Electronics Laboratory<br>The University of Michigan<br>Ann Arbor, Michigan 48105 |

UNCLASSIFIED

Security Classification

**DOCUMENT CONTROL DATA - R&D**

*(Security classification of title, body of abstract and indexing annotation must be entered when the overall report is classified)*

| | |
|---|---|
| ORIGINATING ACTIVITY (Corporate author)<br>Cooley Electronics Laboratory<br>The University of Michigan<br>Ann Arbor, Michigan 48105 | 2a. REPORT SECURITY CLASSIFICATION<br>Unclassified<br>2b. GROUP |

REPORT TITLE

The Phase Synchronization of a Parametric Subharmonic Oscillator

DESCRIPTIVE NOTES (Type of report and inclusive dates)

April 1967 - 7695-8-T - TR 178

AUTHOR(S) (Last name, first name, initial)

Cockrell, James L.

| REPORT DATE | 7a. TOTAL NO. OF PAGES | 7b. NO. OF REFS |
|---|---|---|
| April 1967 | 209 | 116 |

| | |
|---|---|
| a. CONTRACT OR GRANT NO.<br>DA 28-043-AMC-01870(E)<br>b. PROJECT NO.<br>1 PO 21101 AO42. 01. 02<br>c.<br>d. | 9a. ORIGINATOR'S REPORT NUMBER(S)<br>7695-178<br>9b. OTHER REPORT NO(S) (Any other numbers that may be assigned this report)<br>ECOM-01870-8-T |

0. AVAILABILITY/LIMITATION NOTICES

Distribution of this report is unlimited.

| | |
|---|---|
| 1. SUPPLEMENTARY NOTES | 12. SPONSORING MILITARY ACTIVITY<br>U. S. Army Electronics Command<br>Electronic Warfare Laboratory, AMSEL-WL-S, Ft. Monmouth, N. J. 07703 |

3. ABSTRACT

The general problem of phase determination for a parametric subharmonic oscillator is formulated. The analyses of several circuits are reduced to the solution of the canonical Mathieu equation. Solution is effected by the Floquet theorem and the parameters discussed in terms of the range of values encountered in experimental circuits. The transient portion of the solution produces arbitrary constants with two possible signs, yielding the two phase states of a growing oscillation. Conditions of oscillation are discussed, and the influence of signal and noise presented.

DD FORM 1 JAN 64 1473

UNCLASSIFIED

Security Classification

| KEY WORDS | LINK A | | LINK B | | LINK C | |
|---|---|---|---|---|---|---|
| | ROLE | WT | ROLE | WT | ROLE | WT |
| | | | | | | |

## INSTRUCTIONS

ORIGINATING ACTIVITY: Enter the name and address the contractor, subcontractor, grantee, Department of Dense activity or other organization *(corporate author)* issuing e report.

. REPORT SECURITY CLASSIFICATION: Enter the over- l security classification of the report. Indicate whether Restricted Data" is included. Marking is to be in accord- ice with appropriate security regulations.

. GROUP: Automatic downgrading is specified in DoD Di- ctive 5200.10 and Armed Forces Industrial Manual. Enter e group number. Also, when applicable, show that optional arkings have been used for Group 3 and Group 4 as author- ed.

REPORT TITLE: Enter the complete report title in all ipital letters. Titles in all cases should be unclassified. a meaningful title cannot be selected without classifica- on, show title classification in all capitals in parenthesis mediately following the title.

DESCRIPTIVE NOTES: If appropriate, enter the type of port, e.g., interim, progress, summary, annual, or final. ive the inclusive dates when a specific reporting period is vered.

AUTHOR(S): Enter the name(s) of author(s) as shown on in the report. Enter last name, first name, middle initial. military, show rank and branch of service. The name of e principal author is an absolute minimum requirement.

REPORT DATE: Enter the date of the report as day, nth, year; or month, year. If more than one date appears the report, use date of publication.

. TOTAL NUMBER OF PAGES: The total page count ould follow normal pagination procedures, i.e., enter the mber of pages containing information.

. NUMBER OF REFERENCES: Enter the total number of ferences cited in the report.

. CONTRACT OR GRANT NUMBER: If appropriate, enter e applicable number of the contract or grant under which e report was written.

, 8c, & 8*d*. PROJECT NUMBER: Enter the appropriate ilitary department identification, such as project number, bproject number, system numbers, task number, etc.

. ORIGINATOR'S REPORT NUMBER(S): Enter the offi- al report number by which the document will be identified d controlled by the originating activity. This number must unique to this report.

. OTHER REPORT NUMBER(S): If the report has been signed any other report numbers *(either by the originator by the sponsor)*, also enter this number(s).

. AVAILABILITY/LIMITATION NOTICES: Enter any lim- ations on further dissemination of the report, other than those imposed by security classification, using standard statements such as:

(1) "Qualified requesters may obtain copies of this report from DDC."

(2) "Foreign announcement and dissemination of this report by DDC is not authorized."

(3) "U. S. Government agencies may obtain copies of this report directly from DDC. Other qualified DDC users shall request through

_____."

(4) "U. S. military agencies may obtain copies of this report directly from DDC. Other qualified users shall request through

_____."

(5) "All distribution of this report is controlled. Qualified DDC users shall request through

_____."

If the report has been furnished to the Office of Technical Services, Department of Commerce, for sale to the public, indicate this fact and enter the price, if known.

11. SUPPLEMENTARY NOTES: Use for additional explanatory notes.

12. SPONSORING MILITARY ACTIVITY: Enter the name of the departmental project office or laboratory sponsoring *(paying for)* the research and development. Include address.

13. ABSTRACT: Enter an abstract giving a brief and factual summary of the document indicative of the report, even though it may also appear elsewhere in the body of the technical report. If additional space is required, a continuation sheet shall be attached.

It is highly desirable that the abstract of classified reports be unclassified. Each paragraph of the abstract shall end with an indication of the military security classification of the information in the paragraph, represented as *(TS), (S), (C), or (U)*.

There is no limitation on the length of the abstract. However, the suggested length is from 150 to 225 words.

14. KEY WORDS: Key words are technically meaningful terms or short phrases that characterize a report and may be used as index entries for cataloging the report. Key words must be selected so that no security classification is required. Identifiers, such as equipment model designation, trade name, military project code name, geographic location, may be used as key words but will be followed by an indication of technical context. The assignment of links, rules, and weights is optional.